We are grateful to both reviewers for their careful reading and correction suggestions. We accounted for most of their comments for revising a new version of our manuscript. Both referees call for rewriting parts of the manuscript more rigorously regarding the novelties brought and originality of the GO+ model. In the revised version, we took this opportunity to document more accurately the originality of the model, minor our over-enthusiastic statements and shorten some parts of the manuscript. We have organised our reply starting to address first the general comments of both referees and replying then to each specific comment.

1 General comments of referees #1 and #2

1.1 Referee # 1

Referee # 1 raised three main points.

- The linkage between soil water, plant size, plant, hydraulics and stomatal functioning and photosynthesis.
  We agree with the comments of both referees regarding the need for a clear demonstration of the model novelty in this area. Although kept simple, the explicit linkage between plant hydraulics and stomatal conductance in GO+ v3.0 is not implemented in most forest models where, e.g., the Ball-Berry's model is used instead (Guillemot et al. 2014) or a simpler LUE approach is used (Landsberg and Waring 1997) or time resolution is too large for calculating hourly values of the leaf water potential (Reyer et al. 2014). We simply meant that our stomatal and photosynthesis model is not based upon an optimality postulate and doe not link the stomatal conductance to photosynthesis. In the revised version, we propose to illustrate in a new figure (Figure 1) the effect of the leaf water potential on the stomatal conductance and photosynthetic CO2 assimilation at a range of leaf-to-air water vapour pressure deficit, CO2 concentration, and for different tree species. We agree our statement about the originality of this formalism was a bit exaggerated and that our model is actually close from the original Jarvis's (1976). We rewrote accordingly the first part of the discussion. We think that demonstrating the performance of the model for specific processes would lengthen considerably the manuscript and be complex due to the paucity of appropriate data. The evaluation of the canopy fluxes of water vapour and CO2 modelled against flux data measured by eddy covariance makes realise how well / badly the model behaves for simulating photosynthesis and evapotranspiration.

- The effect of the management options implemented in the model on model results.
  There is currently a vivid discussion about the role of forestry in the carbon emissions reduction policy of the countries that are signatories to

the Paris Agreements. This makes crucial to describe realistically the impacts of forest operations on carbon pools in the soil, harvested products and biomass. However, the present and upcoming forest management strategies are poorly represented in most models. The main merit of our model is its versatility that allows to create, assemble and combine the forest operations currently included in management schemes of coppices, plantation forests (soil preparation, intensive harvesting of different tree parts, ground vegetation removal), as well as close-from-nature management schemes (thinnings from the top, from below or random, self thinning). Our model can describe a relatively vast range of sylviculture options for even-aged, monospecific forests. In addition, the soil carbon sub-model, adapted from Roth-C, accounts for the effects of soil operations (tillage, disking, moulding,...) and the improvement of the soil carbon dynamics illustrated in Fig 3 is a substantial progress. However, we agree that the model originality is lesser for assessing deforestation impacts which led us to remove the Figure 4 from the revised version. We add a sentence in the Discussion section making clear that the version 3.0 is not including mixed or multilayered forests.

- The nutrient cycles and related impacts on photosynthesis and respiration. Thanks for the suggestion. The relationship between N and P leaf content, SLA and photosynthetic parameters is still an open area for modelling (Achat et al. 2016, Jiang et al. 2019). Meta-analysis comparing species (Walker et al. 2014) and previous modelling attempts developed in few global or forest models are of course inspiring but cannot be adapted straightforwardly to GO+. Based upon our recent synthesis (Achat et al. 2016)), a module describing the main processes of the nitrogen and phosphorus cycles in the soil-plant system is being developed for GO+ but goes beyond the scope of the v3.0 version .
  Hence, the simulations shown are all based assuming V_{cmax}, J_{max} values at 25 °C are fixed because we have not yet evaluated the next nutrient version with data observed. Though, we implemented the nitrogen content effect on maintenance respiration in the V3.0 version shown because its ecophysiological basis is widely understood (Ryan, 1991) and thus easier to parameterise and make generic among species and plant parts. However, the concentration of nitrogen in each part of the plant is fixed, which would make it superfluous to further detail the photosynthesis - foliar nitrogen relationship.

1.2 Referee # 2

The referee # 2 pointed 1) the usefulness of the verification section and 2) the explanation of the stomatal response functions (Eq. 13).

- The "Verification" section complied with the requirement of the journal but we thank you for the suggestion of changing its title. We thought this section is useful for showing the closure of mass and energy balances on a 22 year-long time series. Here, the lack of closure of the energy balance (9 %) is explained in this section by the approximation made about the atmospheric stability and the related underestimation of the convective heat fluxes by the model.

- We apologise because the sentence P9L10 " *The individual stomatal response functions used are allowed to vary according to the species considered*" is misleading and will be removed from the revised version. Actually, in the version 3.0 of the GO+ model, the response functions of stomatal conductance to short-wave radiation, leaf-to-air vapour pressure deficit, CO2 and leaf water potential are generic among species(see Figure 1), only their parameterisation is species specific. We add to Eq.13 the explicit description of the four response functions (previously shown in the parameterization section).

2 Specific comments referee#1

Abstract: the 2nd half of the abstract only described what the author have done – i.e. examines the sensitivity of the model, compares the model performance with observations. I would like to see some more explicit descriptions of the results of these actions. We changed the second part of the abstract.

P4, L2: This statement really depends on your definition of representations. Many land surface models did incorporate empirical relationships on management effect on soil and vegetation carbon. A recent literature is Felzer and Jiang (2018), who assessed the effect of different land uses on vegetation and soil carbon sequestration, including forest harvests. The relationships in their model are empirical, but so does some relationships described in this study.

We partially agree. Feltzer and Jiang (added in references) nicely described the effects of land use change and timber harvesting at the country scale on the only biomass stocks and related litter input to the soil. They ignored the putative short term effects of soil preparation, timber logging and clearcutting on soil organic matter mineralisation and ground vegetation that are common in European forestry. In European forests, Naudts et al. (2016) and Luyssaert et al. (2018) accounted for the impacts of forestry on the soil carbon dynamics considering the only changes in litter inputs and exports. They do not estimate effects on organic carbon mineralisation and transformation dynamics due to soil preparation techniques. In the forests of Southern Europe, the removal of branches, stumps and foliage of trees and understory are also relatively common but not accounted for by most forest models.

Table 1: Any particular reason why atmospheric O2 concentration is an input in this model? P8, Michaelis-Menten coefficient of Rubisco is depending on CO2 and O2 concentrations.

L13: What depth is the reference depth? Can you specify? This is actually the soil depth. Corrected.

P9, L8: So stomatal conductance is simulated independently of photosynthesis. Can you show, in your model evaluations, how photosynthesis and stomatal conductance is coupled/decoupled under different weather conditions? I think it's important for the readers to know the performance of these two fluxes, especially given the current way you represent these two inter-related fluxes.

We added a new figure deciphering the impact of leaf water potential and air water vapour pressure saturation deficit on the stomatal conductance and photosynthesis of the tree canopy.

P9, L9: Can you perform a sensitivity test on the time constant? This constant seems to potentially have a big effect determining your drought responses.

Yes we could but think it would lengthen the already long paper. We expect substantial effects on understorey exchanges where species with long response time, e..g. Fern species, are common. In tree species, the time constant is rarely exceeding 30-40 mn and has no impact on the model results at an hourly resolution.

Equation 13: How could one derive relationships from observations to drive your model? I can see many assumptions must have gone into the parameterization of this equation. How much confidence can we trust the model prediction, if these parameters were only empirically- determined/assumed?

We have explained this in the parameterisation section. The stomatal model equation is generic and may be parameterised at the canopy scale, using eddy covariance flux data, sap flow measurements, or upscaling gas exchange measurements performed with chambers. The new figure (Figure 1) will be inserted in the parameterisation section.

P10, L25: You have maximum root depth as an input parameter, but how root depth changes with plant age?

There is no changes in soil rooting depth with age in the V3.0 version. We agree that a relationship of the rooting depth with tree size is however missing for forest plantations and younger stands, where root expansion must be accounted for. We warn for this limitation in the discussion part of the version revised.

Equation 24: You did not have nutrient effect on photosynthesis, but you included N effect on respiration? Can you justify the reason to not include N effect on photosynthesis then? That seems a missed opportunity given the current momentum in including nitrogen and phosphorus cycle processes in land surface models, which has been quite nicely reviewed in Achat et al. (2016) and evaluated in Fleischer et al. (2019).

This is being developed in the next version of the GO+ model and will be evaluated using different forest experiments, including input from N fixing species, nitrogen deposition and fertilisation.

P13, L2: "than" grammar issue?
Yes, thanks, corrected.

P13, L6: Does allocation only respond to this water stress index and nothing else (e.g. nutrient, competition, phenology)? This could be quite an important weakness that needs further justification. Also, it seems that this water stress index only changes at annual timestep (P14, L5). Is this too coarse a resolution to simulate drought effect on growth and transpiration fluxes? The model certainly resolves energy, water and carbon budgets at hourly timestep, which implies that the model has the capacity to investigate detailed water-carbon relations under extreme conditions.

Apart from the foliage, the growth of the other tree parts (stem, branches, root parts) is integrated over the year and updated annually. We used therefore an annual index for simulating the impact of water stress on the carbon allocation between above-ground and below-ground tree parts (Eq. 28).

But if the water stress index is only updated at annual timestep, I see little possibility for a realistic simulation of the diurnal and intra-annual variability in carbon-water coupling.

The impact of leaf water stress on transpiration and photosynthesis is implemented hourly through stomatal limitation (Eqs.13 and 16) and leaf growth (understorey). Hence, the water and carbon are coupled at a range of time frequencies:

- Hourly for most canopy processes:
    - changes in leaf temperature, and in turn respiration, controlled by stomatal closure
    - leaf water potential and VPD control of stomatal conductance and in turn the internal CO2 concentration that affects photosynthetic assimilation of carbon
- Daily and yearly for growth, phenology and mortality processes.

These couplings are not covering all possible water stress effects on ecophysiological processes in trees, that are multiple. So, we do not pretend that the model is capturing every ecophysiological process coupling carbon and water metabolism a tree.

Figure 2: Allocation partitioning into different root components – how do you parameterize and evaluate this? For such a simple allocation scheme, maybe the authors want to justify the need for additional complexity in representing root dynamics. What additional insights do you gain by compartmenting roots into 4 categories? This parameterization is empirical and based upon allometric

relationships detailed in Achat et al. 2018. This is detailed in the Suppl Mat. Table S2 and Eqs. S34-S62. This level of details is requested for calculating the biomass maintenance respiration. It has not yet any other implication for the processes described in the V3.0. but, as explained in section 2.9.4, this was needed also for calculating the nutrient export due to harvests (Achat et al. 2018). Moreover, it will be used in the subsequent versions of the model for a number of processes included in N and P nutrient cycles.

Section 2.7: The representation of vegetation phenology includes very little mechanistic understanding – from what I can see, some part of the model only still uses date of year to change phenology. Maybe that's a point of future model improvement, but some acknowledge of the limitation may be needed.

As in most models, the bud burst, leaf unfolding and leaf duration (Fagus) are depending on the accumulated temperature – as chilling or forcing temperatures –, photoperiod (Quercus spp., data not shown) and accumulated radiation. Being more mechanistic would lead to implement detailed physiological processes that are complex and difficult to describe at the canopy scale. So, in this version, only the needle cohort life duration is fixed. All other phenological variables are controlled by temperature, radiation or water stress (Tables S3, S5).

P16, L21 – 22: From reading of this, it appears to me that you consider a tree dead once you can't close the carbon mass balance. Is this a realistic/safe assumption? The thing is, this assumption ignores the role of plant hydraulic and physiological traits in modulating plant responses to extreme conditions. I think some acknowledgement on the lack of process-based representation of tree mortality is needed here.

Yes, thanks it has been added in the discussion. We are aware of the numerous studies relating stomatal function to cavitation avoidance since, e.g., Jones and Sutherland (1991) until Choat et al. (2018). The implementation of variable resistances linked to cavitation and embolism of sapwood tissues and their repair would need to represent individual tree hydraulics that is not feasible with our model.

The negative carbon balance is produced when assimilation has been constrained by prolonged stomatal closure as a result of plant water stress. The stomatal response to leaf water potential is itself a consequence of plant hydraulics function (capacitance in tree and resistances in plant and soil). We assume that the GO+ hypothesis of the death of the tree of a negative carbon balance is a simple and direct modelling shortcut to summarize the impact of water stress in terms of tree mortality.

P16, L25: If I understand this correctly, here potentially coarse woody debris is added to soil pool?

Yes.

Figure 3: Clearly the new prediction still can't capture the exact management

effect, so what's the point of including these management options in your model? Yes the simulation is better matched with observation over the long-term, but the immediate impact should also be represented, I would argue.

Thanks. Our message here is essentially to show how GO+ captures the trajectory of soil carbon following a series of soil preparation operations. The example shown in Fig 3 are a unique time series of soil carbon content measured during the C. Jolivet Ph. D. thesis work in 2000. However, this time series is not fully consistent and should not have been used as such for the following reasons.

- First, the soil density used for calculating the observed values of C stocks was kept constant at a default value (1.13); it may have been changed during ploughing and disking but we have non information on this.
- Second, the slash and ground vegetation were initially accounted for until 1998 but were then piled in rows and left apart when ploughing (operation #5). They are not anymore accounted for in measurements until mid 1999. At that time, they were buried again in mineral soil during the subsequent disking (operation #4).

For consistency, we removed the observed C stock values measured without accounting for the slash and have changed the figure 3 accordingly (Figure 2).

Figure 4: Prediction not necessarily improved, is it?
See above. We removed it.

P21, L10 – 14: these assumptions seem to be very arbitrary – no citations, and not species-specific.
The fractions of understorey biomass destroyed by disking is the observed practices of the fast growing Pines plantations in Europe. We have added an explanation and reference. The calibration of the increase in the mineralisation and humification rates of the soil carbon are explained in section 2.9.1.

Section 2.9.4: I don't think there is much mechanistic basis in these model implementations. And if you have nutrient concentration in leaf, it seems to be logical to include nutrient effect on plant photosynthesis, at least that's what the authors did for respiration. Some justifications are needed as to why the authors did not consider nutrient effect on photosynthesis. There are relationships available to do so (e.g. Walker et al., 2014).
Yes thanks, this remark makes sense. We answered in the "General Comments" section, point #3.

The following section on sensitivity and parameterization test seems thorough, but I do note that the model was parameterized, so it's reasonable to see the model simulation matched with observations to some extent. I think it's more important to test the sensitivity of the assumptions that determine the CO2, temperature, precipitation, etc. responses, which is a different suite of *sensitivity test. This different suite of sensitivity test would allow one to really entrust the model mechanisms to predict future climate change impact.*

Yes we agree with this remark. However, we stress that, apart from the soil descriptive parameters (texture, soil depth), the model was not parameterized or calibrated on each site (L7 p35). Some parameters were obtained from the FR-LBr site and applied for all the othe stands shown in Figs. 13 (Pm-Vielle, Pm-Pomp21). Most model parameters were calibrated from independent experiments not used in the evaluation tests.
Our sensitivity analysis is the basic analysis expected when describing the first version published of such model. Its objective is to show how the model responds to its parameters and climate and how this is affecting the model uncertainty. The sensitivity tests related to the shape of the response of each process to environmental variables would have lengthened substantially the manuscript. We plan to publish this analysis within a GO+ application paper (project $Forets - 21$ funded by the French Ministry of Agriculture and project *Biosylve* funded by the French governmental agency *Ademe*).

Table 6: why "continued"?
A typo, thanks, removed.

P39, L3-4: You haven't evaluated how photosynthesis couples/decouples with stomatal conductance under water stress. I think you need to demonstrate it before you call it a novelty of the paper.
We agree and have added a new figure (see above and Figure 1)).

P40, L5: there is an extra comma in the citation bracket.
Thanks, corrected.

3 Specific comments referee#2

page 3, line 4: better explain the mechanisms (sensible heat flux) We add a short explanation regarding the effect in the boreal zone, the tropical impact of forests being already explained and referenced.

p3L18ff: you do not consider the life cycle of wood products. Your model can provide data that could allow such an analysis....
Agreed. We removed the sentence "It should be accounted for in forest models" that does not bring anything here.

p6L1: "releasing model calculations...": nicely put!

p7l5: "latter" instead of "later"
Thanks, corrected.
*p9l1: "is taken" ... " extended *the* use of Eqs" p9l13:*

Done.

please be a bit mor ?
In the revised version, the stomatal reduction functions have been developed in Eq. 13.

p10l5ff: the concept of dynamic layer dimensions is an interesting approach!
We agree, it is essential for including a groundwater table in the root zone.

p11l19: extra space after "presented here"
Done

p13: please make clear what "individual trees" are and what not
We changed the figure 2 legend and text.

p16l17ff: you state that you do not model tree mortality; what about regeneration? Is this also limited to managed forests (with planting)? You could mention this here (growth/mortality/regeneration as the major demographic processes).
Sound suggestion, thanks. We change this section into "Regeneration and Mortality" and explained how regeneration is prescribed in GO+.

And what is the "carbon balance of individual trees"??? The carbon balance of individual trees is calculated at the end of the year as the difference between its annual carbon gain, GPP_i, and annual carbon loss, $Rm_i + Rg_i$.

$$GPP_i - Rm_i - Rg_i \tag{1}$$

We have added a short explanation in the text.

p17l27: double ".." Corrected.

p19l10: it is not clear what the "number of trees felled" means. How does the number of trees change in the model? By management (thinning, final cuts), right? How is that related to the mortality of trees? You see, I am confused.
Sorry for that ! We changed this to "the number of cut or dead trees". The number of trees is continuously changing by mortality and regeneration. The mortality is mainly caused by the cutting of the stems harvested during thinnings or clearcutting and to a possible negative carbon balance of some individual trees.

p20 Fig5: please add explanations for the pools (DPM, RPM, ...) in the caption. There is a stray label ("L2") in the figure. Captions (e.g. "Long", "Beech" are way too big - or the other text labels are way too small.
The figure was redrawn.

p22l12: maybe use a different term instead of "verification". Maybe something like "testing conservation principles"?

See above.

p26/p27: in my opinion the discussion of results of the sensitivity analysis is too long and too verbose. It is meaningful to have such an analysis, but it is just limited what can be derived from such a general +-10 % approach.
We shortened the text by 25%.

p27Figure7: spell out abbreviations or refer to some table.
We refer now to the tables A1 and S1.

p30l1: How did you select the SDs of the parameters?
When available from their published references. Empirically in few cases

p33l30: "annual increase" instead of "time derivative".
Thanks, corrected.

p34Table 5: Can you add observed/predicted values here?
Yes, done.

p35 Table 6: remove "continued"
Done

p35l10: the sentence is duplicated ("The random errors...") Thanks, corrected.

p36 Table 7: Is this analysis useful? It does basically say that the model is able to discern between summer and winter. I think this is a candidate for shortening the paper
This analysis shows how the model error behave at a range of time frequencies. We agree that some frequencies reflect mainly obvious variations, e.g., the season, but find also useful to show how unsystematic errors tend to cancel out at low frequency.

p39l17: Remove the "the" after GO+
Done.

p39L22: confused again. How do you simulate the dynamics of size distribution??
The size distribution of the regenerating stand is prescribed. Each forest operations or self thinning is then selecting trees to be removed either from the top , the bottom or randomly. The natural death of trees provoked by a negative carbon balance may also affect either the bigger trees, the smaller trees or be random depending on the species-specific ratio between leaf area and respiring biomass.

p40L1: not true. There are gazillions of forest management practices that are not covered. What about single tree selection approaches or other spatial explicit small scale interventions? What about everything related to mixed forests?

See our reply in the General Comments section 1.

p40l28: "Model performance"

New paragraph created

p45: Leaf area is m2/tree, not m-2/tree.

Thanks, corrected.

same for BA. LAI is m2/m2, not m-2/m2. Stem volume is m3, stocking density is stems... this page is a bit messed up.

We agree, there was several typos here. We made all the corrections.

4 References

Choat, B., Jansen, S., Brodribb, T. J., Cochard, H., Delzon, S., Bhaskar, R., Bucci, S. J., Feild, T. S., Gleason, S. M., Hacke, U. G., Jacobsen, A. L., Lens, F., Maherali, H., Martínez-Vilalta, J., Mayr, S., Mencuccini, M., Mitchell, P. J., Nardini, A., Pittermann, J., Pratt, R. B., Sperry, J. S., Westoby, M., Wright, I. J., and Zanne, A. E.: Global convergence in the vulnerability of forests to drought, Nature, 491, 752-755, 2012.

Felzer, B. S. and Jiang, M.: Effect of Land Use and Land Cover Change in Context of Growth Enhancements in the United States Since 1700: Net Source or Sink?, Journal of Geophysical Research: Biogeosciences, 123, 3439-3457, 2018.

Jiang, M., Caldararu, S., Zaehle, S., Ellsworth, D. S., and Medlyn, B. E.: Towards a more physiological representation of vegetation phosphorus processes in land surface models, New Phytol, 222, 1223-1229, 2019.

Jones, H. G. and Sutherland, R. A.: Stomatal control of xylem embolism, Plant, Cell and Environment, 14, 607-612, 1991.

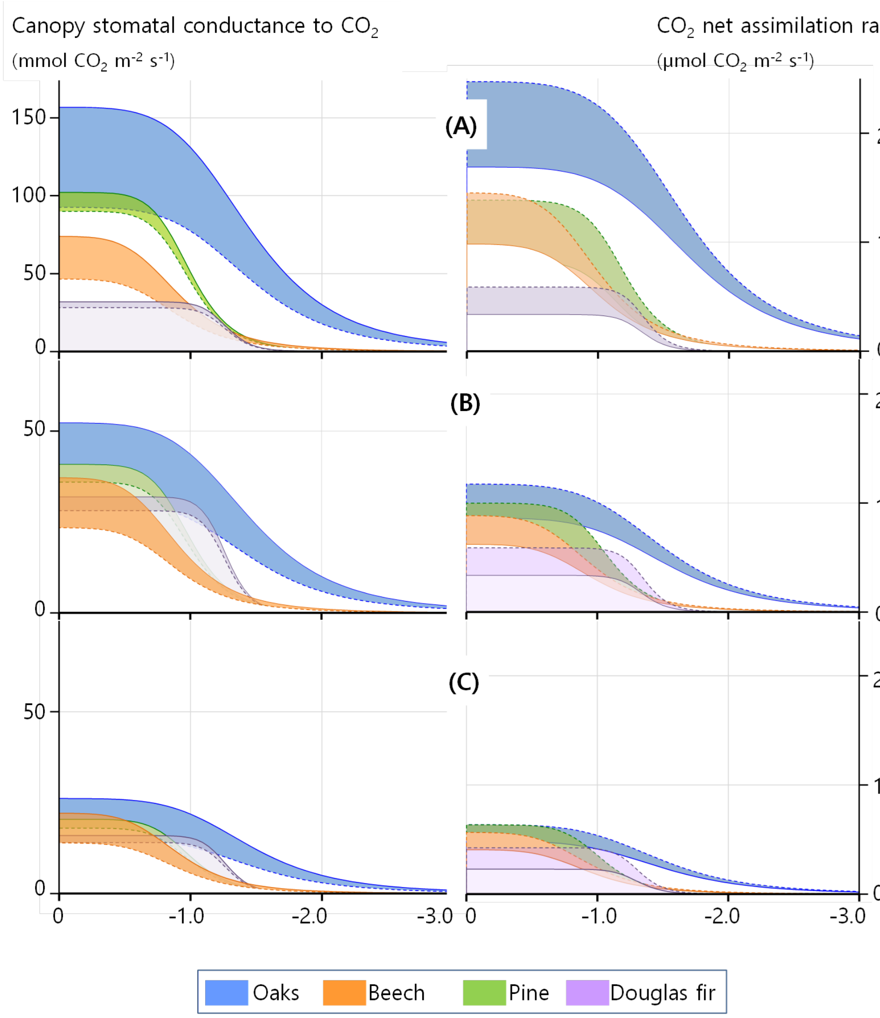

Figure 1: Modelled response of the stomatal conductance (left) and light-saturated photosynthesis (right) to decreasing leaf water potential at three levels of air water vapour saturation deficit, δe_w: (A) 500 Pa, (B) 1500 Pa, (C) 3000 Pa. The response curves delineates the range of response of four tree species for atmospheric concentrations in CO_2 varying between 410 (full line) to 820 ppm (dashed line).

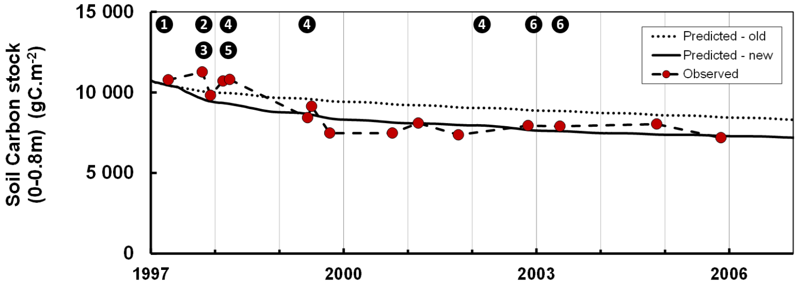

Figure 2: (Revised version of the original Figure 3 of the main manuscript). Changes in the soil organic carbon stock during the regeneration phase following a clear-cut of a maritime pine stand as simulated by the GO+ model with and without adaptation for soil preparation (full and dotted lines respectively) and measured in the field (grey dots). Data taken from Jolivet (2000). The numbers inset in black dots refer to the forest operation. 1: Clear-cutting and logging; 2: Heavy disking; 3: Stump removal; 4: Cover crop; 5: Tillage; 6: Vegetation crushing.

Energy, water and carbon exchanges in managed forest ecosystems : description, sensitivity analysis and evaluation of the INRAE GO+ model, version 3.0.

Virginie Moreaux[1,11], Simon Martel[1,10], Alexandre Bosc[1], Delphine Picart[1], David Achat[1], Christophe Moisy[1], Raphael Aussenac[1], Christophe Chipeaux[1], Jean-Marc Bonnefond[1], Soisick Figuères[1], Pierre Trichet[1], Rémi Vezy[2], Vincent Badeau[3], Bernard Longdoz[3], André Granier[3], Olivier Roupsard[4], Manuel Nicolas[5], Kim Pilegaard[6], Giorgio Matteucci[7], Claudy Jolivet[8], Andrew T. Black[9], Olivier Picard[10], and Denis Loustau[1]

[1]Bordeaux-Sciences-Agro, INRAE, UMR ISPA, Villenave d'Ornon, F-33140, France
[2]AMAP, Univ Montpellier, CIRAD, CNRS, INRAE, IRD, Montpellier, France
[3]INRAE, UMR SILVA 1434, Champenoux, F-54280, France
[4]Eco&Sols, Univ. Montpellier, CIRAD, INRAE, IRD, Montpellier SupAgro, Montpellier, France
[5]ONF, Département RDI, Fontainebleau, F-77300, France
[6]Technical University of Denmark, Department of Environmental Engineering, 2800 Kgs. Lyngby, Denmark
[7]CNR,ISAFOM, I-80056 Ercolano (NA) Italy
[8]INRAE, US1106 InfoSol, Orléans, F-45075, France
[9]Faculty of Land and Food Systems, Vancouver, BC - V6T 1Z4, Canada
[10]CNPF-IDF, Paris, F-75000 France
[11]Université de Grenoble-Alpes,CNRS, UMR IGE 5001, Grenoble, F-38058, France

Correspondence: Denis Loustau (denis.loustau@inrae.fr)

Abstract. The mechanistic model GO+ describes the functioning and growth of managed forests based upon biophysical and biogeochemical processes. The biophysical and biogeochemical processes included are modelled using standard formulations of radiative transfer, convective heat exchange, evapotranspiration, photosynthesis, respiration, plant phenology, growth and mortality, biomass nutrient content, and soil carbon dynamics. The forest ecosystem is modelled as three layers, namely the tree overstorey, understorey and soil. The vegetation layers include stems, branches and foliage and are partitioned dynamically between sunlit and shaded fractions. The soil carbon sub-model is an adaption of the Roth-C model to simulate the impact of forest operations. The model runs at an hourly time-step. It represents a forest stand covering typically 1 ha and can be straightforwardly up-scaled across gridded data at regional, country or continental levels. GO+ accounts for both the immediate and long-term impacts of forest operations on energy, water and carbon exchanges within the soil-vegetation-atmosphere continuum. It includes exhaustive and versatile descriptions of management operations (soil preparation, regeneration, vegetation control, selective thinning, clear-cutting, coppicing, etc.), thus permitting the effects of a wide variety of forest management strategies to be estimated: from close-to-nature to intensive. This paper examines the sensitivity of the model to its main parameters and estimates how errors in parameter values are propagated into the predicted values of its main output variables. The sensitivity analysis demonstrates an interaction between the sensitivity of variables with the climate, soil hydraulic properties being dominant under dry conditions whereas the leaf biochemical properties are most influential on wet soil. The sensitivity profile of the model is changing from short- to long time scales due to the cumulative effects of the fluxes of carbon, energy and water on the stand growth and canopy structure. Apart from few specific cases, the model does not show major discrepancies from observations at simulating the observed values of atmospheric exchanges, tree growth, and soil carbon and water stock changes monitored over Douglas fir, European beech and pine forests of different ages. We also illustrate the capacity of the GO+ model to simulate the provision of key ecosystem services, such as the long-term storage of carbon in biomass and soil under various management and climate scenarios.

1 Introduction

Carbon sequestration by forest ecosystems offsets a significant part of the global carbon emissions from burning fossil fuel (Pan et al. 2011). Forests are assumed to have the potential to be a low-cost effective measure for keeping the global temperature increase below +2°C (Griscom et al. 2017). Hence, the conversion of other land-use types into forests and the management of existing forests have been included in the portfolio of environmental actions to allow compliance with the international agreements proposed at Kyoto, Paris and subsequent conferences (Grassi et al. 2017). The enhanced management of existing forests and new plantations may play a substantial role in attenuating the increase in atmospheric CO2 concentration; especially for forests in temperate Europe and Russia (Bright et al. 2017). Managed forests also constitute the major source of material for wood-derived products. The growth of the world's human population is creating an increasing demand for such wood and fibre products; this demand is also leading to pressure to intensify the management of forests. Indeed, 22% of global ice-free land is covered by forests subject to diverse management strategies for wood production and other services; this compares with 9% occupied by unmanaged forests (IPCC 2019 report). In Europe, 86% of the forested area is managed, although with a large range of intensity. These numbers show that the dynamics of more than two-thirds of the world's forest are dominated by human activities.

In this context, the impacts of the management of European forests on climate are a matter of debate. The biophysical impacts on climate through, e.g., heat and radiation exchanges, and the biogeochemical role of forests, e.g., carbon sequestration, may be antagonistic and could cancel out (Bright et al. 2012, 2017, Luyssaert et al. 2018). In addition, the climate impacts of forest management at local, regional and global scales are diverse. Management affects the entire forest life cycle through many aspects such as the soil preparation, drainage, fertilization, tree stand species composition, age-class distribution, tree regeneration, thinning and harvest, control of diseases, pests and fires, land-use changes, etc. Many forest operations involved in modern forestry drastically change key canopy properties such as its albedo, roughness, leaf area index, standing biomass, and number of stems per hectare (Garcia et al. 2014, Kuusinen et al. 2014, Otto et al. 2014). Important soil properties (heat and water storage capacities, cation exchange capacity, nutrient stocks) are also affected by forest operations that are common in managed forests (logging, soil preparation, drainage, fertilization, liming) with significant but controversial impacts on carbon dynamics (Stromgren et al. 2013, Achat et al. 2015, Jurevics et al. 2016, Erb et al. 2017, Zhang et al. 2018). The forest understorey is also targeted by management practices aimed at decreasing the competition between the trees and understorey vegetation, or reducing the stands' vulnerability to fire (Borys et al. 2016).

Furthermore, the environmental effects of forest management and land-use changes have long been shown to interact with local climate conditions and forest characteristics such as albedo and roughness. Both climate models and observations have shown that the expansion of forests has some contrasting effects in boreal regions: there, the decrease in the snow cover duration and associated enhancement in the amount of net radiation absorbed could have a warming effect, as compared with the tropics, where enhanced evapotranspiration from forested areas reduces the sensible heat flux and enhance cloud formation at regional scale (Cutrim et al. 1995, Betts, 2000, Lee et al. 2011, Bala et al. 2007, IPCC Report 2019). The aridity also plays a key role, giving forests a net effect of slightly warming arid zones, due to the overwhelming impact of enhanced net radiation; in contrast a net cooling effect would result from afforestation or reforestation of humid zones due to enhanced latent heat flux (Huang et al. 2018). Climatic impacts of forest also depend on the tree species, in particular their specific albedo and evapotranspiration (Naudts et al. 2016, Ahlswede and Thomas, 2017). Through changes in albedo and in convective heat exchanges with the lower troposphere, forest management may impact the surface and planetary boundary layer temperature by the same magnitude as that from land-use changes (Bright et al. 2012, Luyssaert et al. 2014, Ahlswede and Thomas 2017). However, quantifying these biophysical impacts on climate is a complex procedure and therefore not accounted for in impact studies (Yousefpour et al. 2018) — as a result they have so far been ignored in climate treaties.

The forest products harvested from managed forests are also accounted for under a controversial "substitution" effect, that is, the replacement of emissions-intensive materials by wood products; a process that reduces emissions in other sectors (IPCC report 2019). This putative substitution effect is difficult to quantify due to the large diversity of wood products, transportation and transformation processes and product life cycles. Indeed, the substitution coefficient, the ratio of fossil carbon avoided to the bio-sourced carbon used, has been found to vary from -2.0 to 15 (Sathre and O'Connor, 2010). Nevertheless, considering the impact of wood products on the emissions of fossil carbon is essential when assessing and comparing the climate impacts of forest management strategies (Schlamadinger and Marland 1996). It should be accounted for in forest models. Including such an effect in impact studies implies that forest growth models must be connected to wood product life cycles, and, among others, to details of how the carbon is apportioned to the different products harvested and of their temporal dynamics (Pichancourt et al. 2018).

Mechanistic, process-based models of forest biophysics and biogeochemistry display a range of ability at representing forest management effects; their ability depends on their temporal and spatial resolution, and on the level to which they have been simplified. The most detailed dynamic stand-scale models, designed for describing a forest patch of typically one hectare area, include operations such as thinning and harvest (Deckmyn et al. 2008, Gutsch et al. 2011, Guillemot et al. 2014), and their frequency and intensity. They also allow the modeller to select the trees to be cut and harvested (Lindner et al. 1997). However, most models restrict the selection of the tree parts harvested to the stem and ignore the impacts on soil carbon of the removal of other elements such as branches, foliage or stumps. Until recently, global vegetation models have prioritized their efforts on the effects of land-use changes and tend to oversimplify the impacts of the management, that are reduced to age-class and functional type distributions (Bellassen et al. 2010 a and b, Harper et al. 2018, but see the implementation of management schemes across Europe by the model ORCHIDEE- CAN by Luyssaert et al. 2018). A few models, e.g., Rasche et al. (2013), do account for the size distribution of the harvested stems which allows one to realistically route the raw harvest products among energy, pulp, fibre, industrial uses, plywood and panels, and other building material (Schlamadinger and Marland 1996, Masera et al. 2003, Felzer and Jiang 2018).

To our knowledge no process-based model, local, regional or global, accounts for the effects of soil preparation techniques and understorey management on the energy balance, canopy properties, and ecosystem water and carbon balances. A few models can be coupled with other models of product life cycles, paving the way for assessing the impacts of the entire forest product life cycle . Models based on forest inventory data, so-called data models, and empirical growth and yield models may represent accurately the management effects on tree growth and wood production (Karjalainen et al., 2003, Kurz et al. 2009, Pilli et al. 2017). However, they do not account for the impact of climate and biogeochemical processes, nor do they allow new management strategies to be implemented. These models are not designed for simulating ecosystem functions — essentially they model growth and production under steady environmental conditions.

To progress our understanding of the role and functions of managed forests and their behaviour in a rapidly changing world, we present a mechanistic, process-based model called GO+. The model simulates the functioning and growth of temperate managed forests. GO+ accounts for both the immediate and long-term effects of forest operations on energy, water and carbon exchanges within the soil-vegetation-atmosphere continuum. It predicts the temporal dynamics of the above-ground and below-ground biomass of standing and harvested trees, ground surface vegetation and soil. The model is designed to be applied at large scale, i.e., over typically 10,000 grid points and 150 years. It has therefore been developed considering the trade-off between the need for a realistic prediction of tree growth, forest production and ecosystem functions at the country and regional levels, and the representation of the main biogeochemical and biophysical processes required for ensuring its robustness under climate and management scenario combinations. GO+ includes a comprehensive and versatile description of management operations (soil preparation, regeneration, vegetation control, selective thinning, clear-cutting, coppicing, etc.) allowing a variety of forest management strategies to be accounted for, from close-to-nature to intensive. In what follows, we first describe, the suite of processes implemented in GO+ from the radiation balance of the plant canopy to growth, phenology and mortality of a forest stand. The parameterization and verification of the model is then presented. We examine the sensitivity of the model to its main parameters and to the driving climate variables. From the results of this analysis, we estimate how errors in parameter values are propagated into the main output variables. Finally, we show how the model performs through comparisons with different sets of observations such as temporal series of forest-atmosphere exchanges of energy, water and CO_2 monitored over Douglas fir, European beech and maritime pine forests (Pseudotsuga Menziesii, Fagus sylvatica and Pinus pinaster, respectively) of different ages, and long time series of tree growth, soil water and soil carbon data recorded at permanent forest plots.

Table 1. List of the forcing meteorological variables driving the GO+ v3.0 model.

Symbol	Description	Entity (1)	Unit
CO_2	Air CO_2 concentration	Air	mol CO_2 mol air $^{-1}$
e_w	Air water vapor pressure	Air	Pa
$LW\downarrow$	Downward flux density of longwave radiation	Atmosphere	W m^{-2}
O_2	Air O_2 concentration	Air	mol O_2 mol air $^{-1}$
P	Atmospheric pressure	Atmosphere	Pa
$Rain$	Gross precipitation	Atmosphere	kg H_2O m^{-2} hr^{-1}
$SW\downarrow$	Downward flux density of shortwave radiation	Atmosphere	W m^{-2}
T_a	Air temperature	Air	°C
Tr_{soil}	Soil reference temperature	Soil	°C
U_{ref}	Horizontal wind speed	Air	m s^{-1}
β	Solar elevation angle	Sun	radians
δe_w	Air vapor pressure saturation deficit	Air	Pa

2 Model description

This section describes version 3.0 of the model GO+. The model has been developed in parallel to a series of experimental and theoretical developments which were formalized in preliminary versions (Loustau et al. 2005, Ciais et al. 2011). The model is primarily aimed at simulating managed forest stands and has been applied to various species (eucalyptus, Douglas fir, European beech, maritime pine) and management schemes (standard, coppice, self-thinning). In the interests of brevity, most of the equations and submodels already published in the literature are reported in the supplementary material; here we present only the main adaptations and innovations of the model.

2.1 Overview

The model runs on an hourly time-step for a forest plot typically covering 1 ha and is forced by meteorological variables (Table 1). It describes the energy balance, biogeochemical functioning and the development, growth and mortality of trees. The complete list of model prognostic variables together with their symbols and units is provided in Appendix A. The model parameters are presented in the supplementary material, Table S1. The vegetation is represented by a two-layer canopy corresponding to the trees and ground vegetation (Fig. 1). The core model includes the main biophysical and geochemical processes of the energy, water and carbon balances, and simulates dynamically the plant growth in height, leaf area, biomass and stem diameter, as well as vegetation dynamics (phenology, regeneration, senescence and mortality induced by ecological events or management). The tree layer is conceived as a collection of trees composed of foliage, branches, stemwood, bark, stump, taproot, coarse roots, small roots and fine roots. The ground vegetation is a simple homogeneous layer including three parts: foliage, roots and a perennial part that corresponds to either rhizomes, seeds or the woody parts of understorey species.

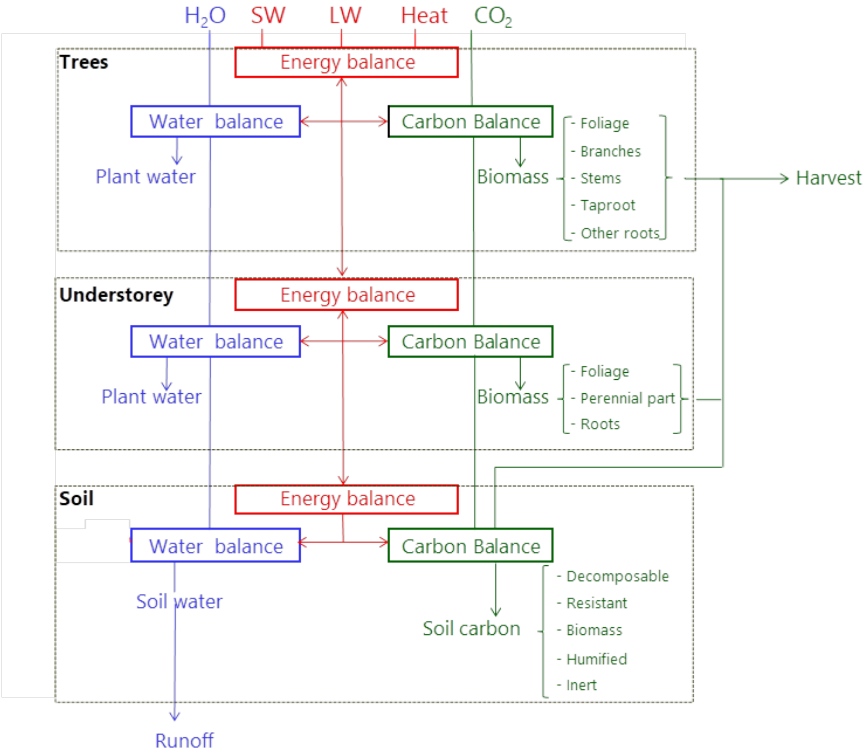

Figure 1. Overview of the GO+ model. The main atmospheric fluxes exchanged with the forest are summarised as H_2O: precipitation ; SW and LW: short-and long-wave radiation; Heat: sensible and latent heat flux; CO_2: carbon dioxyde exchange. The carbon exported as harvested material can be composed of stems, branches, foliage, stumps and coarse roots. The carbon flow from tree and understorey into the soil includes litter from foliage, branches and roots as well as harvest residue and dead parts of the understorey.

The model calculations start from solving the aerodynamic and radiation transfers, energy balance and water cycle and end with the resolution of carbon processes, plant growth and mortality. It includes several feed back processes (not shown in Fig.1 for clarity) namely the effects of soil water and carbon content on vegetation layers, the canopy feedback of the atmospheric exchanges of radiation and wind speed. The competition for light resource between the tree and understorey layers is explicit whereas the two entities are treated equally for the access to the soil water resource. For allowing GO+ to be run over large spatial and temporal domains with sufficient resolution, the 3.0 version of GO+ used two main simplifying assumptions releasing model calculations from time consuming iterative computations as follows. First, the feedbacks of canopy sources on the air temperature, humidity and CO_2 concentration are neglected, implying that the profile of scalar concentrations gradients within the canopy are not accounted for. Second, some simple analytical solutions of the radiation transfer and energy balance calculations are used instead of iterative calculations, which implies a limited number of approximations detailed in the description section.

2.2 Radiation transfer

Each vegetation layer is treated as an isothermal turbid medium where intercepting elements, the foliage and above-ground woody parts, are distributed uniformly or clumped. The calculation is operated for each layer from the top to the bottom layer. The transfer of direct and diffuse shortwave radiation, SW, and long-wave radiation, LW, through each layer is calculated using the Beer-Lambert law of light attenuation with a second order scattering. In the shortwave domain, the GO+ model follows the approach described by de Pury and Farquhar (1997) with few adaptations described below.

2.2.1 Foliage

For both the trees and understorey, GO+ allows a dynamic partitioning between sun and shade components (Eq. S1). The canopy reflection coefficients for diffuse and direct beam irradiance are calculated from (i) the leaf optical characteristics (reflectance, transmittance and absorbance), (ii) the diffuse and direct canopy extinction coefficients, $k_{d,c}$ and $k_{b,c}$ and (iii), for the latter, solar elevation (Eqs S2-S4). The extinction coefficients $k'_{d,c}$ and $k'_{b,c}$, where the primes indicate scattered radiation, are then used to determine the fractions of light absorbed and scattered by the sunlit and shaded parts of the foliage, thus accounting for the second order scattering of shortwave radiation. The shortwave radiation absorbed by the sunlit and shaded fractions of the trees and understorey layers is given by the sum of direct, diffuse and scattered-beam components (Eq. S5-S7). The absorption of the longwave radiation intercepted is also simulated using the isothermal turbid medium analogy and Beer-Lambert's law as detailed in Eq. S8-S9.

2.2.2 Woody parts of the tree canopy

The same formalism used for the foliage is used for modelling the passage of both shortwave and longwave radiation through non-leafy parts of the canopy, i.e. the tree branches and stems. The tree canopy leaf area index, LAI_T, is substituted by the wood area index, WAI_T, the latter being calculated from the above-ground biomass, mean canopy height, stem density per hectare, mean stem diameter and a trunk shape factor (Eq. S10).

2.3 Energy balance

The exchanges of long-wave radiation between soil, canopy and the atmosphere are calculated according to the analytical solution proposed by Jones (1992) with minor adaptations as follows. First, for each layer c, the net isothermal radiation, $Rn_{i,c}$ is calculated from the SW and LW radiative balance, assuming that leaf and air temperature are equal.

$$Rn_{i,c} = SW_{a,c} + LW_{a,c} - 2 \times K_{LW,c} \times \epsilon \times \sigma \times Ta_z^4 \tag{1}$$

where K_{LWc}, the emission coefficient for thermal radiation is calculated following the model by Berbigier and Bonnefond (1995) completed with a term for thermal radiation from the leafless parts of the canopy (stem and branches) as :

$$K_{LWc} = 1 - \exp(k_{LW1} \times LAI_c + k_{LW2} \times LAI_c^2 - k_{d,c,w} \times WAI_c) \tag{2}$$

where $k_{LW1,c}, k_{LW2,c}$ are extinction coefficients of foliage and $k_{d,c,w}$ the extinction coefficient of woody parts for diffuse radiation.

The longwave radiation and heat transfer are calculated using a resistance analogue scheme with a combined resistance to heat transfer, $r_{HR,c}$, that is calculated from the resistances to convective and radiative transfer, $r_{H,c}$ and $r_{R,c}$respectively:

$$r_{H,c} = \frac{U_z}{u*_c^2} \tag{3}$$

$$r_{R,c} = \frac{\rho_a \times c_p}{2 \times 4 \times K_{LWc} \times \sigma \times \epsilon \times Ta_z^3} \tag{4}$$

$$r_{HR,c} = \frac{1}{\frac{1}{r_{H,c}} + \frac{1}{r_{R,c}}} \tag{5}$$

Last, the temperature of each vegetation layer and air, Ts_c, is derived by combining radiative and convective transfers :

$$Ts_c = Ta_z + \frac{Rn_{i,c} \times \dfrac{\gamma}{g_{ctot,c}} \times r_{HR,c}}{\rho_a \times c_p \times (\dfrac{\gamma}{g_{tot,c}} + s \times r_{HR,c})} - \frac{r_{HR,c} \times \delta e_w}{(\dfrac{\gamma}{g_{tot,c}} + s \times r_{HR,c})} \tag{6}$$

Long-wave emission and net radiation absorbed are then given by Eqs. 7-8:

$$LW_{e,c} = 2 \times K_{LW,c} \times \epsilon \times \sigma \times Ts_c^4 \tag{7}$$

$$Rn_c = SW_{a,c} + LW_{a,c} - 2 \times K_{LW,c} \times \epsilon \times \sigma \times Ts_c^4 \tag{8}$$

The changes in storage of heat into the above-ground biomass, and air and water vapour within the canopy is neglected. The soil heat flux, G, is:

$$G = \frac{h}{z_{ref}} \times (Ts_{soil} - Tref_{soil}) \tag{9}$$

where h is the thermal conductivity of soil between the reference depth, the lower limit of the soil, and the top layer of soil in contact with the atmosphere, Ts_{soil} the soil surface temperature and $Tref_{soil}$ the temperature at the lower soil limit taken as the mean annual temperature of the site.

2.4 Momentum and heat transfer

The fluxes of sensible and latent heat from each vegetation layer and the soil into the atmosphere at the reference level z are formalized as a transfer through two resistances in series :

- the aerodynamic resistance to momentum transfer under neutral conditions, (related stability parameters equal zero), $r_{H,c}$ (Eq. 3) is related to the tree –or understorey– height, h_c, stem density, SD_c, and leaf area index, LAI_c, calculated according to the formulation proposed by Nakai et al. (2008):

$$u*_c = U_{ref} \times k \times (\log \frac{z_{ref} - d_c}{z_{0c}})^{-1} \tag{10}$$

with the wind speed at a reference height, U_{ref}, is derived from values provided by meteorological data using a logarithmic attenuation profile. The roughness length, z_{0c}, and displacement height, d_c, are modelled as follows:

$$d_c = [1 - \frac{1-\exp(-k_1 \times SD_c)}{k_1 \times SD_c} \times \frac{1-\exp(-k_2 \times LAI_c)}{k_2 \times LAI_c}] \times h_c \tag{11}$$

$$z_{0c} = 0.264 \times (h_c - d_c) \tag{12}$$

The resistance to heat transfer is taken as resistance to momentum under neutral conditions. We neglected corrections for stable and unstable conditions and extended the use of Eqs. 11-12 to non-neutral conditions.

– the canopy stomatal conductance submodel is based on a hypothetical maximum conductance, $g_{s,max}$, which is modified by empirical stomatal response functions which vary between zero and unity. These functions are combined in a multiplicative polynomial equation (Jarvis, 1976) to model the responses to the air CO_2 concentration, air vapour pressure saturation deficit, δe_w , the incident shortwave radiation, SW, and the leaf water potential, ψ_{leaf} . Since the leaf water potential depends on the tree hydraulic conductivity (Eq. 21), this model accounts for the effects of plant height on stomatal conductance (Delzon et al. 2004). The stomatal response modeled is therefore independent of the photosynthesis rate and allows for putative nighttime positive values. The individual stomatal response functions used are generic but their parameterisation is species-specific. The stomatal model includes a time constant which accounts for the response time of stomata to changing climatic or leaf water potential conditions. The steady state stomatal conductance, $g_{s,c}*$ and its dynamic counterpart, $g_{s,c}$ are :

$$g_{s,c,h}* = g_{s,max} \times f_{SW} \times f_{\delta e} \times f_{\psi} \times f_{CO2}$$

$$g_{s,c,h} = g_{s,c,h}* + (g_{s,c,h-1} - g_{s,c,h}*) \times \exp(\frac{-1}{\tau}) \tag{13}$$

with

$$f_{SW} = \frac{SW_a}{SW_a + k_{SW}}$$

$$f_{\delta e} = (\frac{\delta e}{k_{e1}})^{-k_{e2}}$$

$$f_{\psi} = (1 + \frac{\psi}{k_{\psi 1}})^{-k_{\psi 2}}$$

$$f_{CO2} = 1 - (1 - k_{CO2}) \times (\frac{CO_2}{350} - 1)$$

The sensible heat flux from the vegetation layers and soil is

$$H_c = \frac{1}{r_{Hc}} \times \rho_a \times c_p \times (Ts_c - Ta_z) \tag{14}$$

Since mass transport into the atmosphere is essentially turbulent, resistance and conductance for heat, momentum and mass transport will not be distinguished further in this section. The wet and dry fractions of each canopy and soil layers are calculated dynamically using the Gash's canopy water balance model resolved at an hourly time step (Eqs. S11-S14, Gash (1979)). This model, which needs few parameters, estimates the interception of incident rainfall by the canopy and the depth of water retained on the canopy. The tree trunks are treated as the foliage (Table S1). Under wet canopy conditions the stomatal resistance is assumed to be zero and, the flux of water vapour exchanged with the atmosphere is transferred only across the aerodynamic resistance :

$$\lambda \times E_{wet,c} = min(S_{W,c}, \frac{(1-f_{dry,c}) \times \rho \times c_p \times [\delta e_w + s \times (Ts_c - Ta_z)]}{\gamma \times r_{a,c}}) \tag{15}$$

where $S_{W,c}$ is the water stored at the surface of the canopy and $(1-f_{dry,c})$ is the fraction of canopy that is wet. In the case of condensation, i.e. when $\lambda E_{wet,c} < 0$, the corresponding amount is added to the rainfall and transmitted to the lower layer. The canopy temperature is not differentiated between the wet and dry fractions.

The canopy stomatal resistance is added to estimate the vapour flux emitted from the dry canopy i.e. the plant transpiration:

$$\lambda \times E_{dry,c} = \frac{f_{dry,c} \times \rho \times c_p \times [\delta e_w + s \times (Ts_c - Ta_z)]}{\gamma \times (r_{s,c} + r_{a,c})} \tag{16}$$

The soil is treated using a specific surface resistance calculations as follows:

$$r_{s,soil} = 100 \times \frac{\theta_{SAT} - \theta_{WP}}{\theta_A - \theta_{WP}} - 1 \tag{17}$$

The resulting latent heat flux, λE, is the sum of dry and wet evaporation over the vegetation layers and soil.

2.5 Water transfer

The soil is partitioned into three horizontal layers which are defined by their respective water content and may therefore have a variable depth and thickness:

- the top layer A is unsaturated, i.e. , its water content θ_A, varies between the wilting point, θ_{WP} and maximal water holding capacity, i.e., the field capacity, θ_{FC};
- the water content of the layer B, θ_B, is between the field capacity and saturation, $\theta_{FC} \leq \theta_B < \theta_{SAT}$, and z_{AB} is the lower level of layer A (upper level of layer B);
- the layer C is saturated at θ_{SAT} and z_{BC} is the lower level of layer B (upper level of layer C).

Water is transferred from the soil surface into the three layers according to a 1-D cascading formalism through either (i) as frontal diffusion or (ii) fast gravitational transfer and according to a simple bucket model. Because the water content of B and C cannot vary - only their thicknesses can vary - the layer A, if present, is first filled up until field capacity, further water input is then transferred to the layer C that is filled until it reaches the soil surface when $z_{BC} = 0$. In the absence of sufficient plant water uptake, deep runoff of groundwater occurrs; this depends on the local topography and hydrological environment and is modelled as :

$$D = D_{max} \times (\frac{z_{min} - z_{BC}}{z_{min}})^{k_w} \tag{18}$$

where D_{max} is the maximal drainage rate which will occur when the water table is at the soil surface, z_{min} is the depth at which drainage of the water table ceases and k_w a shape parameter describing the attenuation of drainage rate with the water table depth. In this equation, the depth is counted as a positive number.

The soil evaporation is emitted from the upper layer, that is either A, B or C. Plant transpiration is taken from the soil layers above the maximal root depth according to their respective water availability, first from the saturated layer C , then and if necessary from the intermediate layer B and finally from the upper layer A. Hence, when soil is saturated, i.e. $z_{BC} = 0$ and layers A and B do not exist, the transpiration uptake lowers the level of C and creates a layer B until z_{BC} passes beneath the root level i.e. $z_{BC} < z_{roots}$. The transpiration is then taken from the layer B until its water content, θ_B, drops down to the field capacity, $\theta_B = \theta_{FC}$. Layer A is then created and transpiration is taken from A.

The water withdrawn by plants is transferred from the soil to the roots and from the roots up to the canopy along a series of two hydraulic resistances, the soil-to-root resistance, r_{soil} and the mean root-to-foliage resistance, r_{xyl}.

$$r_{soil} = \frac{[1 + (\alpha_{VG} \times \psi_{soil})^{n_{VG}}]^{m_{VG}/2}}{\{1 - (\alpha_{VG} \times h_P)^{n_{VG}-1} \times [1 + (\alpha_{VG} \times \psi_{soil})^{n_{VG}}]^{-m_{VG}}\}^2} \tag{19}$$

$$r_{xyl,c} = k_{x0} + k_{x1} \times h_c^{k_{x2}} \tag{20}$$

A plant bulk capacitance, C_T, is added in derivation of the two-resistance pathway (Eq. S15 from Loustau et al. 1998). Having defined a global soil-to-foliage resistance, r_c, as $r_{soil} + r_{xyl,c}$, the canopy foliage water potential is:

$$\psi_{c,t} = (\psi_{soil,t-1} - \frac{E_{dry,c} \times r_c}{LAI_c \times 3600}) \times [1 - \exp(-\frac{\delta t}{r_c \times C_T})] + \psi_{c,t-1} \times \exp(-\frac{\delta t}{r_c \times C_T}) \tag{21}$$

2.6 Carbon cycle

The carbon cycle includes a suite of processes starting with the CO_2 uptake from the atmosphere by photosynthesis in the foliage and continuing with the subsequent transport and metabolic processes until carbon is exported out of the ecosystem, being either returned into the atmosphere by the respiration of the vegetation or soil, leached as dissolved carbon in groundwater, or exported during harvest (Fig. 1). Methane fluxes, the emission of volatile organic compounds and herbivory are neglected in version 3.0 of the model.

2.6.1 Photosynthesis

The photosynthetic carbon uptake by each vegetation layer is formalised in GO+ following Farquhar et al. (1980) and de Pury and Farquhar (1997) as the minimum of the RubP (Ribulose -biPhosphate) regeneration by electron transport and its carboxylation rate by RubisCO. The effects of leaf nitrogen and phosphorus content on photosynthesis are not implemented in the version 3.0 of the GO+ model and so are not presented here.The carbon assimilation is calculated separately for shaded and sunlit fraction of the foliage, denoted by subscript s, following the same set of equations (Eqs. 22, S17-S20).

The temperature dependency of the maximal rates of carboxylation by RubisCO and electron transport, $V_{cmax,c}$ and $J_{max,c}$ are computed according to Medlyn et al. (2002) (Eqs S22-S28). The chloroplastic concentration in CO_2, c_x, is estimated from the atmospheric concentration $CO2_a$, accounting for a series of three resistances from atmosphere to chloroplast, the aerodynamic resistance (Eq. 3), stomatal resistance (Eq. 13) and leaf internal resistance, the latter being taken from Ellsworth et al. (2015) (Eq. S21). The combination of the CO_2 transport equation $Anet_{c,s} = g_{CO2,c} \times (CO_{2a} - c_{x,c,s})$, where the total conductance to CO_2 is $g_{CO2,c,s} = \dfrac{1}{r_{H,c} + r_{s,c} + r_{m,c}} \times \dfrac{D_{CO2}}{D_{H2O}}$, with biochemical reaction rates Eqs. (S18-20) leads to a quadratic equation which has the solution:

$$Anet_{c,s} = \frac{b - \sqrt{b^2 + 4 \times c}}{2} \tag{22}$$

with

$$b = \begin{cases} g_{CO2,c,s} \times (CO_{2a} + K_m) + V_{cmax,c} - R_d & \text{if } W_c > W_j \\ g_{CO2,c,s} \times (CO_{2a} + 2 \times \Gamma^*) + \dfrac{J_{c,s}}{4} & \text{otherwise.} \end{cases}$$

and

$$c = \begin{cases} g_{CO2,c,s} \times [(CO_{2a} + K_m) \times R_d - (CO_{2a} - \Gamma^*) \times V_{cmax,c}] & \text{if } W_c > W_j \\ g_{CO2,c,s} \times [(CO_{2a} + 2 \times \Gamma^*) \times R_d - (CO_{2a} - \Gamma^*) \times \dfrac{J_{c,s}}{4}] & \text{otherwise.} \end{cases}$$

where the electron transport rate $J_{c,s}$, is calculated according to Eq. S19. The net photosynthesis is then integrated at canopy layer level using the shaded and sunlit area fractions of foliage LAI_{sun} and LAI_{shade} (Eq. S1) and foliage temperature for estimating K_m , $V_{cmax,c}$, $J_{max,c}$ and Γ^* (Eqs S22-S28). At the ecosystem level, the net assimilation of CO_2 and the gross primary production by the canopy foliage are therefore, respectively:

$$A_{ECO} = \sum_{c=1,s=0}^{2,1} Anet_{c,s} \times LAI_{c,s}$$

$$GPP_{ECO} = A_{ECO} + \sum_{c=1}^{2} R_{d,c} \tag{23}$$

Figure 2 illustrates the shape of the stomatal conductance and photosynthesis responses to the leaf water potential at a range of leaf-to-air vapour pressure deficit. The coloured areas provide the range expected for the effect of a CO_2 concentration change from 410 to 820 ppmv.

2.6.2 Respiration

The respiration from living plants, R_a, is assessed as a mass flux of CO_2 released into the atmosphere. It is partitioned between a growth component and maintenance component. The growth respiration R_g is estimated as a fixed fraction of the carbon allocated to growth that depends on the chemical composition of the organ, leaves, branches, stems, roots (Penning de Vries et al. , 1974). The maintenance respiration, R_m, is a basal metabolic rate of respiration that depends on the living biomass and temperature. It is calculated separately for above-ground parts and below-ground parts as follows.

- The foliage respiration of each layer, $Rm_{\mathrm{c,\,f}}$ is :

$$Rm_{\mathrm{c,\,f}} = LAI_c \times R_{\mathrm{d,\,T15,\,c}} \times \exp\left(E_\mathrm{a}(R_d) \times k_{\mathrm{T,\,c}}\right) \tag{24}$$

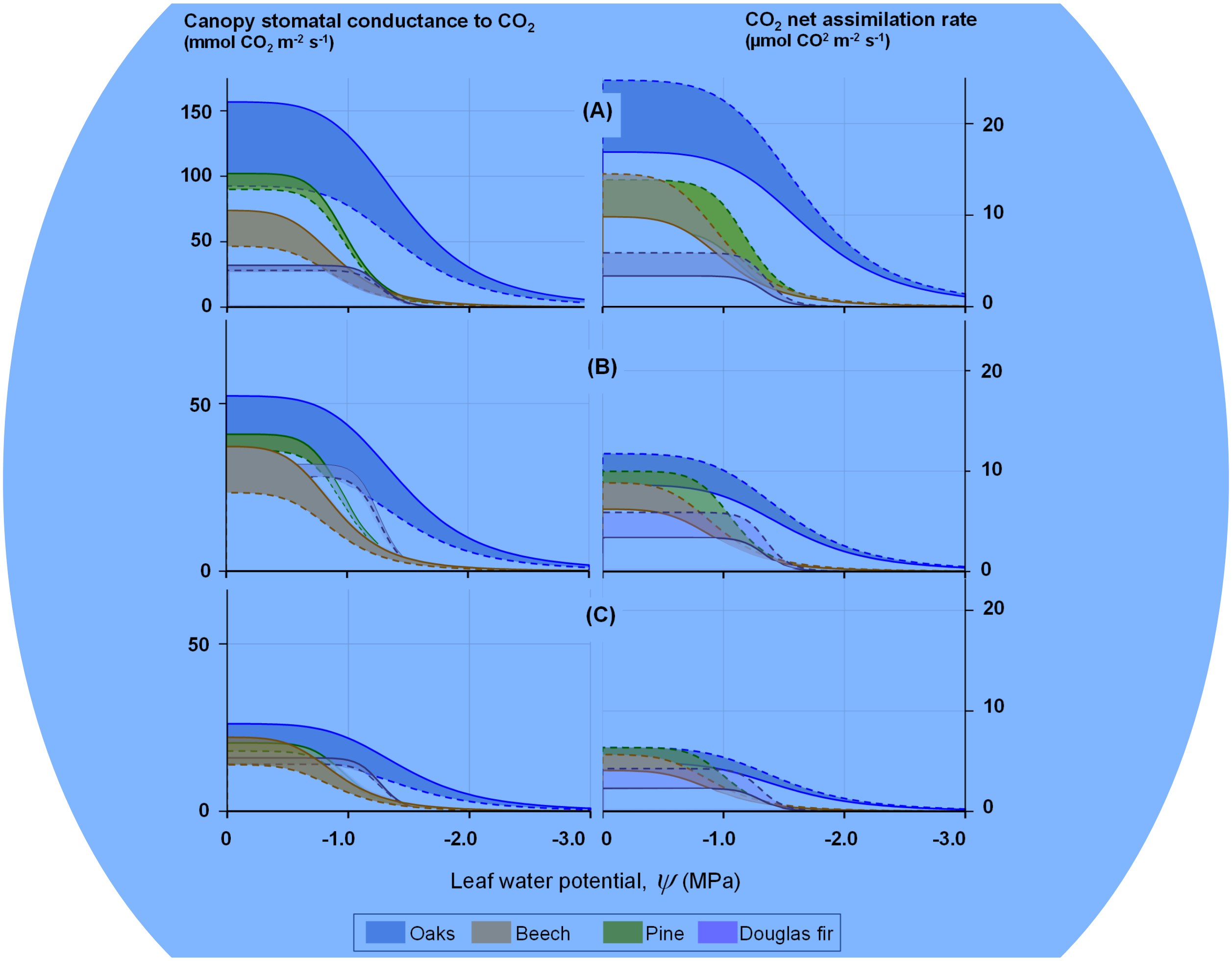

Figure 2. Modelled response of the stomatal conductance (left) and light-saturated photosynthesis (right) to decreasing leaf water potential at three levels of air water vapour saturation deficit, δe_w: (A) 500 Pa, (B) 1500 Pa, (C) 3000 Pa, according to Eqs. 13 and 22. The response curves delineates the range of response of four tree species for atmospheric concentrations in $\mathrm{CO_2}$ varying between 410 (full line) to 820 ppm (dashed line).

where k_{Tc} is a temperature factor also used for the parameters representing the temperature dependency of photosynthesis (Eq. S22).

- The maintenance respiration of other tree parts (stem, branches, taproot, coarse, small and fine roots, denoted by x) is calculated on the basis of the mass of nitrogen in living biomass , N_x^* (Dufrêne et al. 2005).

$$Rm_{\mathrm{T15,x}} = N_x^* \times R_{N,T15} \quad (25)$$

where $R_{N,T15}$ is the rate of maintenance respiration per unit mass of nitrogen (Ryan, 1991). The calculation of N_x^* is resolved at the tree level as detailed in the supplementary material Eqs. S29-33. The temperature dependent respiration integrated over the entire tree layer, Rm_{T} , is then:

$$Rm_{\mathrm{T}} = \sum_{i}^{SD}\sum_{x} Rm_{\mathrm{T15},\,x} \times Q_{10,\,x}^{\frac{T_x - 15}{10}} \tag{26}$$

where the subscript i stands for tree, SD is the number of trees per unit area and $Q_{10,x}$ is multiplier of maintenance respiration of organ x for a 10°C temperature increase.

- The maintenance respiration of the understorey components, foliage, roots and perennial part, is depending on their only biomass and is using the same temperature response than trees.

2.6.3 Carbon allocation and growth

The GO+ allocation scheme allows a flexible allocation of carbon among trees and between above-ground and below-ground tree parts. The allocation scheme of the understorey is fixed. The allocation scheme is summarised in Fig. 3. The carbon allocation between below-ground and above-ground parts is regulated by a water stress index. Subsequently, the carbon is distributed among plant parts based upon empirical allometric equations.

- For the tree stand, the growth is resolved at a daily time-step for the foliage and at an annual step for the stems, branches, taproot, coarse roots and small and fine roots. The tree growth is modelled following a three-step process.
  - (1) The carbon uptake by photosynthesis GPP_T is shared among trees according to their respective contribution, λ_i, to the canopy foliage dry mass $W_{L,T}$.

    $$\lambda_i = \frac{W_{L,i}}{W_{L,T}} \tag{27}$$

    where $i \in [1, SD]$ and $\sum_{i=1}^{SD} \lambda_i = 1$, SD being the number of stems per unit area. For each individual the amount of carbon allocated to growth, NPP_i, is the gross primary production after the respiration of foliage, woody parts and roots have been subtracted, $NPP_i = \lambda_i \times GPP_T - [Rm_{a,i,f} + Rm_{a,i,w,} + Rm_{r,i} + Rg_i]$.
  - (2) NPP_i is partitioned between above-ground and below-ground parts using an root / shoot allocation coefficient Λ. This coefficient depends on the annual water stress index, I_{stress}, that is related to the ratio of the annual tree transpiration, $E_{\mathrm{dry,\,T}}$, to the potential transpiration $E_{\mathrm{pot,\,T}}$. The potential transpiration, $E_{pot,T}$, is calculated with a stomatal model having only SW and CO_2 limitations and corresponds to the transpiration of a canopy unlimited by hydrological or meteorological drought.

    $$\Lambda = k_{\lambda 1} \times \exp(k_{\lambda 2} \times {I_{\mathrm{stress}}}^{k_{\lambda 3}}) \tag{28}$$

    with

    $$I_{stress} = 1 - \frac{E_{dry,T}}{E_{pot,T}} \tag{29}$$

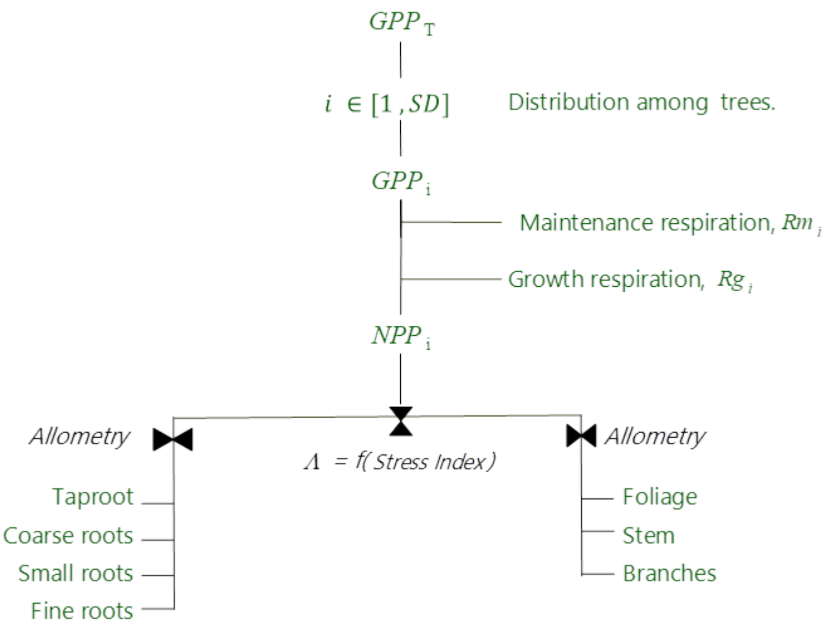

Figure 3. Allocation scheme of carbon for the tree canopy in the GO+ v. 3.0 .GPP_T is the gross primary production of the whole tree layer (Eq. 23), i denotes each individual tree, SD is the number of trees per ha, Rm_i and Rg_i are the maintenance and growth respiration of tree i (Eq. 25-26), NPP_i the net primary production of tree i and Λ is a root-shot allocation coefficient controlled by the water stress index (Eqs. 27-29).

The allocation scheme allows therefore a shift of the annual amount of carbon allocated to growth of below-ground parts, $\mathrm{d}W_{r,T}$, when the stress index increases (Landsberg and Waring, 1997). The annual net amount of carbon available for the structural growth of roots is calculated as:

$$\mathrm{d}W_{r,i} = \Lambda \times NPP_i \tag{30}$$

The corresponding amount of carbon allocated to above-ground structural parts is:

$$\mathrm{d}W_{a,i} = NPP_i - \mathrm{d}W_{r,i} \tag{31}$$

The tree biomass above-ground and below-ground $W_{a,i}$ and $W_{b,i}$ are then updated :

$$\begin{aligned} W_{a,i,year+1} &= W_{a,i,year} + \mathrm{d}W_{a,T,year} \\ W_{b,i,year+1} &= W_{b,i,year} + \mathrm{d}W_{b,T,year} \end{aligned} \tag{32}$$

- (3), GO+ allocates the amount of carbon available for above-ground growth among foliage, branches and stem and for below-ground parts among taproot (stump + main pivotal root), coarse roots (diameter > 20 mm) , small roots (diameter between 2 and 20 mm) and fine roots (diameter < 2 mm) using species-specific sets of allometric equations. Each set of values is specific to the tree species considered. Such equations link the stem diameter at breast height, D_{130}, to the biomass of aerial parts. The D_{130} is substituted from the set of allometric equations so that each compartment biomass can be related to the total above-ground biomass. The foliage growth is distributed over the next growing period meaning that the current cohort of leaves relies upon the previous year NPP_T. This implies that the current year LAI depends on the previous year NPP_T and stress index. The growth of the other parts of each tree is not dynamic but is calculated at a yearly resolution; it is instantaneously updated at the end of the year. The equations used for maritime pine, European beech and Douglas fir are shown as examples in Eqs. S34-S62. The height of each tree is also derived from allometric equations.

- The understorey allocation scheme is resolved dynamically at a daily time step using two ordinary differential equations. We assume the horizontal distribution of the understorey vegetation is uniform and no individual plants are defined. The vegetation includes three compartments, the foliage, f, roots, r, and perennial parts, p. The understorey growth comprises two processes, growth and mortality, that are applied to each compartment, foliage, roots and perennial parts with specific parameter values. The growth of understorey biomass parts is resolved at a daily time step as the minimum of a demand and a supply functions, $dW_{d,j}$ and $dW_{s,j}$ respectively.
  - The demand function of each compartment, foliage, roots and perennial parts, $dW_{d,j}$ at day DOY is the derivative of the sigmoid function s_j times the asymptotic value of biomass $W_{max,j}$:

$$dW_{d,j} = W_{max,j} \times s_j \times (1 - s_j) \quad (33)$$

$$s_j = \frac{1}{1 + exp[-k_p \times (DOY - DOY_{0.5,j})]}$$

where $dW_{d,j}$ is the daily potential biomass increment of compartment j , $k_p = \frac{1}{GD} \times 2 \times Log(\frac{1}{k_s} - 1)$ where GD is the maximal growth duration, k_s a flattening coefficient (kurtosis) and $DOY_{0.5,j} = BB_j + \frac{GD}{2}$ the day of year by which half of the growth has been achieved, BB_j being the day when growth starts.

  - The supply function of compartment j, $W_{s,j}$, is the pool of carbon available for growth. Its is fed by the fraction of the carbon allocated to the compartment, $dW_{s,j}$ calculated as:

$$dW_{s,j} = \lambda_j \times (GPP_U - R_{m,U}) \times \frac{1}{1 + Rg_j} \quad (34)$$

where λ_j is an allocation coefficient to compartment j and Rg_j the respiration cost associated with the compartment j. The NPP_U allocation among the three compartments is fixed by three parameters, λ_j , subscript j standing for f, p or r. The growth starts at the "budburst day", BB_j, according to a simple model of accumulated "degree-days" and is paused when the soil moisture deficit or air temperature drop below a fixed threshold value of SMD_{GU} or T_{GU} respectively.

2.7 Vegetation phenology

Leaf unfolding, senescence and growth

A specific phenological model of leaf development can be specified for any tree species comprising the overstorey layer. This is illustrated for three phenological model types in the supplementary material (Table S3). They include (i) a simple thermal time model (maritime pine), (ii) a parallel model combining simultaneously chilling and forcing temperatures (Douglas fir) and (iii) an alternating model assuming a negative exponential relationship between the sum of forcing units required for completing the quiescent phase and the sum of chilling units received (European beech). A single model is implemented to describe the phenology of the understorey vegetation. It includes a simple thermal time model for leaf unfolding with parameters that are identical for the three compartments, foliage, perennial part and roots (Table S5). The temperature used for accumulating degree-days is the air temperature for above-ground parts and the soil temperature at 0.1 m depth for the roots.

Senescence

The senescence of the different tree and understorey parts is modelled according to the organ-specific turn-over time and to the mortality induced by low temperature, soil moisture deficit or date respectively(Tables S4-S5). The timing of senescence is fixed for the cohort of coniferous needles. For broadleaf species it is a linear function of the sum of the mean daily shortwave radiation($= \frac{1}{24}\sum_0^{24} SW \downarrow$, in W m^{-2}) accumulated from the date of budburst until DOY=258 for European beech, Table S4), as fitted on data provided by the French ICP forest network (http://icp-forests.net/) from 14 beech stands where meteorological data were recorded (Le Bourgeois 2008). This accumulated radiation model explains 60$\%$ of the variance of the leaf senescence date across the data set explored; it compares well with other modelling attempts requiring more parameters and variables (Delpierre et al. 2009). The understorey senescence is triggered by low temperature, soil moisture deficit or date: beyond a fixed threshold, the understorey mortality is set at a fixed rate (Tables S1, S5). The separation of dead parts from the mother plant occurs as a single event either annually at the end of year for tree branches and roots or daily for the tree and understorey foliage. After separation, dead parts are immediately incorporated into the soil.

Mortality

Apart from the management operations (spacing, thinning, clear-cutting), the process of mortality of forest trees is diverse, complex and poorly understood and documented: it is therefore not mechanistically modelled in version 3.0 of GO+. Instead, at the end of each year, the carbon balance of each tree – the difference between its annual carbon assimilation, GPP_i, and its annual respiration, $Rm_i + Rg_i$ – is calculated. A "natural" tree death occurs when the carbon balance of a tree is negative, i.e., the net amount of carbon allocated for growth is negative. This is mainly provoked by combinations of strong soil water deficit, air water vapour deficit and high temperatures.

The understorey cannot "die" naturally but is maintained as a perennial carbon pool that can be regarded as a survival form (seeds, rhizomes, bulbs etc.). This allows regrowth of ground vegetation after clear-cutting. Following natural mortality, thinning or clear-cutting, the parts of harvested trees and understorey that are not exported are added to the soil pool. In particular, the part of the ground vegetation composing the understorey that is destroyed by forest operations such as soil preparation and possible disking prior to tree spacing or thinning interventions is added to the soil.

Tree regeneration

Such as mortality, tree reproduction and regeneration is not mechanistically depicted in GO+. Instead, following the clearcut of a tree stand, the stocking density of the next cohort of trees and the size distribution of young seedlings – or saplings – are specified. The stocking density may vary from few hundreds per hectare in coniferous tree plantations up to ten thousands per hectare in broadleaf standards with natural regeneration.

2.8 Soil carbon

The Roth-C v 6.3 model is implemented in GO+ with only a few modifications (Coleman and Jenkinson 1996). Only one soil layer is considered for soil carbon and the entire organic carbon stock of the soil is assumed to be included between the soil surface and the soil depth down a vertical profile modelled as exponentially decreasing with depth (Arrouays and Pelissier,1994). The inputs of organic matter to the soil are incorporated at the time of death — or harvest — when plants die, or at the time of separation from the mother plant for the senescing parts of foliage, branches, stems and roots. Mineralization and decomposition processes are discretized at an hourly time step and forced by the soil temperature at average depth where the respiration occurs,$T_{S,Rh}$ and soil moisture in layer A. The temperature at the average soil depth where the heterotrophic respiration occurs, $T_{S,Rh}$ is estimated using an empirical force-restore model depending on air and soil reference temperature as follows:

$$T_{S,Rh} = T_{S,Rh} + k_{Ta} \times (T_a - T_{S,Rh}) + k_{Tref} \times (T_{ref} - T_{S,Rh}) \tag{35}$$

The main adaptation introduced concerns the impact of forest operations on mineralization and decomposition rates as described in the next section.

2.9 Management: forest operations and harvesting, nutrient balances, wood products.

The management module of GO+ is separated from the core biophysical and biogeochemical modules. Management intervenes during the model execution as a suite of operations affecting processes involved in the soil carbon dynamics or affecting the understorey layer and tree stand. The forest management schemes are described as itineraries starting from regeneration and running until the next clear-cut thus covering the entire life cycle of the tree stand.Throughout the life of a stand, tree density is thus controlled by regeneration, climatic mortality and thinning and cutting. Two main management strategies are implemented in the GO+ 3.0 version, coppicing and regular stand. So far the former has been used only for eucalyptus whereas regular stand management is the main strategy used for pine, beech and oak species.The GO+ model may thus simulate the main management schemes used in monospecific even-aged forests, from short rotation eucalyptus coppice to stands of coniferous or broadleaved species, unmanaged old-growth forests (self-thinning) and agroforestry systems (coffee plantations). The model results can therefore be used for analysing the interactive effects of management and climate change on forest energy, water and carbon balances as well as commercial production. Further developments that will account for tree species mixture and irregular forests are ongoing but not yet implemented in version 3.0.

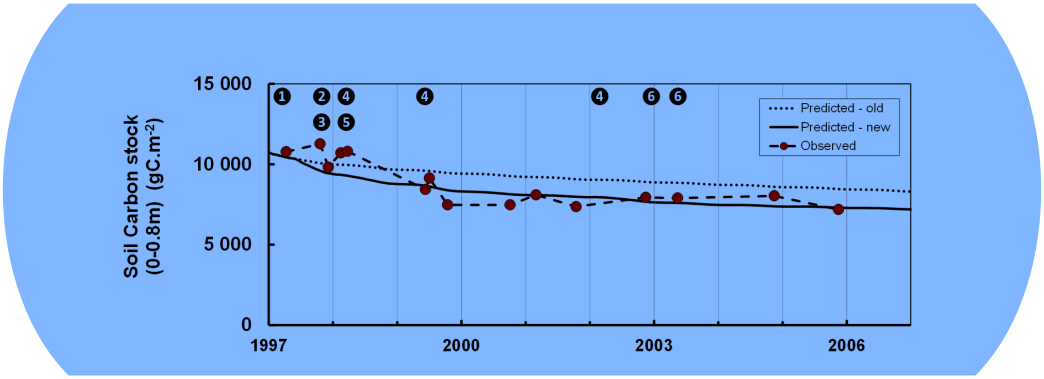

Figure 4. Changes in the soil organic carbon stock during the regeneration phase following a clear-cut of a maritime pine stand as simulated by the GO+ model with and without adaptation for soil preparation (full and dotted lines respectively) and measured in the field (grey dots). Data taken from Jolivet (2000). The numbers inset in black dots refer to the forest operation. 1: Clear-cutting and logging; 2: Heavy disking; 3: Stump removal; 4: Cover crop; 5: Tillage; 6: Vegetation crushing.

2.9.1 Soil preparation

Although Roth-C was initially calibrated for arable soils subject to periodic ploughing, it may underestimate the abrupt effect of ploughing on forest soils (Balesdent et al. 1998, Gottschalk et al., 2010). In managed forests, soil preparation may include techniques such as tillage, moulding and disking which may occur at only decade-long time intervals and therefore induces some drastic changes in the structure and microclimate of the upper soil horizons and organic layers. This may explain the effects of the preparation of forest soils on mineralization (Wang et al. 2018) and decomposition of the soil organic matter (Chen et al. 2004). In the GO+ model, we introduced a ploughing effect specifically for forest soils.. With this scheme the effects on the soil carbon of the preparation techniques such as ploughing, moulding and disking can be prescribed in the management module at any specific time during the rotation, e.g., after clear-cut, before every or specified spacing, thinning and clear-cutting operation or before regeneration. Immediately after any operation affecting the soil, the mineralization and decomposition rates of the soil carbon fraction affected are enhanced, this enhancement then decreases exponentially with time. Fig.4 shows the dataset taken from Jolivet (2000) which is used for calibrating the enhancement factor and its life half-life. The Table S1 provides the default values of the parameters. This approach is simple but easier to implement on multiple sites and spatial scales than the more mechanistic Gottschalk et al. (2010)'s which differentiates the ploughing effect according to the carbon pools described in Roth-C and to their linkage with the mineral fraction. We also evaluated the model on soil carbon data collected by Arrouays and Pelissier (1994). Those data provide a time series of soil carbon stocks following deforestation and continuous maize cropping in Les Landes forest in southwest France. The difference between the original version of Roth-C and the GO+ version is substantial, i.e., 5 to 12% of the total modelled soil carbon; this difference is maintained over time. The simulations output from the improved GO+ version are closer to the observations for both the short-term changes observed during soil preparation (stump removal, slash burial, vegetation crushing) (Fig.4) and long term soil carbon chronosequence following deforestation (data not shown, Arrouays and Pelissier, 1994).

2.9.2 Tree stand management

The tree stand management has a dramatic impact on forest ecosystems and their functioning. The model GO+ describes mechanistically the effects of the main management alternatives applied to even-aged monospecific forest stands that dominate European forests. To this end a large framework of forest operations is implemented in the model and can be assembled to construct different technical itineraries. The operations prescribed in a given itinerary are triggered according to forest management rules as follows.

- The stand regeneration can result from either natural processes, sowing or planting, the number of seedlings and their age and size distribution being flexible.

- The tree harvests are defined by the number and size of trees felled at each thinning and the final clear-cut. Successive spacings, coppicing, thinning and final clear-cutting occur either at given stand ages; they can be triggered by a competition index (Le Moguedec and Dhote 1992, Bellassen et al. 2010, 2011, Guillemot et al. 2014), or by target values of stand variables commonly used in forestry such as the mean tree diameter and height, stand basal area, or mean diameter and height of the 100 biggest trees per hectare at a given age. The selection of trees to be felled is flexible and can be either random, from the top, i.e., the bigger trees, or from below. A wide range of thinning strategies of varying complexity can thus be simulated by the model from the relative density index used for broadleaved species to the application of the "natural" self-thinning rule (Reineke, 1933).

- Specifying which tree parts are to be harvested may be any combination of stemwood, branches, foliage, stumps and roots. The harvest residues are input into the soil. GO+ predicts the size distribution of the stems harvested thus allowing raw wood products to be routed into life-cycle models, such as the C.A.T. model (Pichancourt et al. 2014), at large spatial scales.

- Coppicing is modelled as a clear-cut followed by the resprouting of a variable number of stems, which grow from the stumps left behind. The growth of the new stems is fed by a carbon pool that corresponds to the basal part of the stem having a diameter of 1.2 × D_{130} and a variable height (default value is 0.1 m) that is assumed to be residue. At this stage, the allocation of NPP to the above-ground part is increased until the root/shoot ratio is restored to its equilibrium value ($k_{\lambda 1}$, Eq. 29). This allows the stand LAI to increase rapidly after cutting, as is observed for coppices.

The Fig. 5 illustrates the impacts on the biomass and soil carbon stocks of typical management cycles implemented in GO+ and applied commonly in European forestry. The coniferous and broadleaf standards are managed according to "Long", "Short" and "Standard" rotations. The eucalyptus coppice includes one ("Long") or two ("Short" and "Standard") cuttings between each plantation, the"Short" option having a smaller diameter threshold for cutting than the "Standard"option. The levelling off of the beech biomass with stand age in the long, and to a lesser extent in the standard, options is mainly provoked by a decline

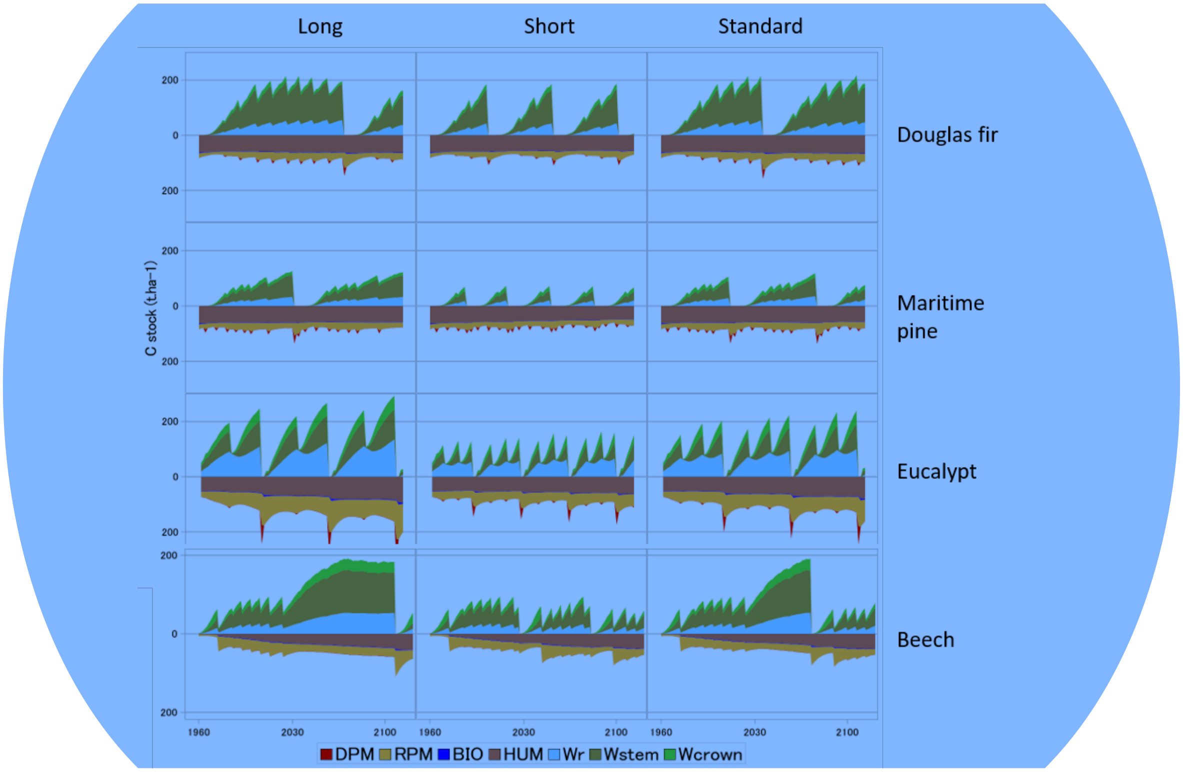

Figure 5. Biomass and soil carbon stocks simulated for four species and three management alternatives. The simulations were forced by the RCP 2.6 climate scenario. The grid point location is close to the centre of the French geographical distribution of each species. The pine and Douglas fir are grown in plantations managed with thinning rules and a final clear-cut based upon the mean stem diameter. Harvested parts are the stem only (Long) or crown and stem (Short and Standard). The eucalyptus is managed as coppice with two cuttings of sprouts before new planting. The stump age is used to trigger coppicing and final cut. The beech stand is managed according to the relative density index (Le Moguedec et Dhôte 1992). In the examples shown, the beech stand simulated was regenerated on a bare soil with low organic matter content and no understorey. In the legend, DPM, RPM, HUM and BIO are soil carbon pools of the decomposable, resistant , humidifed and biological parts respectively. W$_r$, W$_{stem}$ and W$_{crown}$ stand for the root, stem and branch+foliage carbon pools respectively. The soil fractions "BIO" and "DPM" have low values that are barely visible.

in NPP due to increased biomass respiration but also by a decrease in GPP. The predicted levelling-off of production is less marked or absent for other species and management options because the thinning regime prevents the tree stand biomass to saturate. Apart from the beech stand that was simulated on a bare soil, the soil carbon dynamics is mainly marked by the periodic massive input of resistant plant material leftover following harvest operations. The soil carbon dynamics contrast sharply with the forest management options for the eucalyptus coppice and much less for the other species.

An application of the model at the country level is illustrated by Fig. 6 where two afforestation scenarios, the "Short" and "Standard" alternatives, were run from 2006 to 2100 in dynamic mode under RCP 4.5, starting from cultivated soils with low

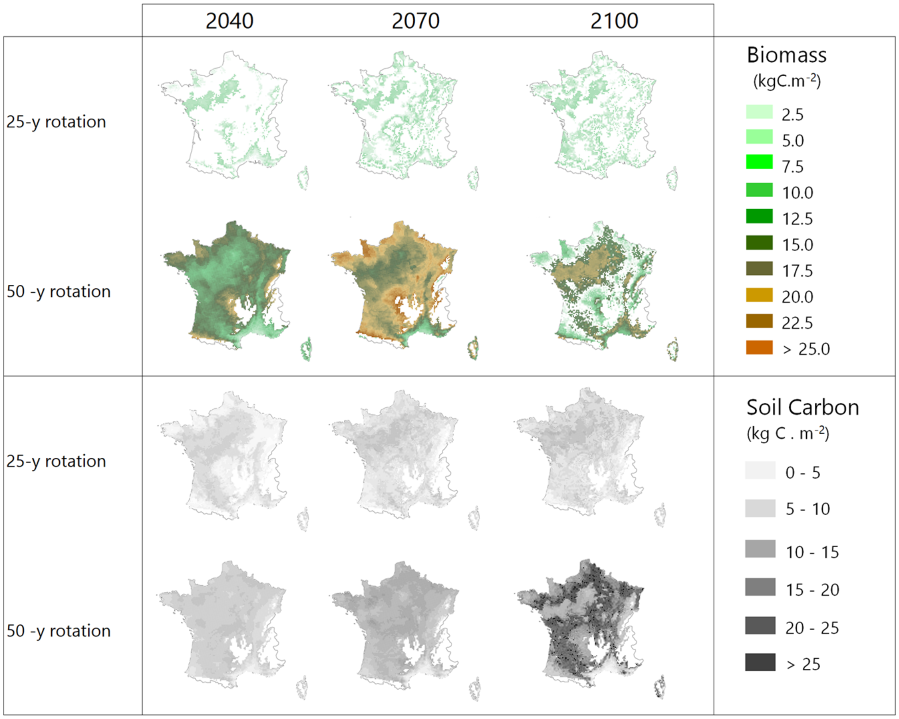

Figure 6. Biomass and soil carbon stocks of maritime pine stands simulated over the entire French metropolitan area for two management alternatives under climate scenario RCP 4.5. GO+ was run dynamically from 2006 to 2100 and initialised on bare soils with new stands in 2006, mimicking as the afforestation of cultivated soils.

organic content. The short rotation is cut at 25 years and includes deep ploughing and fertilisation, the Standard rotation is cut at 50 years and includes partial tillage. The simulation covers the whole French metropolitan area at 8x8 km resolution (9600 pixels) and is shown only as an illustration, all simulated pixels being afforested simultaneously.

2.9.3 Vegetation control

The vegetation management operations are described in terms of area affected and fraction of the understorey vegetation biomass destroyed. For releasing the trees from vegetation competition for light, water and nutrients, or during soil preparation a variable fraction of ground vegetation is affected and the corresponding fractions of the above-ground and below-ground understorey biomass are assumed to be destroyed and added to the soil carbon pool (Subedi et al. 2014). Prior to spacing, thinning or clear-cutting, a variable fraction of understorey biomass is also prescribed to be destroyed. For instance, in the pine forests of southwest Europe, rolling heavy disk trails is a common practice at plantation and before each thinning or clear-cutting. These disking operations are applied between rows of trees on three quarters of the soil surface area and affect typically 15% of the soil carbon. The model simulates this practice through the following:

- mortality of 75% of the above-ground biomass (foliage and perennial parts) and 50% of the below-ground biomass (roots) of understorey vegetation;

- as described previously in section 2.9.1, a three-fold increase in the mineralisation, decomposition and conversion-into-CO_2 parameters of the Roth-C model for 15% of the soil carbon with a half-life of 92 days.

2.9.4 Nutrient export

Achat et al. (2018) provide a detailed description of the nutrient module that was recently added to the core GO+ model in order to quantify the export of nutrients from the ecosystem through harvesting and soil preparation. This module evaluates the nutrient (N, P, K, Ca and Mg) stocks in standing tree biomass and soil. The nutrient outputs from these stocks through biomass harvesting can then be calculated. In short, this module calculates the main nutrient content of the soil, tree and understorey parts from literature values and combines them with predicted values of biomass and soil components.This calculation is based on allometric equations which account for the age and size of each tree part allowing the nutrient content of trees to vary with age and size. Realistic estimates of the nutrient exports related to forest practices can thus be produced under a range of climate-management combinations, as is illustrated by Achat et al. (2018). In their simulation, the harvested tree parts were allocated to size categories, allowing them to predict the nutrient balance of management schemes according to the harvest intensity.

3 Verification and parameterisation

3.1 Testing conservation principles

The verification tests consisted of checking the conservation of energy and mass of carbon and water for a long time series of model simulation. The period covered a typical forest stand rotation from the seedling stage to the final clear-cut; thinning and the impact of extreme natural events were included. We selected the Le Bray site to provide the benchmark data for the sensitivity analysis and evaluation of the model. The tree stand demography at this site was monitored from 1987 to 2008, with measurements of sensible heat, CO_2 and H_2O fluxes and meteorological variables starting in 1996. The period starts in 1984 and ends in 2010. It includes a series of dry years (1989–1991, 2002–2003, 2005–2007) and the December 1999 "Klaus" storm that fell or broke 22% of the trees. The model was run from 1984 to 2001 forced with meteorological data measured at the French synoptic network station being interpolated across the 8x8 km SAFRAN grid. The number and size of the trees thinned and felled for this period in 1991, 1996, 2001 and 2005 were also used to prescribe the thinned and windthrown trees. The verification test results are summarised in Table 2.

- The average hourly gap in the energy balance $R_n = H + LE + G$ was 8 Wm^{-2}, that is 9%. This gap results from the extension of neutral regime to stable and unstable conditions which results primarily in a slight underestimation of the convective heat fluxes, LE and H. The Nakai's model for estimating roughness length and displacement height leads to underestimate H for low value of Leaf Area Index that is below 1.5 m^{-2} m^{-2}.

Table 2. Verification tests operated on the model. The test is a simple conservation test applied to the annual values of energy, water and carbon fluxes over the 1984 to 2010 period.

Test	Input	Output					Balance (I-O)
Energy balance	Rn	H	λE	G			
(W m^{-2})	89	52	29	0.0			8
Water balance	$Rain$	E_{wet}	E_{dry}	$\Delta(\theta_{rootlayer} \times z_{root})$	D		
(kg H_2O m^{-2} yr^{-1})	960	249	422	3	291		5
Carbon balance	GPP	R_a	R_h	W_h	ΔW	ΔC_{soil}	
(gC m^{-2} yr^{-1})	2336	1401	664	148	64	65	-6

- For the water balance, we checked independently that the annual amount of precipitations from 1984 to 2010, $Rain$, was correctly allocated among (i) interception by the canopy and soil layers, E_{wet}, vegetation transpiration, E_{dry}, groundwater discharge or runoff, D, and the variation of the soil water stock over this period, $\Delta(\theta_{rootlayer} \times z_{root})$. The discrepancy found was 5 mm yr^{-1}over a total amount of 960 mm yr^{-1} that is 0.5%.

- The closure of the carbon balance was also satisfactory, the balance between the gross primary production and the sum of carbon stock changes in biomass and soil, harvested carbon plus the ecosystem respiration being less than 0.3%. The mean annual NEE over the period was 266 gC m^{-2} and is partitioned among three parts, the amount of carbon exported by harvesting, W_h and the net annual increments in biomass, ΔW, and soil organic carbon, ΔC_{soil}.

3.2 Parameterisation

The complete list of the parameters of the model is provided in the supplementary material Table S1 together with an appropriate reference. Most of the main parameters of the model have direct observational counterparts and their values were extracted from the literature or open data sources.

Soil.

The soil parameters of the GO+ model — as listed in Table S1 — are essentially functional and not descriptive. The rooting depth, z_{roots}, is the depth equivalent of the soil volume affected by the root water uptake. It should not be interpreted as the maximal depth at which roots can be observed — that can be substantially deeper. The parameters θ_{FC}, θ_{SAT}, θ_{WP}, have been estimated by pedotransfer functions from the kinetics of soil humidity retention curves collected over Europe and France (Wosten et al. 1999, Dobarco et al. 2019) . The parameters are dynamic and depend upon the organic matter content of the soil calculated at a daily resolution. The soil water potential ψ_{soil} (MPa) and hydraulic resistance, r_{soil} (Eq.19) are calculated from the soil texture and water content following Van Genuchten (1980) with soil texture - dependent parameters estimated using the approach developed in Ghanbarian-Alavijeh et al. (2019).

Initialisation of the soil carbon stock is prescribed by the user and may correspond either to observed values or to steady state values simulated by model spin-up. The organic layers above-ground, eventually including coarse woody debris, are conceptually included in the DPM and RPM fractions of the model. They are not separated from the mineral soil (layers A, B, C) for the calculations of energy and water exchange. Each type of plant material either foliage, branches, stem, roots, perennial part of the understorey etc. is characterised by a specific prescribed composition of decomposable and resistant plant material for each species considered.

Vegetation layers

The model parameters generally refer to the entire vegetation layer, i.e. to either the tree foliage, tree stems, understorey or soil layers. This is certainly the case for carbon metabolism parameters related to the vegetation respiration or photosynthesis. The main model assumption concerns the horizontal homogeneity of vegetation layers and implies within-population variations in canopy parameters are ignored. Ideally, the optical and radiative parameters of the canopy layers will have been estimated from data observed either at leaf or canopy levels, in situ or remotely (Hassika et al. 1997, Breda 2003). The stomatal conductance model is parameterised from measurements upscaled to the canopy level (Granier and Loustau 1994, Granier et al. 2000a, Rayment et al. 2000, 2002). The response functions have been thus parameterised based upon the data available from Granier and Loustau (1994), Granier and Breda (1996), Delzon and Loustau, (2005) and Granier et al. (2000a) for pine, oaks and beech respectively or Van Wijk et al. (2000) for Douglas fir, Medlyn et al. (2001) for the CO_2 response.

The bulk root-to-leaf tree hydraulic resistance is modelled empirically from literature data documenting combined measurements of transpiration or sap flow and soil and leaf water potential (e.g. Loustau et al. 1990, 1996, Delzon et al. 2003, Granier et al. 2000). The parameters used for describing the rainfall interception and its retention by the canopy layers were extracted from field data analysis (see discussion on parameters estimates in Muzylo et al. 2009). In the version 3.0 of the model, the value of the fraction of carbon allocated to growth is identical for all biomass parts and fixed at 0.28 (Penning de Vries, 1974). The phenology model of understorey vegetation is based on the understorey at Le Bray and other sites (Loustau and Cochard, 1991, Moreaux, 2012).

The allometric parameters used for allocating the net carbon produced to the different tree parts are derived from sets of allometric equations published in the literature and commonly available for the main commercial tree species. Most of them are robust enough to be applied to a range of soil, climate and management conditions (e.g., Gholz et al., 1979, Wutzler et al. 2007, Shaiek et al. 2011). The leaf area index is calculated from the total foliage biomass using the specific leaf area as follows;

$$LAI_T = W_{f,T} \times SLA_T \times \xi \tag{36}$$

$$LAI_U = W_{f,U} \times SLA_U \tag{37}$$

where ξ is the leaf area to LAI ratio.

4 Sensitivity and uncertainty assessments

We focused the sensitivity analysis presented below on the Le Bray site that was monitored from 1987 to 2010. It is a well-documented site and the data meet our objective, which was to verify the consistency of the model rather than to investigate geographical or climate variations of ecosystem functioning. A one-at-a-time (OAT) sensitivity test was carried out considering first the model parameters, and second the climate variables. This analysis aimed to: (i) check the consistency of the model behaviour in response to step changes in its main parameters and meteorological forcing variables; (ii) investigate possible interactions between the model sensitivity and climate; and (iii) compare the short-term to the long-term sensitivities of the model.

We used the time series of meteorological data interpolated across the SAFRAN grid from 1970 (planting) to 2010 (final cut) as well as the parameters related to soil characteristics and the forest tree stand (stocking density, soil preparation, understorey removal, thinning and harvest). The data used are available at the ISI-MIP project web site and the Fluxnet database (http://dx.doi.org/10.18140/FLX/1440163). We analysed the sensitivity at three temporal resolutions, hourly, annual and full rotation (40 years). The parameters' mean values, the meteorological and soil datasets as well as initial stand conditions were all taken from the European data cluster database (http://gaia.agraria.unitus.it/home). The sensitivity index of a given model variable Y to a parameter — or variable — k was calculated as its response to a step variation of k as:

$$I_k = \frac{Y(1.1 \times k_{ref}) - Y(0.9 \times k_{ref})}{2} \qquad (38)$$

where k_{ref} is the reference value for the parameter. All the other parameters are fixed at a nominal value (mean or final value). This index is the variation of Y in response to a 10% step change in k. To some extent, the I_k values are more meaningful than mean — or sigma — normalised indices, especially for variables that may take values close to zero such as, NEE. The relative values were also computed for easing the comparison between parameters across Figs. 7–9. The relative values

$$I_{k,rel} = \frac{I_k}{Y(k_{ref})}$$

were also computed for easing the comparison between parameters.

4.1 Sensitivity assessment: model parameters

The sensitivity analysis of model parameters was restricted to a subset of the 28 parameters with the aim of giving a general assessment of the model behaviour in response to its parameter variations. The parameters considered are distributed among six groups related to different processes or vegetation layers: structure and allometry, phenology, radiation transfer, soil parameters, tree physiological parameters and understorey physiological parameters. They cover, therefore, the main processes accounted for by the model: leaf unfolding, growth and senescence, radiation and energy balances, hydrology, photosynthesis, respiration, soil carbon balance, tree growth and production. The parameters are assumed independent, i.e. their effect on output variables is approximately additive. The effects of factor interactions on the output variance are neglected with OAT methods, which are therefore only applicable to strictly additive models (Campolongo and Saltelli, 1997). The Y output variables describe the energy balance, water and carbon cycles, carbon balance and tree canopy growth and structure, resulting in a total of 21 variables. The sensitivities of variables related to canopy growth and structure are shown only for the entire rotation. The hour and year sensitivities were calculated separately for a wet year and a dry year, 1994 and 2005, which received precipitation of 1271 and 681 mm, respectively. For each year, the same set of parameter values and the same initial soil and stand conditions were used. Since the hour and year sensitivities provided essentially the same sensitivity profile, only the year sensitivity is shown. The Figs. 7 –9 show the relative sensitivity index for selected parameters whereas the complete table of results are given in supplementary material Figs S1-S3.

Independent of the annual climate, the most influential groups of parameters were first the soil characteristics (the rooting depth and water contents at field capacity and at wilting point); second, the tree canopy physiological parameters and the specific leaf area of both tree and understorey foliage. The model parameters related to the radiation transfer, $\alpha_{soil}, k_{b,T}, k_{d,T}, \rho_{T,f}$, and phenology, BB_T and GD_U had a lesser influence. The relative sensitivity of output variables increased according to their position in the process chain, the sensitivity of end variables, e.g., NEE, being the largest and reaching 14 and 45% for the 1994 (wet) and 2005 (dry) year, respectively. The higher sensitivity of NEE is because its sensitivity accumulates the impacts of parameter changes on the canopy photosynthesis GPP , and autotrophic respiration,R_a. Conversely, the energy balance and water balance components, Rn, H, λE and runoff, D, exhibited a low relative sensitivity, their relative change being close from 0.04 and exceeding 0.10 only for the soil water content at field capacity, θ_{FC}, that has enhanced the soil water storage and mitigated the water stress impact. Comparatively, the model outputs were more dramatically affected by the changes in the wilting point θ_{WP} because of its larger impact on the soil pressure head, water potential and hydraulic resistance and in turn on leaf water potential (Eq. 21), canopy stomatal conductance (Eq. 13), photosynthesis (Fig. 2), stress index and allocation (Eq. 29, see also Table S5 the impact on understorey). The sensitivity of the carbon balance components was distributed more evenly among the parameter groups. Comparing the sensitivity of the variables groups between 1994 and 2005 revealed also differences that can be related to the contrasting amount of precipitations and related impacts on soil moisture deficit and plant water stress. The absolute sensitivity was higher for the wet year 1994 because the absolute annual values of most variables were higher for this year. Apart from the respiration components R_a, R_{ECO} and R_h, the relative sensitivity of output variables almost doubled in 2005. We observed a shift of the sensitivity of the carbon balance components NEE, GPP and NPP to the photosynthetic quantum efficiency, α_T and carboxylation efficiency, V_{cmax}, that was prominent in 1994(wet year) and minor in 2005 (dry year). The opposite was observed in 2005 for the soil water content at wilting point whose sensitivity increased from $14.4, 3.4$ and 6.2% in 1994 to $45.5, 8.6$ and 13.7%.

The pattern of the long-term sensitivity evaluated from 1970 to 2010 is shown in Fig. 8 for the "flux" variables and Fig. 9 for the tree growth and "stock" variables. The main features previously shown on annual values were confirmed except that the impacts of the tree foliage SLA and diffuse light attenuation coefficient k_d were enhanced whereas the understorey related parameters had less influence. The sensitivity of the biomass and soil carbon stocks, W and C_{soil}, mean stem diameter and height reached in 2010, D_{130}, H_c and cumulated harvestable production $W_{h,stem}$ was consistent with the patterns observed previously on fluxes. The commercial production was the most sensitive to the model parameters SLA, θ_{WP} and to the allometric parameters, $k_{D_{130}1}$, $k_{Istress1}$ and $k_{stem,1}$.

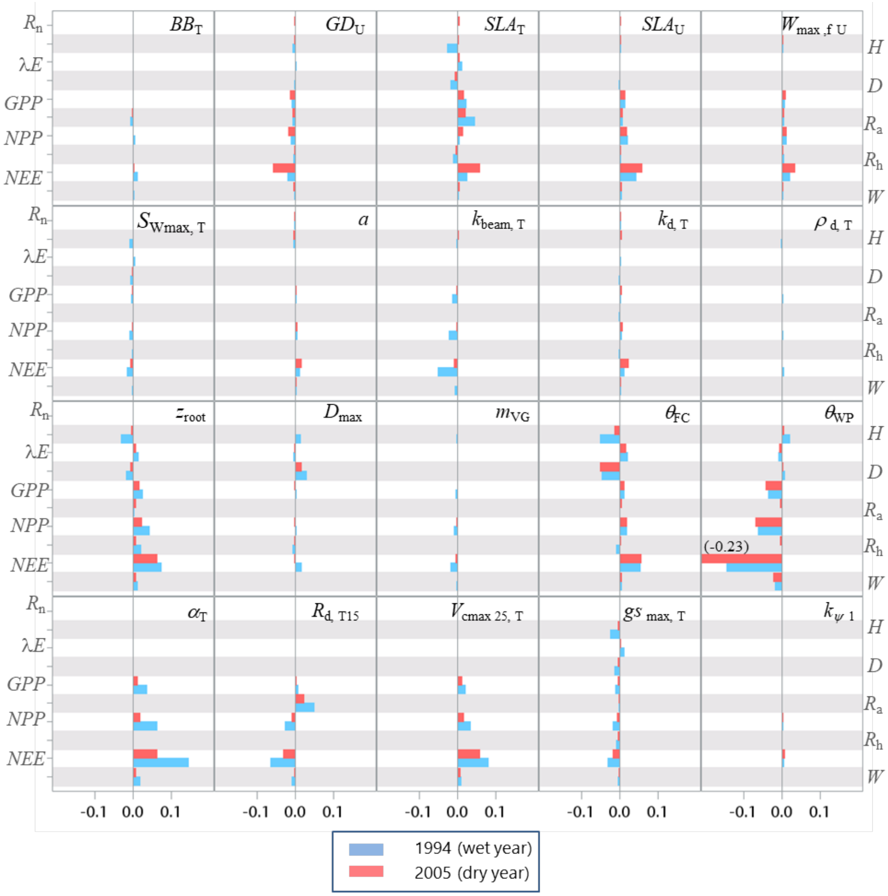

Figure 7. Relative sensitivity index values of the main variables related to the energy, water and carbon fluxes to model parameters for the years 1994 (wet, in blue) and 2005 (dry, in red) at the Le Bray site. The abbreviations of the variables (vertical axes) are explained in the Table A1 and the parameters abbreviations (inset) are detailed in Table S1. The horizontal bars in each box gives the relative sensitivity of 10 variables listed along the y axis to the parameters named in the box. A positive value means that the output variable increased in response to an increase in the parameter value.

4.2 Sensitivity assessment: meteorological variables

The model behaviour in response to variations in meteorological variables was analysed following a similar approach. We considered the following variables: air temperature, atmospheric pressure, precipitation, mean horizontal wind speed, downward shortwave and longwave atmospheric radiation, ambient CO_2 concentration and water vapour pressure saturation deficit, and the fraction of diffuse radiation. The air temperature and air vapour saturation deficit were changed by $\pm 1^{o}$C and ± 200 Pa, respectively, and other variables were changed by $\pm 10\%$. The results are presented in Fig. 10 for the annual sensitivity and in the supplementary material (Fig. S4) for the long-term sensitivity. The main conclusions are summarised below. The model overall behaviour was consistent with the current knowledge about canopy responses to climate for the ecosystem considered:

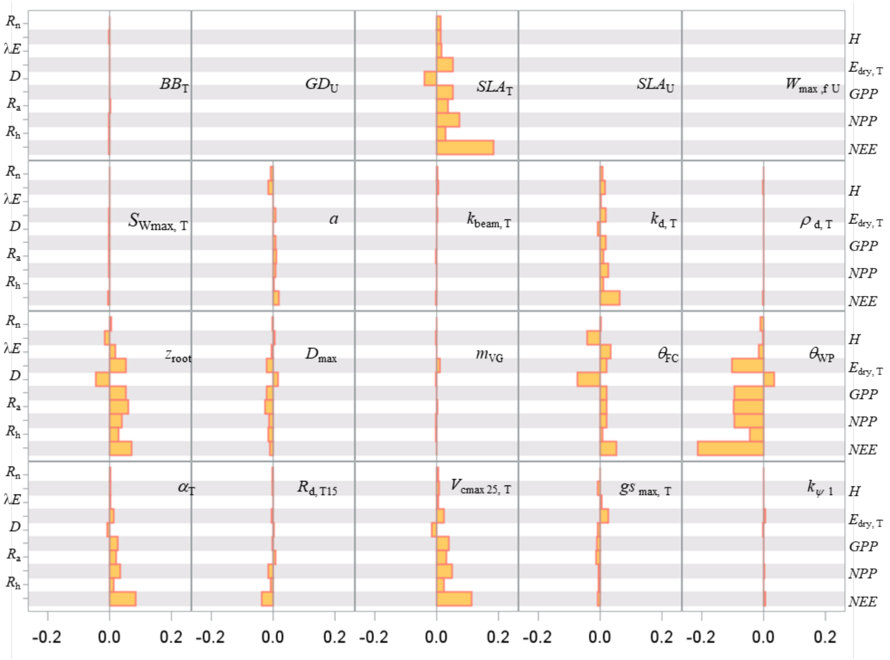

Figure 8. Sensitivity index values of the main variables related to the energy, water and carbon fluxes to model parameters over a full rotation (1970-2010) at the Le Bray site. The abbreviations of the variables (vertical axes) are explained in the Table A1 and parameters abbreviations (inset) are detailed in Table S1.

a temperate Atlantic coniferous ecosystem growing on a well drained sandy soil for the present case (Granier and Loustau 1994, Medlyn et al., 2001, 2002, 2003, Davi et al. 2006, Moreaux et al. 2011, 2020). On an annual basis, the energy balance components, $Rn, H, \lambda E$, were mainly affected by incident radiation, $LW\downarrow$ and $SW\downarrow$ and T_{air} whereas the carbon balance variables, GPP, R_a, NPP, R_h and NEE were more sensitive to $\mathrm{CO_2}$, f_{dif} and precipitations $Rain$. The negative response of the sensible heat flux H to the air temperature was essentially due to the asymmetric response of H with respect to the sign of $T_s - T_{air}$ that was amplified when $T_s - T_{air}$ was negative. Changes in the air temperature and water vapour saturation deficit had a negative effect on all variables except the latent heat flux and respiration for the air temperature. It is worth noting that the effects of $\mathrm{CO_2}$ and f_{dif} were first to impact GPP, then to affect NPP $(= GPP - R_a)$, and last NEE $(= NPP - R_h)$. The air temperature and incident long-wave radiation also had significant impacts on the respiration terms R_a and R_h. The weak response of the carbon processes to a 10% change in $SW\downarrow$ has also been observed, e.g. by Delpierre et al. (2012) under temperate climate was not unexpected since the light is not limiting at this site. The main contrast between the 1994 and 2005 climates was observed on NEE and H, the sensitivity of the former being enhanced in 2005 while H was conversely more sensitive in 1994 . The full rotation sensitivity profile of the "flux" variables (Fig. S4) was identical to the annual sensitivity profile, apart from the biomass and soil respiration, R_a and R_h, and consequently NEE. In particular, the sensitivity of R_a to the air temperature and longwave incident radiation was positive on an annual basis, as expected from Eqs. 24–26 but became

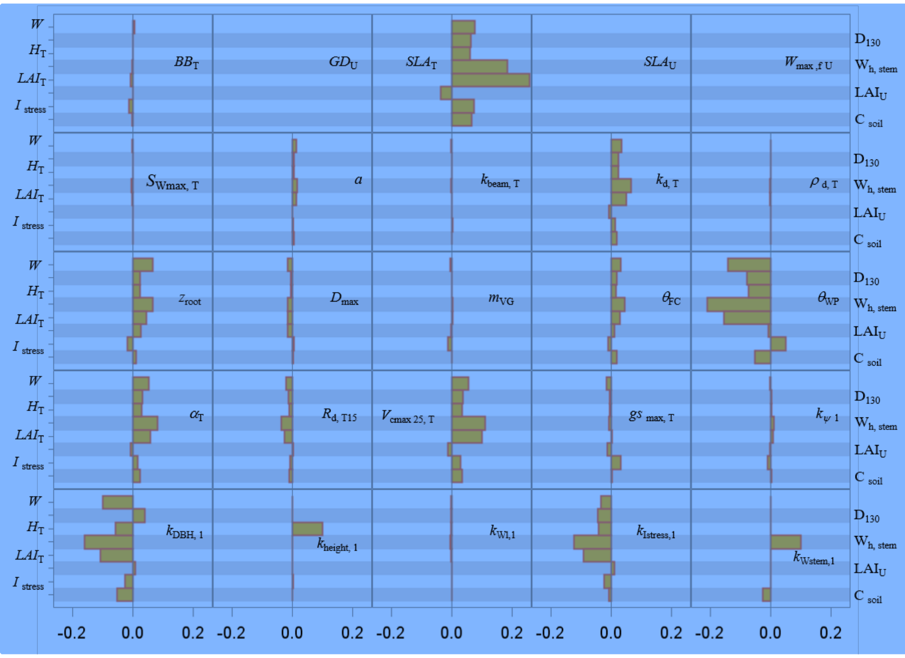

Figure 9. Sensitivity index values of the main variables related to the carbon stocks in biomass and soil to model parameters over a full rotation (1970-2010) at the Le Bray site. The abbreviations of the variables (vertical axes) are explained in the Table A1 and parameters abbreviations (inset) are detailed in Table S1.

negative over the long rotation. This reversal is induced the long term impacts of atmospheric and soil droughts correlated with the temperature step increase as shown by the enhancement of the stress index in response to temperature (Fig. S5). The temperature step–increase depleted the biomass growth, W, and in turn photosynthesis GPP and respiration R_a. The same response is shown to the long wave radiation $LW\downarrow$ that increased the water stress index I_{stress} on the long term.

4.3 Uncertainty assessment

For assessing the uncertainty of the main variables simulated by GO+, we used a simple Monte Carlo approach where 2500 sets of parameter values were randomly drawn from their distribution range. For each set, the model was run for the year 1994 at Le Bray. Based upon the previous sensitivity analysis, we retained the 14 most sensitive parameters for assessing how errors in parameter values are projected on GO+ output variables. The parameters selected were assumed independent. We are aware this assumption may not hold for biological and physiological parameters but we lack of quantitative relationships that would allow us to link them and define a more sound sampling design. The probability distribution assigned to each parameter was by default a normal distribution function whose standard deviation was derived from literature, unpublished field observations or, when lacking, fixed empirically (Table 3). The resulting distributions are shown in Figs. 11- 12 for the ecosystem variable values.

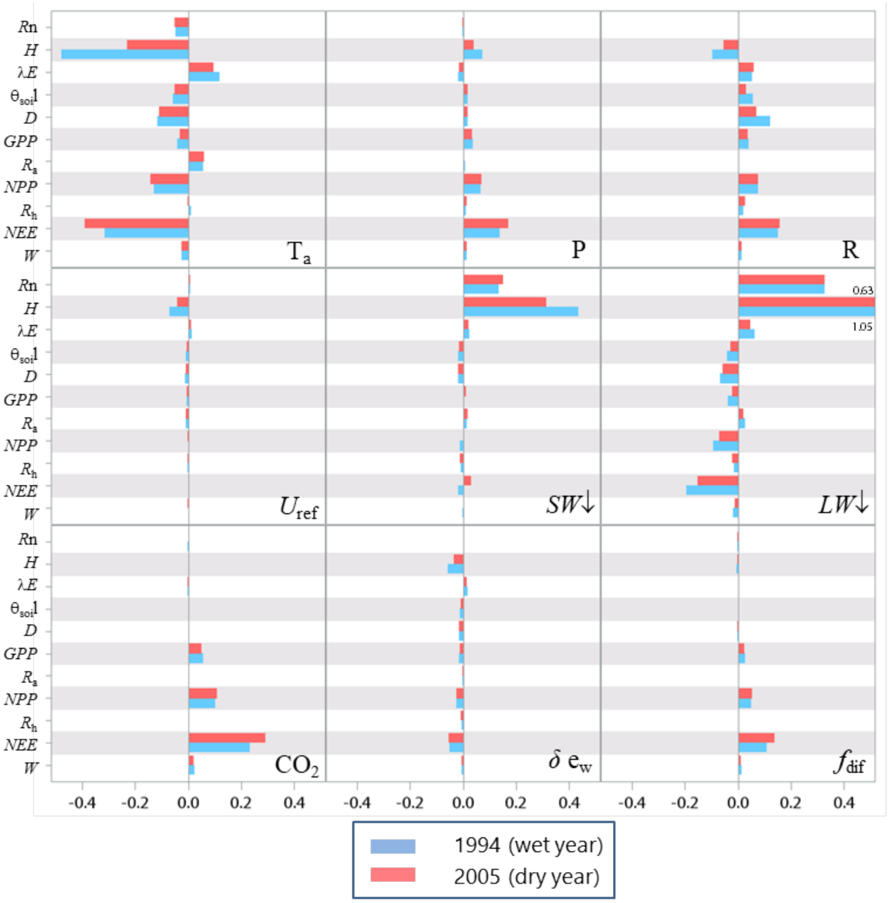

Figure 10. Relative sensitivity of the main variables related to fluxes of energy, water and carbon to meteorological variables for a wet (1994) and dry year (2005) at the Le Bray site . The definition of the variables is provided in the Tables 1 and A1.

The output variables were standardised to their mean value in order to compare the uncertainties among variables and vegetation layers. Only the ecosystem variables are shown, the uncertainty in variables referring to canopy and soil layers are reported in the supplementary material (Figs. S6-S8).The uncertainty range of the energy balance components and ecosystem shortwave albedo was relatively small. It was highest for sensible heat flux, H , and lowest for the net radiation, Rn. This was attributed to the relative accuracy of the attenuation coefficients in direct and diffuse light that were both measured at this site (Berbigier and Bonnefond, 1995), and the fact that the uncertainty of the longwave emissivity was not considered. In addition, compensation effects between canopy layers and soil might have reduced the range of simulated net radiation. Compensation between layers may also explain the relative precision of the model on the ecosystem albedo because any error on the radiation transfer through the upper canopy will mechanistically induce an opposite change in the understorey balance. Indeed, the error generated on the energy balance components of the vegetation canopy was higher for the understorey and the soil; these were poorly constrained as compared to the tree and ecosystem energy balance. The uncertainty on carbon flux variables was higher

Table 3. List of the parameters used for uncertainty propagation in the GO+ model, their reference value and standard deviation.

Parameter	Symbol	Reference value	Standard deviation	Unit
Tree SLA	SLA_T	6.5	0.50	m^2kg dm^{-1}
Understorey SLA	SLA_U	20	1.5	m^2kg dm^{-1}
Heat sum for the tree foliage bud burst	BB	1400	50	^oCday
Growth duration of understorey foliage	$GD_{U,f}$	130	15	day
Maximal understorey foliage biomass	$W_{max,f}$	0.25	0.03	kg dm m^{-2}
Canopy extinction coefficient for a beam normal to the surface	$k_{bh,T}$	0.33	0.02	
Canopy extinction coefficient for diffuse SW radiation	$k_{b,T}$	0.467	0.03	
Rooting depth	z_{root}	0.7	0.1	m
Maximal drainage rate	D_{max}	2.5	0.25	kg H_2Om^{-2} hr^{-1}
Van Genuchten m	m_{VG}	0.75	0.08	
Water content at field capacity	θ_{FC}	205	10	kg H_2O m^{-3} soil
Water content at wilting point	θ_{WP}	65	5	kg H_2O m^{-3} soil
Quantum efficiency	α_T	0.14	0.02	mol e^-mol^{-1}photons
Foliage mitochondrial respiration at 25^{o}C	$R_{d,T}$	8.0E-7	1.0E-7	mol $CO_2m^{-2}s^{-1}$
Maximal carboxylation rate at 25^{o}C	$V_{cmax,T}$	45.0E-6	7.5E-6	mol CO_2 $m^{-2}s^{-1}$
Canopy water storage capacity	$S_{wmax,T}$	0.25	0.03	kg H_2O m^{-2} soil
Maximal stomatal conductance	$g_{smax,T}$	4.24E-3	3.5E-4	m s^{-1}

than that for the energy balance, especially the net ecosystem exchange, NEE, that accumulated the errors generated on both the gross primary production, GPP, and the autotrophic, R_a , and heterotrophic, R_h , respiration components. Our experiment might have exaggerated the error on NEE and NPP since the values of photosynthetic and respiration parameters were drawn independently ignoring the functional link between photosynthesis and respiration. Nevertheless, this relatively large error on NEE will limit the use of its observational counterpart for evaluating the model.

The uncertainty in the annual variation in soil carbon stocks showed contrasting patterns depending on the components considered. The high accuracy on RPM and DPM were to some extent artefacts since the litter biomass was prescribed so that the only error source was caused by the mineralization and humidification processes. Conversely, the HUM component showed very large uncertainty which was attributed mainly to the fact that uncertainty was related to the stock change that was very small over a year. Overall, the annual change in soil carbon stock was constrained with a standard deviation of 15%. The

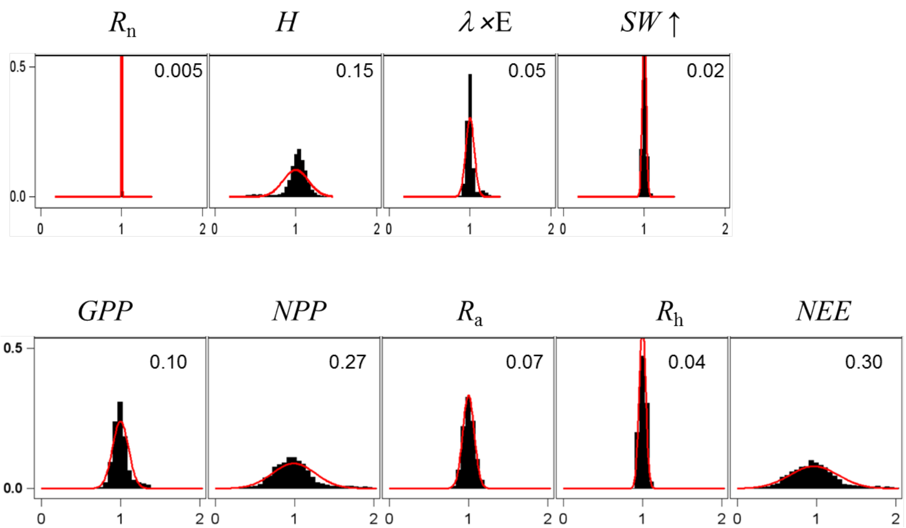

Figure 11. Normalised uncertainty on the annual mean values of flux variables predicted by the GO+ model. Each graph shows the distribution of variable values generated from 14 parameter distributions (Table 3). Red curve is the normal distribution fitted and number inset is the standard deviation. The variables abbreviation is explained in Table A1.

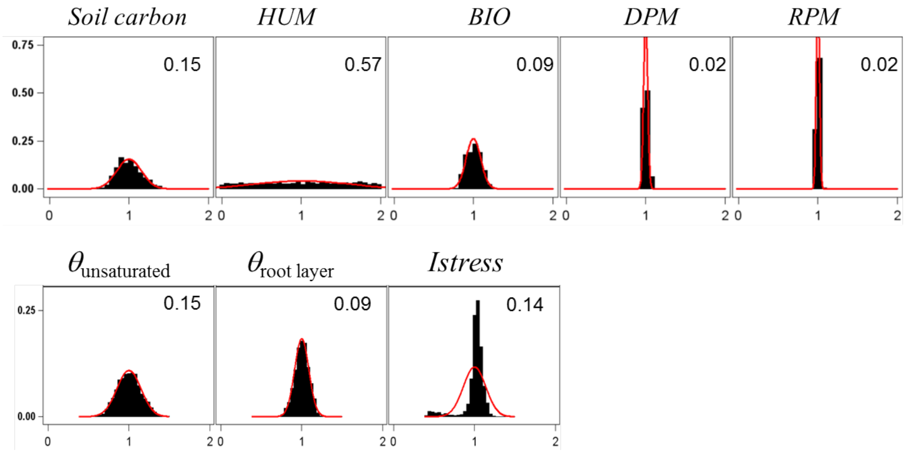

Figure 12. Normalised uncertainty on the main soil variables simulated by the GO+ model. Each graph shows the distribution of variable values generated from 14 parameter distributions (Table 3). The red curve is the normal distribution fitted and the numbers inset is the standard deviation. The variable abbreviations is explained in Table A1.

same magnitude was found for the annual change in the soil water content of the unsaturated layer, whereas the annual change in the total amount of water in the rooted zone was estimated with a precision of 9%. The annual changes in biomass and its components were not well constrained, its standard deviation exceeding 0.3 in the tree layer and 0.5 in the understorey (Fig. S8). This was not unexpected because the net biomass change is the end result of the whole chain of processes described in the model (phenology, radiation transfer, energy balance and evaporation, photosynthesis, respiration and allocation, and growth), and this chain accumulates their related errors. In addition, the assumption that the parameters are independent might have inflated the uncertainty in biomass changes.

5 Comparison with observed data

Because GO+ encompasses full rotation duration, we were able to test the model against long time series of fluxes and stocks at both daily and annual resolution (Thum et al. 2017). To this end, two types of data were used and the model performance was assessed through two comparisons. First, is a comparison of hourly values of flux data between observed and predicted values. The second uses annual values of stand growth data. The statistics used are the root mean square error between observations and simulated values, RMSE, the variance fraction explained by the model, R^2 , and the systematic and unsystematic model errors which assess the bias and precision of the model respectively (Wallach and Goffinet, 1989).

5.1 Data

The time series of daily values of energy water and carbon dioxide fluxes, i.e. net radiation, Rn, latent heat flux, λE, and net $\mathrm{CO_2}$ fluxes, NEE, used in experiment 1) and 3) were obtained from tower stations and taken from the European fluxes database cluster and the Fluxnet Database (URL: http://fluxnet.fluxdata.org) for Douglas-fir sites. The variables used are determined from site measurements of $SW\uparrow, SW\downarrow$ and $LW\uparrow, LW\downarrow$, vertical fluctuations of wind speed, U, and fluctuations of CO_2 and water vapour concentrations. The values are further processed for quality checking, filtering and gap filling. Unless mentioned, they are all Level-3 type for Rn and Level-4 type for λE and NEE. The Level-3 data are standard files provided by stations. The Level-4 data are filtered, gap-filled using the Marginal Distribution Sampling method (Papale et al. 2006, Moffat et al. 2007) and aggregated at different time resolutions, from half-hourly to yearly. Other variables commonly used for model testing such as ecosystem GPP, RE or NPP are derived indirectly from primary measurements. They were, therefore, not used in the model evaluation because that would have introduced redundancy with the test on NEE. Table 4 presents the datasets used and their origin. Seven stations were selected because they cover a large part of the geographical range of three important European commercial tree species and also embrace a wide range of tree stand age.

The data used in experiment 2) is a set of 11 long-term records of stand growth that were mostly taken from the Profound project database (Reyer et al. 2019). The site characteristics and data sources are detailed in the Table S6. In this evaluation, the model performance was assessed using the annual series of stem diameter at 1.3 m height (D_{130}) and basal area (BA) of the tree stands. Three common commercial species are represented: maritime pine, European beech and Douglas fir at different locations across Europe and British Columbia. Various tree ages and thinning regimes are used. We compared the annual change of the stem mean diameter, ΔD_{130} (cm $\mathrm{yr^{-1}}$), and basal area, ΔBA ($\mathrm{m^2\ ha^{-1}\ yr^{-1}}$), that is the cross sectional area of tree stems at 1.3 m height over one hectare. The later can be taken as a proxy for the carbon storage in biomass for which no direct measurement method exists. Moreover, compared to flux values determined from turbulent variables, the stem diameter

Table 4. Characteristics of the sites selected for long term series of daily fluxes of net radiation, latent heat and $\mathrm{CO_2}$.

Site name (Fluxnet code)	Lat / Lon (°)	Annual T (°C) Precip.(mm $\mathrm{yr^{-1}}$)	Main species	Tree age (yr)	Period	Source
BC-Campbell 49	49.86 / -125.33	8.4 / 1245	Douglas fir	51	2000–2010	(1)
BC-Campbell 88	49.50 / -124.90	9.6 / 1546	Douglas fir	14	2002–2008	(2)
Hesse (FR-Hes)	48.67/7.07	9.2 / 820	European beech	33	1996–2010	(3)
Soroe (DK-Sor)	55.49/11.6	8.2 / 660	European beech	88	1998–2012	(4)
Collelongo (IT-Col)	41.85/13.59	6.3 / 1180	European beech	130	1997–2014	(5)
Le Bray (FR-LBr)	44.71 / -0.77	13.5/ 930	maritime pine	26	1996–2008	(6)

1-2. Fluxnet,Humphreys et al. (2006)
3.European database, Granier et al. (2000b)
4.European database, Pilegaard et al. (2011)
5.European database, Scartazza et al. (2013)
6.European database, Berbigier et al. (2002)

Table 5. Statistics of the model evaluation with daily flux values of net radiation, R_n, latent heat flux, λE, and net ecosystem exchnage, NEE, at 6 sites: R^2 and RMSE.The daily average of the observed (O) and predicted values (P) is given.

	Rn (Watts $\mathrm{m^{-2}}$)				λE (Watts $\mathrm{m^{-2}}$)				NEE (gC day $^{-1}$ $\mathrm{m^{-2}}$)			
	O	P	R^2	RMSE	O	P	R^2	RMSE	O	P	R^2	RMSE
BC Campbell 49	75.7	71.9	0.97	15.7	32.0	40.3	0.76	13.9	-0.05	-0.10	0.67	1.7
BC Campbell 88	66.4	64.3	0.95	15.6	30.5	33.0	0.67	13.3	-0.58	-1.81	0.25	1.8
Collelongo	96.0	70.5	0.60	54.8	29.9	46.1	0.41	41.7	-2.2	-2.33	0.30	5.5
Hesse	68.8	72.1	0.75	41.4	25.5	36.2	0.70	28.2	-1.15	-0.89	0.56	3.0
Soroe	99.9	110.6	0.59	58.0	33.2	23.3	0.65	56.8	-0.45	-1.2	0.51	4.0
Le Bray	86.7	93.6	0.61	44.3	48.1	50.2	0.26	23.0	-1.00	-1.38	0.22	2.9

and basal area are measured with a low uncertainty (1–5% error) and cover a wide range of climatic, soil and management conditions. [t]

5.2 Results

To assess the overall performance of the model, we need to relate the RMSE and its systematic and unsystematic components (Table 5) to the model uncertainty in Rn, λE and NEE. The model errors were larger than the respective uncertainty of the three variables calculated in the previous section. Indeed, our uncertainty analysis used parameter values that had been obtained from local measurements — no site calibration was carried out in this comparison, i.e., a single set of parameters was applied

Table 6. Statistics of the model evaluation with daily flux values at 6 sites: systematic and unsystematic errors.

	Rn		λE		NEE	
	W m^{-2}		W m^{-2}		gC d $^{-1}m^{-2}$	
	s	u	s	u	s	u
BC Campbell 49	3.8	13.1	8.5	13.5	1.2	1.7
BC Campbell 88	2.8	15.6	6.2	13.3	1.6	1.8
Collelongo	13.3	53.1	8.4	41.7	0.7	5.5
Hesse	3.3	36.4	17.0	28.2	0.2	2.9
Soroe	12.6	55.4.	43.3	56.8	1.8	4.0
Le Bray	18.0	41.0	22.1	23.0	0.6	2.9

s: systematic error; u: unsystematic error;

to every species, ignoring the acclimation and plasticity of most vegetation traits (Bloomfield et al. 2018). It shows that the model itself introduces a substantial epistemic error in addition to the uncertainty linked to the parameter values. The model error was smallest for Rn and largest for H (not shown), λE and NEE. The error on H may be due to the model making the approximation that the aerodynamic resistance to heat transfer can ignore stability corrections. The NEE predictions might be affected by the simplifications made to the timing of secondary and primary growth of trees and related respiration. In addition, the model represents the source/sink activity and not the transport of water, or $\mathrm{CO_2}$ to the reference level. Such a transfer is included in the flux values measured at ecosystem stations and adds a substantial random noise to flux values. Testing the model predictions against observed values at increasing time integrals from an hour to 365 days, we observed that the variance fraction of Rn , $NEE$and E explained by the model increased with the time span until the (90–day) season-length and then drops at longer time spans (Table S7).

The sources of error are multiple and it should be noted that the data themselves are subject to measurement and calculation errors currently assumed to lie within 10–15% of the daily values used. The meteorological data used may also be a source of errors, i.e., at Le Bray where they were interpolated from the main French national meteorological network. Second, the fact that long time series of variables were used for this evaluation exercise makes the model results affected not only by possible errors and approximations in processes directly involved in the energy balance and carbon cycle, but also by possible faults affecting the processes describing the vegetation dynamics, i.e., phenology, carbon allocation, tree growth, mortality, forest operations or soil carbon. For this evaluation, the model was run actually from the start to the end of the decadal time series without recalibration. This is in particular the case of the Le Bray site where simulations were initiated in 1984 and run until 2000.

The evaluation of the model by comparing its output with long term inventory records reveals that the predictions are relatively close to the observed values, both in terms of accuracy and precision (Fig. 13). Since only few data were available from inventories, we pooled together in this figure the results of the 11 sites analysed. The data observed are prone to smaller errors (typically 5%) than the previous flux data but the information about the station characteristics and meteorological data used for modelling is more uncertain. This uncertainty is because reliable series of meteorological data, i.e., measured on site, are not available and the information on soil characteristics can be poor. In addition and apart from the Le Bray site, we had only vague information about the criteria used to select which trees are thinned. We used the annual increment rather than the annual raw values of D_{130} and BA because the latter are actually cumulative variables including large temporal autocorrelation. The predicted ΔBA were close to the observed ones in general, with most values being positive but close to zero. Interestingly, the model accuracy was mainly constant along all values ranging from -7 to +5 m^{-2} ha^{-1} yr^{-1} . The predicted ΔD_{130} was satisfactorily simulated by GO+. Given these uncertainties and the fact that no site-specific calibration of parameters was used, the evaluation test shows that the model departs only slightly from measurements on average, with relatively small biases. Its performance was similar across sites despite the range of species, age, management and location covered by the data set.

An interesting product of the Go+ model is its evaluation based upon simultaneous values observed and predicted of several variables over decades-long time series. To our knowledge few models have been tested using long-term sets of multiple variables. Figure 14 shows an example for the Collelongo broadleaf forest, Vancouver Island Douglas Fir stand and the Le Bray coniferous forest. In Collelongo and Le Bray, 20– and 25–year long inventories of tree diameters were available, respectively. A series of soil water stock — or groundwater level — and flux measurements were also available in the three sites. The comparison shows that the long-term trajectory of energy, water and carbon fluxes as well as soil water, tree growth and LAI were captured without significant bias by the model for a period marked by severe droughts (2002 and 2005), a heatwave (2003), several thinnings (1992, 1997, 2005 at Le Bray) and storm damage (at Le Bray 20% of trees suffered windthrow in December 1999). Some inconsistencies are also evident, such as the overestimation of respiration and primary production at Collelongo, that may be related to LAI overestimation. The behaviour of the soil moisture predicted at the Douglas Fir site is also challenged by the observations when soil becomes close from saturation. Because we did not calibrate the parameters for every site, these discrepancies are mainly caused by errors in the values of influential parameters such as the soil depth and hydraulic parameters, the leaf mass-to-area ratio or the root-shoot ratio. The comparison of multiple variables between observed and predicted values also reveals that the performance of the model was clearly affected by the quality of observed flux data. At Le Bray, the flux values were more scattered after 2003 due to a change in instrumentation (closed-path analyser until 2003; open-path from 2004 onward) and related quality assessment criteria: the R^2 of the predicted versus observed values of NEE was 0.36 for the period 1997–2003 but dropped to 0.22 when calculated for the entire period 1997–2008. Testing the model against data of different quality levels also produced substantial differences, up to 0.15, in the calculated value of R^2.

6 Discussion

Essentially, the GO+ model brings together robust representations of canopy and carbon cycle processes that can be evaluated straightforwardly against observed data. From a biogeochemical point of view it offers three main innovations: (i) GO+ explicitly links the stomatal functioning of the tree canopy to the leaf water potential and plant hydraulics; (ii) it allows us to connect

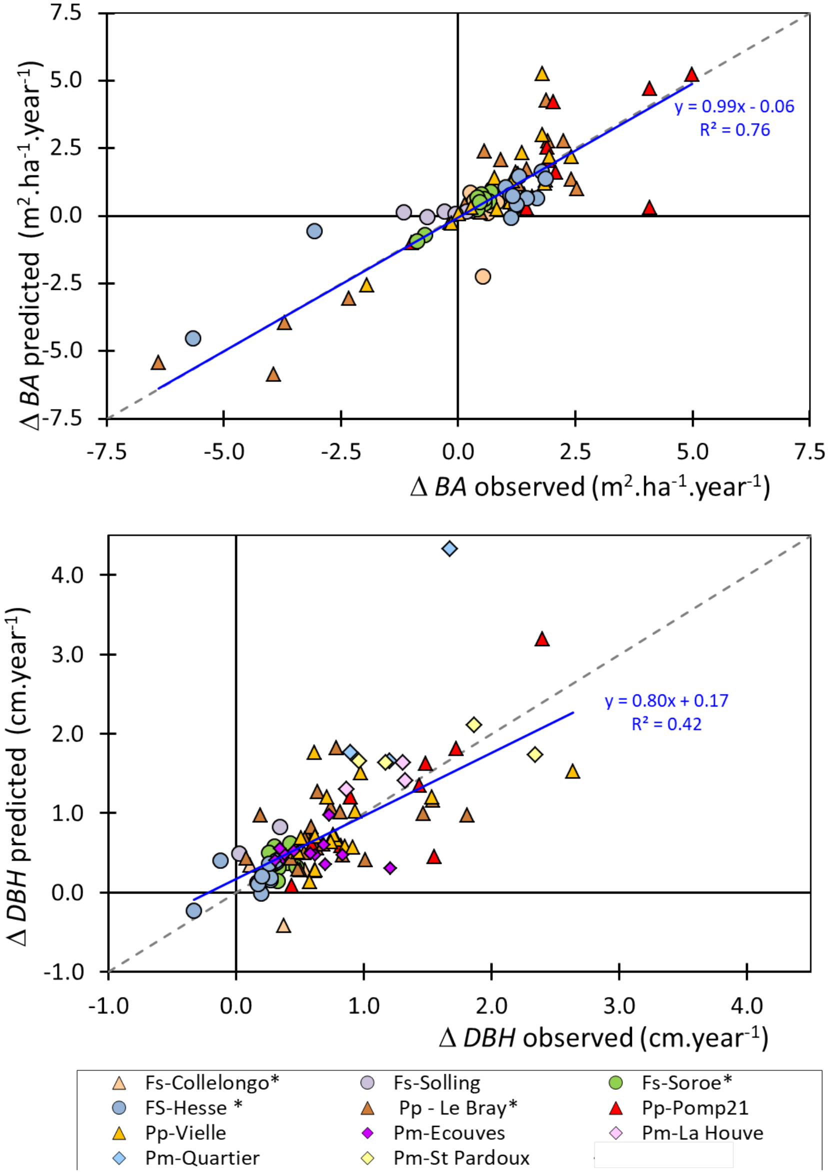

Figure 13. Predicted versus observed values of annual increment in basal area, ΔBA, upper diagram, and stem mean diameter, ΔD_{130} (lower diagram) for sites described in Table S6 of the supplementary material. The sites used for both flux and inventory data are annotated with a star (*). The 1:1 line (dashed line) and linear regression (blue) are shown.

fast biophysical and biogeochemical processes to slower plant growth and soil carbon transformation processes; and (iii) provides for a range of options in specifying management operations and harvest exportation for monospecific forest stands. In this section, we first discuss these three points and further model specificities. We then return to a discussion of model performance.

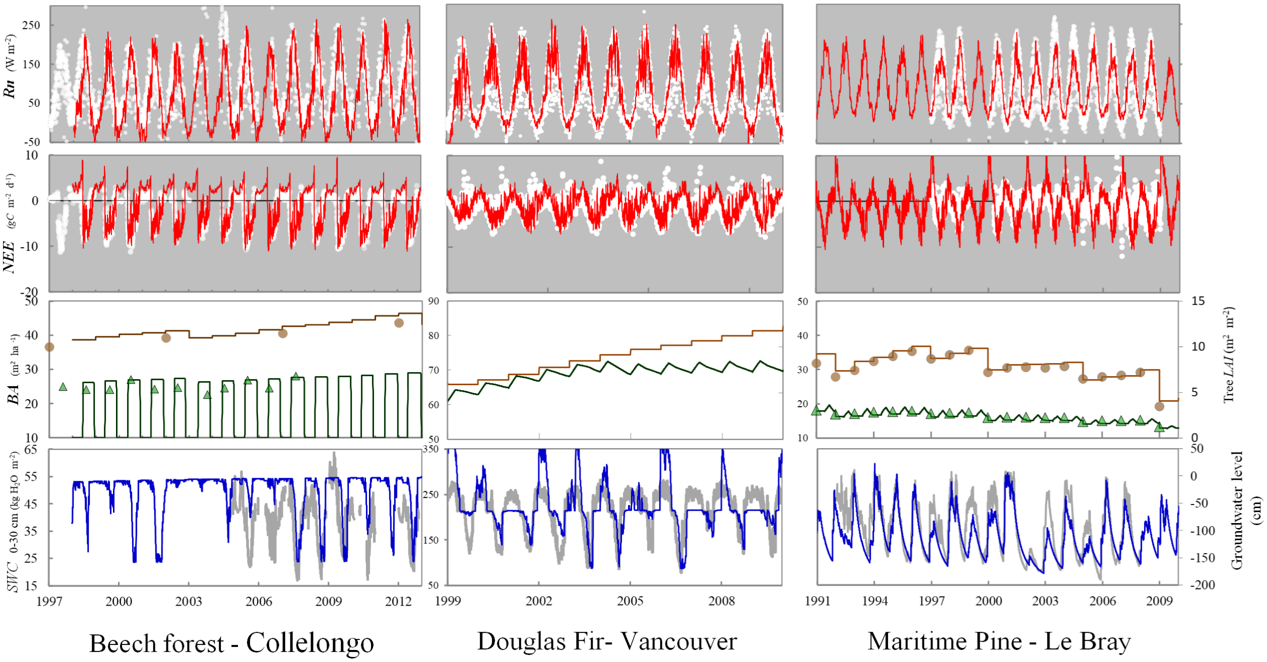

Figure 14. Time series of net radiation and CO_2 fluxes observed (white dots and grey lines) and predicted (heavy lines), top diagrams, together with stand basal area, leaf area index and soil water stock or groundwater level, bottom diagrams. Left: Collelongo European beech forest. Centre: Douglas Fir stand in British Columbia. Right: Le Bray pine forest. Source of the data used are detailed in Table 4. The model was initiated in 1997 for the Collelongo experiment, 1998 in the Douglas Fir and 1987 for the Le Bray experiment. The soil water content in the top 30 cm or 60 cm observed at the Collelongo or Douglas Fir sites (left axis of bottom diagrams) are compared with SWC in the rooted zone simulated by GO+. At the Le Bray site, the groundwater level is compared for the 1994–2008 period (right axis).

First, the tree hydraulics model accounts for the effect of the mean tree height and therefore reflects the effects of age on the leaf water potential and stomatal conductance (Delzon et al. 2003). The hydraulic scheme is kept as simple as possible allowing the description of leaf water potential to be calculated dynamically as a function of transpiration and soil water. The water potential function of canopy stomatal conductance (Eq. 13) is close to the Mencuccini et al. (2015) model, the stomatal closure being smoother in our case. The GO+ stomatal conductance model includes three essential features of the soil-to-leaf water transport, i.e., (i) the soil water potential and conductance dependencies on water content (Eqs. S16 and 21), (ii) the relationship between the tree hydraulic conductance and tree height (Eq. 20), and (iii) its capacitance in relation to the total biomass. We think it is a satisfying compromise between more sophisticated models, that would be difficult to parameterize and calibrate at large spatial scales, and the need for describing the temporal fluctuations of leaf water potential and related effects on stomatal conductance. Second, the GO+ net primary production allocation scheme among trees and within tree parts satisfies the need to simulate realistically the tree stand size distribution and the harvested wood product categories. This is required for coupling GO+ to models of wood-product life cycles and thus route raw harvest products into a range of product categories, namely:

pulp, biofuel, industrial products, furniture and construction (Pichancourt et al. 2018). The allocation scheme is sensitive to the environmental stresses and management, and satisfies the mass conservation principle. Although simple, this allocation scheme has proven its ability to realistically simulate the dynamics of size distribution in mono-specific stands where the selection of trees thinned is crucial (not shown). It summarises the end result of the carbon transfer processes within a tree. A mechanistic simulation of carbohydrate transport within trees at large spatial scales is still beyond computational capacity and constitutes a research challenge (Mencuccini et al. 2015).The inclusion of a species-specific set of allometric equations is therefore a trade-off allowing us to constrain the growth allocation within trees. It is relatively parsimonious in terms of parameters, yet confers to GO+ a capacity to account for a variety of forest tree species. Moreover, tree allometric equations and parameter values are available for the main tree species of the tropical, temperate and boreal zones (Chave et al. 2014, Forrester et al. 2017). In addition, the prediction of tree size allows the assessment of model performance with data covering a range of temporal scales from hourly to the complete forest rotation time (Thum et al. 2017) as illustrated by its evaluation at the Collelongo and Le Bray sites. The dynamic allocation scheme implemented in the understorey vegetation results in a temporal dynamics that is consistent with our current understanding of understorey vegetation growth in managed stands, but could not be evaluated yet at a large spatial scale because of data paucity. Unfortunately, long time series of the annual tree growth for the entire population of trees are still rare and difficult to obtain.

Third, most current practices of forest management in monospecific stands are implemented in the GO+ v3.0 code and can be combined in a wealth of forest management options, including: the drainage (not shown) and mechanical preparation of soil, control of vegetation, thinning, coppicing and clear-cutting of the tree stand. The model is being further developed to allow it to simulate tree stands that are not even-aged and mix two to three tree species. Other process-based models also account for a variety of forestry practices (ORCHIDEE-FM, Bellassen et al. 2011, Reyer et al. 2014), but rarely with documented impacts on soil carbon or how the carbon is apportioned to the different harvested products. Regarding the soil carbon, the Roth–C model and its subsequent development, ECOSSE, had been proven useful and relatively accurate for estimating the dynamics of carbon in the top 1.0 m of the soil following afforestation (Romanya et al. 2000, Dondini et al. 2015) or in temperate forests under different climate change scenarios (Smith et al. 2006). The adaptation of the ROTH -C model to include the effects of soil mechanical disturbances, as implemented in the GO+ model, substantially improves the predictions of soil carbon changes observed following clear-cutting in the pine forests of southwest France. Nevertheless, the model still has to be evaluated at large scale. It is worth noting the GO+ code inherently accounts for the light resource competition between trees and understorey. By construction, the access of the vegetation foliage to light is prioritized from the top to the bottom of the canopy allowing the ground vegetation to respond to thinning and to recover first after clear-cutting. The tree layer subsequently dominates when trees have regrown. This version of the GO+ model also suffers from a number of limitations. It does not yet include a biogeochemistry module and does not allow us to simulate mixed-stand forests or stands that are not even-aged; this is because so far very few evaluation data sets are available. The uptake of water from the soil is not prioritized, with understorey vegetation and trees having access to the same soil volume and their transpiration being withdrawn from the soil simultaneously. Both this limitation, and the canopy and soil layers homogeneity assumption, could be overcome in subsequent versions of this model through adding a dynamic partitioning of the canopy and rooted soil. When necessary, the number of layers could also be increased to some extent provided observed data exist to calibrate and validate the canopy structure and simplifying assumptions required. However, the De Pury and Farquhar's radiation and photosynthesis canopy model has proven effective as compared with complex multi-layer models and may well suffice for simulating more complex canopies.

With the above limitations in mind, the overall sensitivity profile of the model is consistent with the current understanding of the role of the different processes involved and their functional hierarchy. The sensitivity analysis demonstrates an interaction between the sensitivity of variables with the climate — the water holding capacity of soil being limiting under dry conditions, i.e., the year 2005 at Le Bray, and the photosynthetic quantum and carboxylation efficiencies becoming the most influential parameters on wet soil. We have also shown how the time scale modifies the sensitivity profile of model due to the cumulative effects of the fluxes of carbon, energy and water on the stand growth and canopy structure. The GO+ model simulates the seemingly contradictory sensitivity of the autotrophic and heterotrophic respiration to temperature between the short-term (positive direct thermal) effect and the long-term (neutral or negative) effect, which is linked to reduced productivity (Janssens et al. 2001, Atkin and Tjoelker 2003, Knorr et al. 2005). Although simple, the mechanistic link established between instantaneous canopy processes (radiation and energy balance, transpiration, assimilation and respiration) and longer term processes, such as primary and secondary stem growth, wood production, and soil carbon and water dynamics, allows us to capture dynamically the main trajectory and energy, water and carbon fluxes and stocks over decades. The main limitation of our model in that respect is the time resolution of the tree growth processes, which does not account for the seasonality of growth in tree biomass, height and diameter, and may therefore introduce errors, e.g., when predicting the autotrophic respiration at an hourly time-step. This gap may induce some errors for very fast growing species but not for slower growing tree species, as shown in Fig. S3 for the allometric parameters. The sensitivity analysis of GO+ demonstrates that the dynamic representation of stand growth processes is a key feature for capturing the ecosystem behaviour in the long term. We are aware that the conclusions drawn depend on the sensitivity experiment chosen, in terms of climate, soil, tree species and canopy structure, but we think they will be applicable beyond the specific case examined here, at least for canopies with persistent foliage. Whereas the model performances for energy, water vapour and CO_2 flux predictions may compare with other current models (Davi et al. 2005, Collalti et al. 2016, Chen et al. 2016), an essential feature of GO+ is its ability to also capture the long term trends in tree and stand growth and at the same time produce a realistic prediction of the dynamics of understorey vegetation (not shown) and soil carbon. A shift of influence of meteorological variables at day–month scales to biological factors at yearly resolution and beyond was observed by Delpierre et al. (2012) and Stoy et al. (2005, 2009) for many ecosystems through spectral analysis of NEE, GPP and ecosystem respiration sensitivity. This observation suggests the importance of the processes controlling the vegetation dynamics such as phenology, management, growth, and mortality, that are currently described in the GO+ v3.0 model. The accuracy of the model assessed against flux data may appear relatively poor but it should be noted that a single set of parameter values was used and no site-specific calibration was made. In addition, the most influential site characteristics, the rooting depth and soil hydraulic properties, are unfortunately prone to substantial errors because of the difficulty in determining them, and their being subject to large spatial variations at the scale of the footprint of flux measurements. Careful examination of the kinetics of predicted and observed flux values reveal that the modelled phenology was not a substantial source of error despite the fact that this process is poorly documented and difficult to parameterise for species such as European beech or maritime pine. Increasing the complexity of the canopy representation, e.g., by taking into account the heterogeneity of sources and sinks within the vegetation layers, might improve the energy balance and flux modelling (see e.g,. Naudts et al. 2015), but at the expense of the model's ability to simulate sites where no such information is available. Considering the diversity of data sources used for evaluation, the model does not show major discrepancies from observations and performed relatively well, with low biases, at simulating the observed values of atmospheric exchanges, tree growth, and soil carbon and water stock changes. The satisfactory results obtained from the comparison with long-term historical series of tree and stand growth and soil carbon and water are particularly promising because they confirm the model's ability to capture low frequency variations of forest ecosystem functioning for managed forests and demonstrate its ability to simulate management scenarios under different climate scenarios at regional scale. We could not identify why the GO+ performance for simulating canopy fluxes was so site dependent. It may be in part attributed to the uneven data quality within and between sites; this may be due to changing instrumentation, data gaps and data processing. Indeed, using data obtained on site (level 3) instead of reconstructed (level 4) quality data produced better performances (not shown). The unique species-specific sets of parameter values used per vegetation layer for all sites may also generate deviations from observed values since most influencial plant traits, e.g. SLA, $V_{cmax,25}$, J_{max} or k_N, exhibit substantial spatial and temporal variations that are not accounted for in our model evaluations (Fajardo and Siefert 2016, Hamada et al. 2016, Bloomfield et al. 2018). Most advanced forest models are more finely tuned for specific processes, e.g., PnET-BGC for forest hydrology (Gbongo-Gupdawa et al. 2001, Pourmokhtarian et al. 2012), ANAFORE for cambial growth and carbohydrate storage (Deckmyn et al. 2011), CANOAK, or ORCHIDEE-CAN for light and turbulence attenuation within the canopy (Harley and Baldocchi 1995, Naudts et al. 2015), but are more restricted in terms of temporal scales, process continuity and exhaustiveness. Very few models that can be run over large gridded datasets can implement canopy processes at an hourly time scale: ORCHIDEE-CAN v1.0 (Naudts et al. 2015, Luyssaert et al. 2018), JULES (Best et al. 2011, Clark et al. 2011) or, optionally, LPJ-Guess v3.0 (Smith et al. 2014). The majority run at daily time scale; that resolution may impair the sensitivity of non-linear processes to climate and $\mathrm{CO_2}$ such as photosynthesis, respiration or stomatal function.

7 Conclusions

The GO+ model allows us to take a new step forward in developing our understanding of the interactive effects of climate and management on forest ecosystems. The model integrates biophysical, biogeochemical, growth and management processes across a range of temporal scales from hour to century and beyond. It thus integrates short time scales, at which ecophysiological reactions take place, into the temporal framework at which the ecosystem functions, thereby covering the entire forest rotational cycle. The low biases in the model predictions of the exchanges of energy, water and carbon explains the model's ability to capture the long-term trajectory of tree and understorey growth and production, which is essential for modelling managed forests. The subtantial set of forest management options included in GO+ allows a wealth of combinations of forest operations to be implemented and tested. We believe that apart from the nutrient cycles, GO+ includes all the key processes that are needed for understanding the interactions of forest with climate through radiation and the energy, water and carbon cycles, and their impacts on soil and plants, plant growth, phenology and mortality, and wood product exports.

Code and data availability. The GO+V3.0 Python code (doi:10.15454/5K9HCS) together with a short user manual and example files (parameters for sites and species, output files, meteorological data sets) can be downloaded from
https://github.com/DenisLOUSTAU/GOplus_model_INRAE.
The code is also available from the data.inrae.fr repository (https://data.inrae.fr/dataverse/eos) although with fewer example files. The data used for evaluating GO+ were from the Fluxnet database located at the European Fluxes Database Cluster (http://gaia.agraria.unitus.it/home). The DOI of the data sets of flux sites used are as follows:

- Le Bray:10.18140/FLX/1440163
- Collelongo: 10.18140/FLX/1440167
- Soroe: 10.18140/FLX/1440155

The forest inventory data used for Douglas fir and partly maritime Pine were provided by the "GIS" data cooperative (Seynave et al. 2018, https://www6.inra.fr/giscoop), and from the PROFOUND project database (Reyer et al. 2019, http://doi.org/10.5880/PIK.2019.008) for beech forests (Soroe, Collelongo, Solling).

Table A1: List of the prognostic variables of the GO+ v3.0 model. The table is split among the main processes. The entity subscripts T, U, and S are standing for tree canopy, understorey canopy and soil respectively. The subscript "t" is for individual trees.

Symbol	Description	Entity (1)	Unit
1. Radiative balance			
$LW\uparrow$	Upward flux density of longwave radiation	T, U, S	W m^{-2}
$SW\uparrow$	Upward flux density of shortwave radiation	T, U, S	W m^{-2}
SW_a	Shortwave radiation absorbed, each separated into shaded and sunlit fractions	T, U, S	W m^{-2}
2.Energy balance			
λE	Latent heat flux	T, U, S	W m^{-2}
G	Heat storage in the soil	S	W m^{-2}
H_c	Sensible heat flux	T, U, S	W m^{-2}
$r_{HR,c}$	Resistance analog to combined heat and radiative transfer	T, U, S	s m^{-1}
$r_{R,c}$	Resistance analog to radiative transfer	T, U, S	s m^{-1}
Rn	Net radiation	T, U, S	W m^{-2}
$T_{s,c}$	Surface temperature	T, U, S	°C or K
3. Aerodynamic profiles			
d	Zero plane displacement height	T, U, S	m
$u*$	Friction velocity	T, U, S	m s^{-1}
z_0	Roughness length for momentum	T, U, S	m
4. Water balance and hydrology			
D	Groundwater discharge in absence of evaporation	S	kg H_2O m^{-2} hr^{-1}
E_c	Evapotranspiration	T, U, S	kg H_2O m^{-2} hr^{-1}
$E_{wet,c}$	Evaporation from wet surfaces	T, U, S	kg H_2O m^{-2} hr^{-1}
$E_{dry,c}$	Transpiration	T, U, S	kg H_2O m^{-2} hr^{-1}
$f_{dry,c}$	Dry fraction of the canopy	T, U, S	-
$g_{s,c,h}$	Surface conductance	T, U, S	m s^{-1}
I_{stress}	Stress index[0, 1]	T	-
r_H, c	Aerodynamic resistance	T, U, S	m s^{-1}
r_{xyl}	Root-to-leaf hydraulic resistance	T	[kg H_2O m^{-2} s^{-1} $MPa^{-1}]^{-1}$

Table A1: (continued) Variables of the GO+ v3.0 model.

Symbol	Description	Entity	Unit
r_{soil}	Soil hydraulic resistance	S	[kg H_2O m^{-2} s^{-1} $MPa^{-1}]^{-1}$
z_W	Groundwater depth	S	m
ψ_c	Leaf water potential (canopy average)	T	MPa
ψ_{soil}	Soil water potential (average of the rooted zone)	S	MPa
θ	Water content (split among soil layers A, B, C)	S	kg H_2O m^{-3}
$\theta_{rootlayer}$	Water content of the soil root zone	S	kg H_2O m^{-3}
5.Carbon balance			
$Anet_c$	Net assimilation (split among sunlit and shaded fractions of foliage)	T, U	mol CO_2 m^{-2} leaf area s^{-1}
c_c	Internal concentration in CO_2	T, U	mol CO_2 mol air $^{-1}$
$g_{m,c}$	Leaf internal resistance to CO_2 transfer	T, U	mol CO_2 m^{-2} s^{-1}
GPP	Gross primary production	T, t, U	gC m^{-2} hr^{-1}
NEE	Net Ecosystem CO_2 exchange	T,U	gC m^{-2} hr^{-1}
NPP	Net primary production	T, t, U	gC m^{-2} hr^{-1}
R_d	Mitochondrial respiration during day	T, t, U	mol CO_2 m^{-2} leaf area s^{-1}
R_{ECO}	Ecosystem respiration	E	gC m^{-2} hr^{-1}
R_a	Autotrophic (plant) respiration	T, t, U	gC m^{-2} hr^{-1}
R_g	Growth respiration	T, t, U	gC m^{-2} hr^{-1}
R_m	Maintenance respiration	T, t, U	gC m^{-2} hr^{-1}
W_T	Carbon stock in tree biomass (split into stem, branch, leaves, stump, coarse, small and fine roots)	T, t	gC m^{-2} or gC $individual^{-1}$
W_U	Carbon stock in understorey biomass (split into leaves, perennial part, roots)	U	kg DM m^{-2}
6. Soil carbon			
BIO	Carbon stock in soil: biological fraction	S	gC m^{-2}
C_{soil}	Total stock of carbon in soil	S	gC m^{-2}
DPM	Carbon stock in soil: decomposable fraction	S	gC m^{-2}
HUM	Carbon stock in soil: humified fraction	S	gC m^{-2}
RPM	Carbon stock in soil: resistant fraction	S	gC m^{-2}

Table A1: (continued) Variables of the GO+ v3.0 model.

Symbol	Description	Entity	Unit
R_h	Soil microbial respiration (or heterotrophic respiration)	S	gC m^{-2} hr^{-1}
7. Canopy structure, phenology and growth			
A$_l$	Leaf area	t	m^2 tree^{-1}
BA	Basal area (projected cross sectional area of tree stems)	T	m^2 m^{-2}
D_{130}	Tree diameter at z=1.3 m above-ground	T, t	m
DOY$_B$	Budburst date	T, U	day of year
DOY$_S$	Senescence date	T, U	day of year
H_c	Canopy height	T, t, U	m
LAI_c	Canopy leaf area index	T, t, U, E	m^2 m^{-2}
SD	Stocking density	T, U	m^{-2}
V	Stem volume	T, t	m^3 m^{-2}
WAI	Branch and stem area index	T, t	m^2 m^{-2}
ΔH_c	Annual increment in height	T, t, U	m yr^{-1}
ΔD_{130}	Annual increment in stem diameter	T, t	m yr^{-1}
8. Harvest and mortality			
$D_{130,h}$	Stem diameter at 1.3m height of trees harvested	t	m
h_h	Stem height of trees harvested	t	m
M	Mortality (harvest excluded)	T	number of trees.m^{-2} yr^{-1}
S_{stem}	Stem senescence	T, t	kg DM m^{-2} year^{-1}
S_r	Root senescence	T, t	kg DM m^{-2} year^{-1}
S_{br}	Branch senescence	T, t	kg DM .m^{-2} year^{-1}
T_h	Trees harvested	T	number of trees m^{-2} year^{-1}
W_h	Carbon exported by harvest (split into stem, branch, leaves, stump)	T, t	gC m^{-2} year^{-1}

Author contributions. VM developed different modules of the model, the understorey, soil and part of the management and she synthesized and reviewed the final version of the manuscript. DA, AB , CC, SM, D P-D, RV, and RA co-developed the model, its adaptation to different species, different modules and parts of the sensitivity and uncertainly analysis. CM did implement the code over gridded datasets using parallel computing. VB, ATB, J-MB, AG, CJ, BL, GM, MN and KP provided the data sets used about the soil carbon, tree and understorey phenology, forest inventories and canopy fluxes of energy and CO_2 and contributed to data analysis and model evaluation. OP and OR were leading the projects supporting the development of the version 3.0 GO+. They supervised the manuscript structure, content and lay-out. DL developed preliminary versions of the model, made the numerical experiments described in the verification and model evaluation sections and wrote the first version of the manuscript article.

Competing interests. The authors declare that they have no conflict of interest.

Acknowledgements. The datasets used for evaluating the GO+ model with stand growth data and tree species phenology were provided by C. Meredieu (INRAE UEFP0570) for maritime pine permanent plot, the ‘GIS Coopérative de données’ https://www6.inra.fr/giscoop/ (Douglas fir and maritime pine data sets), French ICP-Forest network (French part of ICP-Forests Level II network –Renecofor–) and Christopher Reyer (PIK - Potsdam) and the ISI-MIP project for the beech data sets. The data sets of flux measurements were downloaded from the European Data Cluster and Fluxnet (La Thuile 2015 dataset). During their work on this article, D P-D and RV were supported by the ANR projects ORACLE (10-CEPL-0011) and MACCAC (13-AGRO-0005) and DA by the ADEME project "Evafora" (13-60-C0092). VM was supported by the European project RINGO (730944).The authors thank J.H.C. Gash for reviewing the English and style of the manuscript.

References

Achat, D. L., Martel, S., Picart, D., Moisy, C., Augusto, L., Bakker, M. R., and Loustau, D.: Modelling the nutrient cost of biomass harvesting under different silvicultural and climate scenarios in production forests, Forest Ecol Manag, 429, 642-653, 10.1016/j.foreco.2018.06.047, 2018.

Achat, D. L., Fortin, M., Landmann, G., Ringeval, B., and Augusto, L.: Forest soil carbon is threatened by intensive biomass harvesting, Sci Rep -UK, 5, 10.1038/srep15991, 2015.

Ahlswede, B. J., and Thomas, R. Q.: Community Earth System Model Simulations Reveal the Relative Importance of Afforestation and Forest Management to Surface Temperature in Eastern North America, Forests, 8, 10.3390/f8120499, 2017.

Arrouays, D., and Pelissier, P.: Changes in Carbon Storage in Temperate Humic Loamy Soils after Forest Clearing and Continuous Corn Cropping in France, Plant Soil, 160, 215-223, 1994.

Atkin, O. K., and Tjoelker, M. G.: Thermal acclimation and the dynamic response of plant respiration to temperature, Trends Plant Sci, 8, 343-351, 10.1016/s1360-1385(03)00136-5, 2003.

Augusto, L., Achat, D. L., Bakker, M. R., Bernier, F., Bert, D., Danjon, F., Khlifa, R., Meredieu, C., and Trichet, P.: Biomass and nutrients in tree root systems-sustainable harvesting of an intensively managed Pinus pinaster (Ait.) planted forest, Global Change Biology Bioenergy, 7, 231-243, 2015.

Bala, G., Caldeira, K., Wickett, M., Phillips, T. J., Lobell, D. B., Delire, C., and Mirin, A.: Combined climate and carbon-cycle effects of large-scale deforestation, P Natl Acad Sci USA, 104, 6550-6555, 10.1073/pnas.0608998104, 2007.

Bathiany, S., Claussen, M., Brovkin, V., Raddatz, T., and Gayler, V.: Combined biogeophysical and biogeochemical effects of large-scale forest cover changes in the MPI earth system model, Biogeosciences, 7, 1383-1399, 10.5194/bg-7-1383-2010, 2010.

Bellassen, V., Le Maire, G., Dhôte, J. F., Ciais, P., and Viovy, N.: Modelling forest management within a global vegetation model—Part 1: Model structure and general behaviour, Ecol Model, 221, 2458-2474, https://doi.org/10.1016/j.ecolmodel.2010.07.008, 2010.(a)

Bellassen, V., le Maire, G., Guin, O., Dhote, J. F., Ciais, P., and Viovy, N.: Modelling forest management within a global vegetation model-Part 2: Model validation from a tree to a continental scale, Ecol Model, 222, 57-75, 2010.(b)

Berbigier, P., and Bonnefond, J. M.: Measurement and Modeling of Radiation Transmission within a Stand of Maritime Pine (Pinus-Pinaster Ait), Ann For Sci, 52, 23-42, 1995.

Berbigier, P., Bonnefond, J. M., and Mellmann, P.: CO2 and water vapour fluxes for 2 years above Euroflux forest site, Agric For Meteorol, 108, 183-197, 2001.

Best, M. J., Pryor, M., Clark, D. B., Rooney, G. G., Essery, R. L. H., Ménard, C. B., Edwards, J. M., Hendry, M. A., Porson, A., Gedney, N., Mercado, L. M., Sitch, S., Blyth, E., Boucher, O., Cox, P. M., Grimmond, C. S. B., and Harding, R. J.: The Joint UK Land Environment Simulator (JULES), model description – Part 1: Energy and water fluxes, Geosci Model Dev, 4, 677-699, 10.5194/gmd-4-677-2011, 2011.

Betts, R. A.: Offset of the potential carbon sink from boreal forestation by decreases in surface albedo, Nature, 408, 187-190, 10.1038/35041545, 2000.

Bloomfield, K. J., Cernusak, L. A., Eamus, D., Ellsworth, D. S., Prentice, I. C., Wright, I. J., Boer, M. M., Bradford, M. G., Cale, P., Cleverly, J., Egerton, J. J. G., Evans, B. J., Hayes, L. S., Hutchinson, M. F., Liddell, M. J., Macfarlane, C., Meyer, W. S., Prober, S. M., Togashi, H. F., Wardlaw, T., Zhu, L. L., and Atkin, O. K.: A continental-scale assessment of variability in leaf traits: Within species, across sites and between seasons, Funct Ecol, 32, 1492-1506, 2018.

Borys, A., Suckow, F., Reyer, C., Gutsch, M., and Lasch-Born, P.: The impact of climate change under different thinning regimes on carbon sequestration in a German forest district, Mitig Adapt Strat Gl, 21, 861-881, 10.1007/s11027-014-9628-6, 2016.

Breda, N. J. J.: Ground-based measurements of leaf area index: a review of methods, instruments and current controversies, Journal of Experimental Botany, 54, 2403-2417, 2003.

Bright, R. M., Cherubini, F., and Strømman, A. H.: Climate impacts of bioenergy: Inclusion of carbon cycle and albedo dynamics in life cycle impact assessment, Environ Impact Asses, 37, 2-11, https://doi.org/10.1016/j.eiar.2012.01.002, 2012.

Bright, R. M., Davin, E., O'Halloran, T., Pongratz, J., Zhao, K. G., and Cescatti, A.: Local temperature response to land cover and management change driven by non-radiative processes, Nat Clim Change, 7, 296-+, 10.1038/nclimate3250, 2017.

Campolongo, F. and Saltelli, A.: Sensitivity analysis of an environmental model an application of different analysis methods, Reliability Engineering & System Safety, 57, 49-69, 1997.

Chave, J., Rejou-Mechain, M., Burquez, A., Chidumayo, E., Colgan, M. S., Delitti, W. B., Duque, A., Eid, T., Fearnside, P. M., Goodman, R. C., Henry, M., Martinez-Yrizar, A., Mugasha, W. A., Muller-Landau, H. C., Mencuccini, M., Nelson, B. W., Ngomanda, A., Nogueira, E. M., Ortiz-Malavassi, E., Pelissier, R., Ploton, P., Ryan, C. M., Saldarriaga, J. G., and Vieilledent, G.: Improved allometric models to estimate the above-ground biomass of tropical trees, Glob Change Biol, 20, 3177-3190, 10.1111/gcb.12629, 2014.

Chen, C. R., Xu, Z. H., and Mathers, N. J.: Soil carbon pools in adjacent natural and plantation forests of subtropical Australia, Soil Sci Soc Am J, 68, 282-291, 10.2136/sssaj2004.2820, 2004.

Chen, Y., Ryder, J., Bastrikov, V., McGrath, M. J., Naudts, K., Otto, J., Ottlé, C., Peylin, P., Polcher, J., Valade, A., Black, A., Elbers, J. A., Moors, E., Foken, T., van Gorsel, E., Haverd, V., Heinesch, B., Tiedemann, F., Knohl, A., Launiainen, S., Loustau, D., Ogée, J., Vesala, T., and Luyssaert, S.: Evaluating the performance of land surface model ORCHIDEE-CANv1.0 on water and energy flux estimation with a single- and multi-layer energy budget scheme, Geosci Model Dev, 9, 2951-2972, 10.5194/gmd-9-2951-2016, 2016.

Ciais, P., Loustau, D., Bosc, A., Ogée, J., Dufrêne, E., François, C., Viovy, N., and Delage, F.: How will the production of French forests respond to climate change? An integrated analysis from site to country scale. In: Forests, carbon cycle and climate change, Loustau, D. (Ed.), Quae, Paris.

Clark, D. B., Mercado, L. M., Sitch, S., Jones, C. D., Gedney, N., Best, M. J., Pryor, M., Rooney, G. G., Essery, R. L. H., Blyth, E., Boucher, O., Harding, R. J., Huntingford, C., and Cox, P. M.: The Joint UK Land Environment Simulator (JULES), model description – Part 2: Carbon fluxes and vegetation dynamics, Geosci Model Dev, 4, 701-722, 10.5194/gmd-4-701-2011, 2011.

Coleman K., and Jenkinson:, D.D.: RothC - 26.3 - A model for the turnover of carbon in soil. , in: Evaluation of soil organic matter models using existing, long-term datasets., edited by: Powlson D.S., Smith P., and J.U., S., NATO ASI Series I, Springer Verlag, Heidelberg, Germany, 237-246, 1996.

Cutrim, E., Martin, D. W., and Rabin, R.: Enhancement of Cumulus Clouds over Deforested Lands in Amazonia, Bulletin of the American Meteorological Society, 76, 1801-1805, 1995.

Collalti, A., Marconi, S., Ibrom, A., Trotta, C., Anav, A., D'Andrea, E., Matteucci, G., Montagnani, L., Gielen, B., Mammarella, I., Grunwald, T., Knohl, A., Berninger, F., Zhao, Y., Valentini, R., and Santini, M.: Validation of 3D-CMCC Forest Ecosystem Model (v.5.1) against eddy covariance data for 10 European forest sites, Geosci Model Dev, 9, 479-504, 10.5194/gmd-9-479-2016, 2016.

Davi, H., Dufrene, E., Granier, A., Le Dantec, V., Barbaroux, C., Francois, C., and Breda, N.: Modelling carbon and water cycles in a beech forest Part II: Validation of the main processes from organ to stand scale, Ecol Model, 185, 387-405, 2005.

Davi, H., Dufrêne, E., Francois, C., Le Maire, G., Loustau, D., Bosc, A., Rambal, S., Granier, A., and Moors, E.: Sensitivity of water and carbon fluxes to climate changes from 1960 to 2100 in European forest ecosystems, Agr Forest Meteorol, 141, 35-56, 10.1016/j.agrformet.2006.09.003, 2006.

Deckmyn, G., Verbeeck, H., de Beeck, M. O., Vansteenkiste, D., Steppe, K., and Ceulemans, R.: ANAFORE: A stand-scale process-based forest model that includes wood tissue development and labile carbon storage in trees, Ecol Model, 215, 345-368, 10.1016/j.ecolmodel.2008.04.007, 2008.

Delpierre, N., Dufrêne, E., Soudani, K., Ulrich, E., Cecchini, S., Boé, J., and François, C.: Modelling interannual and spatial variability of leaf senescence for three deciduous tree species in France, Agr Forest Meteorol, 149, 938-948, https://doi.org/10.1016/j.agrformet.2008.11.014, 2009.

Delpierre, N., Soudani, K., Francois, C., Le Maire, G., Bernhofer, C., Kutsch, W., Misson, L., Rambal, S., Vesala, T., and Dufrene, E.: Quantifying the influence of climate and biological drivers on the interannual variability of carbon exchanges in European forests through process-based modelling, Agr Forest Meteorol, 154, 99-112, 10.1016/j.agrformet.2011.10.010, 2012.

Delzon, S., Sartore, M., Burlett, R., Dewar, R., and Loustau, D.: Hydraulic responses to height growth in maritime pine trees, Plant Cell Environ, 27, 1077-1087, 2004.

Delzon, S., and Loustau, D.: Age-related decline in stand water use: sap flow and transpiration in a pine forest chronosequence, Agr For Meteorol, 129, 105-119, 10.1016/j.agrformet.2005.01.002, 2005.

DePury, D. G. G. and Farquhar, G. D.: Simple scaling of photosynthesis from leaves to canopies without the errors of big-leaf models, Plant Cell Environ, 20, 537-557, 1997.

Dobarco, M.R., Cousin, I., Le Bas, C., and Martin, M. P.: Pedotransfer functions for predicting available water capacity in French soils, their applicability domain and associated uncertainty, Geoderma, 336, 81-95, 2019.

Dondini, M., Jones, E. O., Richards, M., Pogson, M., Rowe, R. L., Keith, A. M., Perks, M. P., McNamara, N. P., Smith, J. U., and Smith, P.: Evaluation of the ECOSSE model for simulating soil carbon under short rotation forestry energy crops in Britain, GCB Bioenergy, 7, 527-540, doi:10.1111/gcbb.12154, 2015.

Dufrene, E., Davi, H., Francois, C., le Maire, G., Le Dantec, V., and Granier, A.: Modelling carbon and water cycles in a beech forest Part I: Model description and uncertainty analysis on modelled NEE, Ecol Model, 185, 407-436, 2005.

Ellsworth, D. S., Crous, K. Y., Lambers, H., and Cooke, J.: Phosphorus recycling in photorespiration maintains high photosynthetic capacity in woody species, Plant Cell Environ, 38, 1142-1156, 2015.

Erb, K.-H., Kastner, T., Plutzar, C., Bais, A. L. S., Carvalhais, N., Fetzel, T., Gingrich, S., Haberl, H., Lauk, C., Niedertscheider, M., Pongratz, J., Thurner, M., and Luyssaert, S.: Unexpectedly large impact of forest management and grazing on global vegetation biomass, Nature, 553, 73, 2017.

Fajardo, A. and Siefert, A.: Phenological variation of leaf functional traits within species, Oecologia, 180, 951-959, 2016.

Farquhar, G. D., von Caemmerer, S., and Berry, J.: A biochemical model of photosynthetic CO2 assimilation in leaves of C3 species, Planta, 149, 78-90, 1980.

Felzer, B. S. and Jiang, M.: Effect of Land Use and Land Cover Change in Context of Growth Enhancements in the United States Since 1700: Net Source or Sink?, Journal of Geophysical Research: Biogeosciences, 123, 3439-3457, 2018.

Forrester, D. I., Tachauer, I. H. H., Annighoefer, P., Barbeito, I., Pretzsch, H., Ruiz-Peinado, R., Stark, H., Vacchiano, G., Zlatanov, T., Chakraborty, T., Saha, S., and Sileshi, G. W.: Generalized biomass and leaf area allometric equations for European tree species incorporating stand structure, tree age and climate, Forest Ecol Manag, 396, 160-175, 10.1016/j.foreco.2017.04.011, 2017.

Ghanbarian-Alavijeh, B., Liaghat, A., Huang, G.-H., and Van Genuchten, M. T.: Estimation of the van Genuchten Soil Water Retention Properties from Soil Textural Data, Pedosphere, 20, 456-465, 2010.

Garcia, M., Ozdogan, M., and Townsend, P. A.: Impacts of forest harvest on cold season land surface conditions and land-atmosphere interactions in northern Great Lakes states, J Adv Model Earth Sy, 6, 923-937, 10.1002/2014ms000317, 2014.

Gash, J. H. C.: Analytical model of rainfall interception by forests, Q J Roy Meteor Soc, 105, 43-55, 10.1002/qj.49710544304, 1979.

Gbondo-Tugbawa, S. S., Driscoll, C. T., Aber, J. D., and Likens, G. E.: Evaluation of an integrated biogeochemical model (PnET-BGC) at a northern hardwood forest ecosystem, Water Resour Rese, 37, 1057-1070, doi:10.1029/2000WR900375, 2001.

Gholz, H. L. : Limits on aboveground net primary pro- duction, leaf area, and biomass in vegetational zones of the Pacific Northwest. Dissertation. Oregon State University, Corvallis, Oregon, USA, 1979.

Gottschalk, P., Bellarby, J., Chenu, C., Foereid, B., Smith, P., Wattenbach, M., Zingore, S., and Smith, J.: Simulation of soil organic carbon response at forest cultivation sequences using C-13 measurements, Org Geochem, 41, 41-54, 10.1016/j.orggeochem.2009.04.017, 2010.

Granier, A. and Bréda, N.: Modelling canopy conductance and stand transpiration of an oak forest from sap flow measurements, Ann. For. Sci., 53, 537-546, 1996.

Granier, A., and Loustau, D.: Measuring and modelling the transpiration of a maritime pine canopy from sap-flow data, Agr Forest Meteorol, 71, 61-81, 1994.

Granier, A., Loustau, D., and Bréda, N.: A generic model of forest canopy conductance dependent of climate, soil water availability and leaf area index, Ann Forest Sci, 57, 755-765, 2000a.

Granier, A., Ceschia, E., Damesin, C., Dufrene, E., Epron, D., Gross, P., Lebaube, S., Le Dantec, V., Le Goff, N., Lemoine, D., Lucot, E., Ottorini, J. M., Pontailler, J. Y., and Saugier, B.: The carbon balance of a young Beech forest, Funct Ecol, 14, 312-325, 2000b.

Grassi, G., House, J., Dentener, F., Federici, S., den Elzen, M., and Penman, J.: The key role of forests in meeting climate targets requires science for credible mitigation, Nature Climate Change, 7, 220-+, 2017.

Griscom, B. W., Adams, J., Ellis, P. W., Houghton, R. A., Lomax, G., Miteva, D. A., Schlesinger, W. H., Shoch, D., Siikamaki, J. V., Smith, P., Woodbury, P., Zganjar, C., Blackman, A., Campari, J., Conant, R. T., Delgado, C., Elias, P., Gopalakrishna, T., Hamsik, M. R., Herrero, M., Kiesecker, J., Landis, E., Laestadius, L., Leavitt, S. M., Minnemeyer, S., Polasky, S., Potapov, P., Putz, F. E., Sanderman, J., Silvius, M., Wollenberg, E., and Fargione, J.: Natural climate solutions, P Natl Acad Sci USA, 114, 11645-11650, 10.1073/pnas.1710465114, 2017.

Guillemot, J., Delpierre, N., Vallet, P., François, C., Martin-StPaul, N. K., Soudani, K., Nicolas, M., Badeau, V., and Dufrêne, E.: Assessing the effects of management on forest growth across France: insights from a new functional–structural model, Ann Bot-London, 114, 779-793, 10.1093/aob/mcu059, 2014.

Gutsch, M., Lasch, P., Suckow, F., and Reyer, C.: Management of mixed oak-pine forests under climate scenario uncertainty, Forest Syst, 20, 453-463, 10.5424/fs/20112003-11073, 2011.

Hamada, S., Kumagai, T., Kochi, K., Kobayashi, N., Hiyama, T., and Miyazawa, Y.: Spatial and temporal variations in photosynthetic capacity of a temperate deciduous-evergreen forest, Trees-Structure and Function, 30, 1083-1093, 2016.

Harley, P. C., and Baldocchi, D. D.: Scaling carbon-dioxide and water-vapor exchange from leaf to canopy in a deciduous forest .1. Leaf model parameterization, Plant Cell Environ, 18, 1146-1156, 10.1111/j.1365-3040.1995.tb00625.x, 1995.

Harper, A. B., Wiltshire, A. J., Cox, P. M., Friedlingstein, P., Jones, C. D., Mercado, L. M., Sitch, S., Williams, K., and Duran-Rojas, C.: Vegetation distribution and terrestrial carbon cycle in a carbon cycle configuration of JULES4.6 with new plant functional types, Geoscientific Model Development, 11, 2857-2873, 2018.

Hassika, P., Berbigier, P., and Bonnefond, J. M.: Measurement and modelling of the photosynthetically active radiation transmitted in a canopy of maritime pine, Ann Sci Forest, 54, 715-730, 1997.

Huang, L., Zhai, J., Liu, J. Y., and Sun, C. Y.: The moderating or amplifying biophysical effects of afforestation on CO2-induced cooling depend on the local background climate regimes in China, Agr Forest Meteorol, 260, 193-203, 10.1016/j.agrformet.2018.05.020, 2018.

Humphreys, E.R., Black, T.A., Morgenstern, K., Cai, T., Drewitt, G.B., Nesic, Z., Trofymow, J.A., 2006. Carbon dioxide fluxes in coastal Douglas-fir stands at different stages of development after clearcut harvesting. Agr Forest Meteorol 140, 6-22.

IPCC, 2019. Climate Change and Land. An IPCC special report on climate change, desertification, land degradation, sustainable land management, food security, and greenhouse gas fluxes in terrestrial ecosystems. https://www.ipcc.ch/srccl-report-download-page/

Janssens, I. A., Lankreijer, H., Matteucci, G., Kowalski, A. S., Buchmann, N., Epron, D., Pilegaard, K., Kutsch, W., Longdoz, B., Grunwald, T., Montagnani, L., Dore, S., Rebmann, C., Moors, E. J., Grelle, A., Rannik, U., Morgenstern, K., Oltchev, S., Clement, R., Gudmundsson, J., Minerbi, S., Berbigier, P., Ibrom, A., Moncrieff, J., Aubinet, M., Bernhofer, C., Jensen, N. O., Vesala, T., Granier, A., Schulze, E. D., Lindroth, A., Dolman, A. J., Jarvis, P. G., Ceulemans, R., and Valentini, R.: Productivity overshadows temperature in determining soil and ecosystem respiration across European forests, Glob Change Biol, 7, 269-278, 10.1046/j.1365-2486.2001.00412.x, 2001.

Jarosz, N., Brunet, Y., Lamaud, E., Irvine, M., Bonnefond, J. M., and Loustau, D.: Carbon dioxide and energy flux partitioning between the understorey and the overstorey of a maritime pine forest during a year with reduced soil water availability, Agr Forest Meteorol, 148, 1508-1523, 2008.

Jarvis, P. G.: The interpretation of the variation in leaf water potential and stomatal conductance found in canopies in the field, Philos T Roy Soc B, 273, 593-610, 1976.

Jolivet, C.:Le carbone organique des sols des Landes de Gascogne variabilité spatiale et effets des pratiques sylvicoles et agricoles, Ph D THesis, Université de Bourgogne, Dijon, 306p, 2000.

Jones, H.G.: Plants and microclimate: a quantitative approach to environmental plant physiology, Cambridge University Press, Cambridge, 1992.

Jurevics, A., Peichl, M., Olsson, B. A., Stromgren, M., and Egnell, G.: Slash and stump harvest have no general impact on soil and tree biomass C pools after 32-39 years, For Ecol Manag, 371, 33-41, 10.1016/j.foreco.2016.01.008, 2016.

Karjalainen, T., Pussinen, A., Liski, J., Nabuurs, G. J., Eggers, T., Lapvetelainen, T., and Kaipainen, T.: Scenario analysis of the impacts of forest management and climate change on the European forest sector carbon budget, Forest Policy Econ, 5, 141-155, 2003.

Knorr, W., Prentice, I. C., House, J. I., and Holland, E. A.: Long-term sensitivity of soil carbon turnover to warming, Nature, 433, 298-301, 10.1038/nature03226, 2005.

Kurz, W. A., Dymond, C. C., White, T. M., Stinson, G., Shaw, C. H., Rampley, G. J., Smyth, C., Simpson, B. N., Neilson, E. T., Tyofymow, J. A., Metsaranta, J., and Apps, M. J.: CBM-CFS3: A model of carbon-dynamics in forestry and land-use change implementing IPCC standards, Ecol Model, 220, 480-504, 2009.

Kuusinen, N., Lukes, P., Stenberg, P., Levula, J., Nikinmaa, E., and Berninger, F.: Measured and modelled albedos in Finnish boreal forest stands of different species, structure and understory, Ecol Model, 284, 10-18, 10.1016/j.ecolmodel.2014.04.007, 2014.

Landsberg, J. J., and Waring, R. H.: A generalised model of forest productivity using simplified concepts of radiation-use efficiency, carbon balance and partitioning, Forest Ecol Manag, 95, 209-228, 1997.

Lebourgeois, F., Pierrat, J.-C., Perez, V., Piedallu, C., Cecchini, S., Ulrich, E.: Phenological timing in French temperate forests - a study on stands in the renecofor network, Revue Forestiere Française, 60, 323-343,2008

Lee, X., Goulden, M. L., Hollinger, D. Y., Barr, A., Black, T. A., Bohrer, G., Bracho, R., Drake, B., Goldstein, A., Gu, L. H., Katul, G., Kolb, T., Law, B. E., Margolis, H., Meyers, T., Monson, R., Munger, W., Oren, R., Kyaw, T. P. U., Richardson, A. D., Schmid, H. P., Staebler, R., Wofsy, S., and Zhao, L.: Observed increase in local cooling effect of deforestation at higher latitudes, Nature, 479, 384-387, 10.1038/nature10588, 2011.

Le Moguedec, G. and Dhote, J. F.: Fagacees: a tree-centered growth and yield model for sessile oak (Quercus petraea L.) and common beech (Fagus sylvatica L.), Ann For Sci, 69, 257-269, 2012.

Lindner, M., Bugmann, H., Lasch, P., Flechsig, M., and Cramer, W.: Regional impacts of climatic change on forests in the state of Brandenburg, Germany, Agr Forest Meteorol, 84, 123-135, 10.1016/s0168-1923(96)02381-7, 1997.

Loustau, D., and Cochard, H.: Use of a portable transpiration chamber for estimating evapotranspiration in the Molinia caerulea understorey of a maritime pine stand, Ann Forest Sci , 48, 29-45, 1991.

Loustau, D., Berbigier, P., Roumagnac, P., Ferreira, M. I., Pereira, J. S., Arruda-Pacheco, C., David, J. S., and Tavares, R.: Transpiration of a 64-year-old maritime pine stand in Portugal. I : Seasonal course of water flux through maritime pine, Oecologia, 107, 33-42, 1996.

Loustau, D., Domec, J. C., and Bosc, A.: Interpreting the variations in xylem sap flux density within the trunk of maritime pine (Pinus pinaster Ait.): application of a model for calculating water flows at tree and stand levels, Ann Forest Sci, 55, 29-46, 1998.

Loustau, D., Bosc, A., Colin, A., Ogee, J., Davi, H., Francois, C., Dufrene, E., Deque, M., Cloppet, E., Arrouays, D., Le Bas, C., Saby, N., Pignard, G., Hamza, N., Granier, A., Breda, N., Ciais, P., Viovy, N., and Delage, F.: Modeling climate change effects on the potential production of French plains forests at the sub-regional level, Tree Physiol, 25, 813-823, 2005.

Luyssaert, S., Jammet, M., Stoy, P. C., Estel, S., Pongratz, J., Ceschia, E., Churkina, G., Don, A., Erb, K., Ferlicoq, M., Gielen, B., Grunwald, T., Houghton, R. A., Klumpp, K., Knohl, A., Kolb, T., Kuemmerle, T., Laurila, T., Lohila, A., Loustau, D., McGrath, M. J., Meyfroidt, P., Moors, E. J., Naudts, K., Novick, K., Otto, J., Pilegaard, K., Pio, C. A., Rambal, S., Rebmann, C., Ryder, J., Suyker, A. E., Varlagin, A., Wattenbach, M., and Dolman, A. J.: Land management and land-cover change have impacts of similar magnitude on surface temperature, Nature Climate Change, 4, 389-393, 10.1038/nclimate2196, 2014.

Luyssaert, S., Marie, G., Valade, A., Chen, Y.-Y., Njakou Djomo, S., Ryder, J., Otto, J., Naudts, K., Lansø, A. S., Ghattas, J., and McGrath, M. J.: Trade-offs in using European forests to meet climate objectives, Nature, 562, 259-262, 10.1038/s41586-018-0577-1, 2018.

Masera, O. R., Garza-Caligaris, J. F., Kanninen, M., Karjalainen, T., Liski, J., Nabuurs, G. J., Pussinen, A., de Jong, B. H. J., and Mohren, G. M. J.: Modeling carbon sequestration in afforestation, agroforestry and forest management projects: the CO2FIX V.2 approach, Ecol Model, 164, 177-199, 2003.

Medlyn, B. E., Barton, C. V. M., Broadmeadow, M. S. J., Ceulemans, R., De Angelis, P., Forstreuter, M., Freeman, M., Jackson, S. B., Kellomaki, S., Laitat, E., Rey, A., Roberntz, P., Sigurdsson, B. D., Strassemeyer, J., Wang, K., Curtis, P. S., and Jarvis, P. G.: Stomatal conductance of forest species after long-term exposure to elevated CO2 concentration: a synthesis, New Phytol, 149, 247-264, 2001.

Medlyn, B. E., Dreyer, E., Ellsworth, D., Forstreuter, M., Harley, P. C., Kirschbaum, M. U. F., Le Roux, X., Montpied, P., Strassemeyer, J., Walcroft, A., Wang, K., and Loustau, D.: Temperature response of parameters of a biochemically based model of photosynthesis. II. A review of experimental data, Plant Cell Environ, 25, 1167-1179, 2002.

Medlyn, B. E., Berbigier, P., Clement, R., Grelle, A., Loustau, D., Linder, S., Wingate, L., Jarvis, P. G., Sigurdsson, B. D., and McMurtrie, R. E.: Carbon balance of coniferous forests growing in contrasting climates: Model-based analysis, Agric For Meteorol, 131, 97-124, 2005.

Mencuccini, M., Minunno, F., Salmon, Y., Martínez-Vilalta, J., and Hölttä, T.: Coordination of physiological traits involved in drought-induced mortality of woody plants, New Phytol, 208, 396-409, doi:10.1111/nph.13461, 2015.

Moffat, A. M., Papale, D., Reichstein, M., Hollinger, D. Y., Richardson, A. D., Barr, A. G., Beckstein, C., Braswell, B. H., Churkina, G., Desai, A. R., Falge, E., Gove, J. H., Heimann, M., Hui, D. F., Jarvis, A. J., Kattge, J., Noormets, A., and Stauch, V. J.: Comprehensive comparison of gap-filling techniques for eddy covariance net carbon fluxes, Agric For Meteorol, 147, 209-232, 2007.

Moreaux, V., Lamaud, E., Bosc, A., Bonnefond, J.-m., Medlyn, B. E., and Loustau, D.: Paired comparison of water, energy and carbon exchanges over two young maritime pine stands (Pinus pinaster Ait.): effects of thinning and weeding in the early stage of tree growth, Tree Physiol, 31, 903-921, 2011.

Moreaux, V.: Observation et modélisation des échanges d'énergie et de masse de jeunes peuplements forestiers du Sud-Ouest de la France., Ph. D.thesis., Ecole Doctorale 304 "Sciences et Environnements", Thématique "Physique de l'Environnement", Université de Bordeaux-1, Bordeaux, 262 pages pp., 2012.

Moreaux, V., Longdoz, B., Berveiller, D., Delpierre, N., Dufrêne, E., Bonnefond, J.-M., Chipeaux, C., Joffre, R., Limousin, J.-M., Ourcival, J.-M., Klumpp, K., Darsonville, O., Brut, A., Tallec, T., Ceschia, E., Panthou, G., and Loustau, D.: Environmental control of land-atmosphere CO2 fluxes from temperate ecosystems: a statistical approach based on homogenized time series from five land-use types, Tellus B: Chemical and Physical Meteorology, 72, 1-25, 2020.

Muzylo, A., Llorens, P., Valente, F., Keizer, J. J., Domingo, F., and Gash, J. H. C.: A review of rainfall interception modelling, J Hydrol, 370, 191-206, https://doi.org/10.1016/j.jhydrol.2009.02.058, 2009.

Nakai, T., Sumida, A., Daikoku, K. i., Matsumoto, K., van der Molen, M. K., Kodama, Y., Kononov, A. V., Maximov, T. C., Dolman, A. J., Yabuki, H., Hara, T., and Ohta, T.: Parameterisation of aerodynamic roughness over boreal, cool- and warm-temperate forests, Agr For Meteorol, 148, 1916-1925, https://doi.org/10.1016/j.agrformet.2008.03.009, 2008.

Naudts, K., Ryder, J., McGrath, M. J., Otto, J., Chen, Y., Valade, A., Bellasen, V., Berhongaray, G., Bönisch, G., Campioli, M., Ghattas, J., De Groote, T., Haverd, V., Kattge, J., MacBean, N., Maignan, F., Merilä, P., Penuelas, J., Peylin, P., Pinty, B., Pretzsch, H., Schulze, E. D., Solyga, D., Vuichard, N., Yan, Y., and Luyssaert, S.: A vertically discretised canopy description for ORCHIDEE (SVN r2290) and the modifications to the energy, water and carbon fluxes, Geosci Model Dev, 8, 2035-2065, 10.5194/gmd-8-2035-2015, 2015.

Naudts, K., Chen, Y. Y., McGrath, M. J., Ryder, J., Valade, A., Otto, J., and Luyssaert, S.: Europe's forest management did not mitigate climate warming, Science, 351, 597-600, 10.1126/science.aad7270, 2016.

Otto, J., Berveiller, D., Breon, F. M., Delpierre, N., Geppert, G., Granier, A., Jans, W., Knohl, A., Kuusk, A., Longdoz, B., Moors, E., Mund, M., Pinty, B., Schelhaas, M. J., and Luyssaert, S.: Forest summer albedo is sensitive to species and thinning: how should we account for this in Earth system models?, Biogeosciences, 11, 2411-2427, 10.5194/bg-11-2411-2014, 2014.

Pan, Y. D., Birdsey, R. A., Fang, J. Y., Houghton, R., Kauppi, P. E., Kurz, W. A., Phillips, O. L., Shvidenko, A., Lewis, S. L., Canadell, J. G., Ciais, P., Jackson, R. B., Pacala, S. W., McGuire, A. D., Piao, S. L., Rautiainen, A., Sitch, S., and Hayes, D.: A Large and Persistent Carbon Sink in the World's Forests, Science, 333, 988-993, 10.1126/science.3, 2011.

Papale, D., Reichstein, M., Aubinet, M., Canfora, E., Bernhofer, C., Kutsch, W., Longdoz, B., Rambal, S., Valentini, R., Vesala, T., and Yakir, D.: Towards a standardized processing of Net Ecosystem Exchange measured with eddy covariance technique: algorithms and uncertainty estimation, Biogeosciences, 3, 571-583, 2006.

Penningdevries, F. W., Brunsting, A. H., and Vanlaar, H. H.: Products, requirements and efficiency of biosynthesis - Quantitative approach, J Theor Biol, 45, 339-377, 1974.

Pichancourt, J. B., Manso, R., Ningre, F., and Fortin, M.: A carbon accounting tool for complex and uncertain greenhouse gas emission life cycles, Environ Modell Softw, 107, 158-174, 2018.

Pilegaard, K., Ibrom, A. Courtney, M. S., Hummelshøj, P., Jensen, N. O.: Increasing net CO2 uptake by a Danish beech forest during the period from 1996 to 2009. Agr Forest Meteorol, 151, 934-946, https://doi.org/10.1016/j.agrformet.2011.02.013, 2011.

Pilli, R., Grassi, G., Kurz, W. A., Fiorese, G., and Cescatti, A.: The European forest sector: past and future carbon budget and fluxes under different management scenarios, Biogeosciences, 14, 2387-2405, 10.5194/bg-14-2387-2017, 2017.

Pourmokhtarian, A., Driscoll, C. T., Campbell, J. L., and Hayhoe, K.: Modeling potential hydrochemical responses to climate change and increasing CO2 at the Hubbard Brook Experimental Forest using a dynamic biogeochemical model (PnET-BGC), Water Resour Rese, 48, doi:10.1029/2011WR011228, 2012.

Rasche, L., Fahse, L., and Bugmann, H.: Key factors affecting the future provision of tree-based forest ecosystem goods and services, Climatic Change, 118, 579-593, 10.1007/s10584-012-0664-5, 2013.

Rayment, M. B., Loustau, D., and Jarvis, P. G.: Measuring and modeling conductances of black spruce at three organizational scales: shoot, branch and canopy, Tree Physiol, 20, 713-723, 2000.

Rayment, M. B., Loustau, D., and Jarvis, P. J.: Photosynthesis and respiration of black spruce at three organizational scales: shoot, branch and canopy, Tree Physiol, 22, 219-229, 2002.

Reineke L.H. : Perfecting a stand-density index for even-aged forests. J Agric Res, 46 (1933), pp. 627-638, 1933.

Reyer CPO, Silveyra Gonzalez R, Dolos K, Hartig F, Hauf Y, Noack M, Lasch-Born P, Rötzer T, Pretzsch H, Meesenburg H, Fleck S, Wagner M, Bolte A, Sanders T, Kolari P, Mäkelä A, Vesala T, Mammarella I, Pumpanen J, Matteucci G, Collalti A, D'Andrea E, Foltýnová L, Krejza J, Ibrom A, Pilegaard K, Loustau D, Bonnefond J-M, Berbigier P, Picart D, Lafont S, Dietze M, Cameron D, Vieno M, Tian H, Palacios A, Cicuendez V, Recuero L, Wieze K, Büchner M, Lange S, Volkholz J, Kim H, Weedon GP, Sheffield J, Vega del Valle I, Suckow F, Horemans J, Martel S, Bohn F, Steinkamp J, Chikalanov A, Frieler K (2019) The PROFOUND database for evaluating vegetation models and simulating climate impacts on forests. V.0.1.12. GFZ Data Services. http://doi.org/10.5880/PIK.2019.008

Romanya, J., Cortina, J., Falloon, P., Coleman, K., and Smith, P.: Modelling changes in soil organic matter after planting fast-growing Pinus radiata on Mediterranean agricultural soils, Eur J Soil Sci, 51, 627-641, 2000.

Ryan, M. G.: Effects of climate change on plant respiration, Ecol Appl, 1, 157-167, 1991.

Sathre, R., and O'Connor, J.: Meta-analysis of greenhouse gas displacement factors of wood product substitution, Environ Sci Policy, 13, 104-114, 10.1016/j.envsci.2009.12.005, 2010.

Scartazza, A., Moscatello, S., Matteucci, G., Battistelli, A., and Brugnoli, E.: Seasonal and inter-annual dynamics of growth, non-structural carbohydrates and C stable isotopes in a Mediterranean beech forest, Tree Physiol, 33, 730-742, 2013.

Schlamadinger, B., and Marland, G.: The role of forest and bioenergy strategies in the global carbon cycle, Biomass Bioenerg, 10, 275-300, 10.1016/0961-9534(95)00113-1, 1996.

Shaiek, O., Loustau, D., Trichet, P., Meredieu, C., Bachtobji, B., Garchi, S., and El Aouni, M. H.: Generalized biomass equations for the main above-ground biomass components of maritime pine across contrasting environments, Ann Forest Sci, 68, 443-452, 2011.

Smith, P., Smith, J., Wattenbach, M., Meyer, J., Lindner, M., Zaehle, S., Hiederer, R., Jones, R. J. A., Montanarella, L., Rounsevell, M., Reginster, I., and Kankaanpaa, S.: Projected changes in mineral soil carbon of European forests, 1990-2100, Can J Soil Sci, 86, 159-169, 2006.

Smith, B., Wårlind, D., Arneth, A., Hickler, T., Leadley, P., Siltberg, J., and Zaehle, S.: Implications of incorporating N cycling and N limitations on primary production in an individual-based dynamic vegetation model, Biogeosciences, 11, 2027-2054, https://doi.org/10.5194/bg-11-2027-2014, 2014.

Stoy, P. C., Katul, G. G., Siqueira, M. B. S., Juang, J. Y., McCarthy, H. R., Kim, H. S., Oishi, A. C., and Oren, R.: Variability in net ecosystem exchange from hourly to inter-annual time scales at adjacent pine and hardwood forests: a wavelet analysis, Tree Physiol, 25, 887-902, 10.1093/treephys/25.7.887, 2005.

Stoy, P. C., Richardson, A. D., Baldocchi, D. D., Katul, G. G., Stanovick, J., Mahecha, M. D., Reichstein, M., Detto, M., Law, B. E., Wohlfahrt, G., Arriga, N., Campos, J., McCaughey, J. H., Montagnani, L., U, K. T. P., Sevanto, S., and Williams, M.: Biosphere-atmosphere exchange of CO2 in relation to climate: a cross-biome analysis across multiple time scales, Biogeosciences, 6, 2297-2312, 10.5194/bg-6-2297-2009, 2009.

Stromgren, M., Egnell, G., and Olsson, B. A.: Carbon stocks in four forest stands in Sweden 25 years after harvesting of slash and stumps, Forest Ecol Manag, 290, 59-66, 10.1016/j.foreco.2012.06.052, 2013.

Subedi, P., Jokela, E. J., Vogel, J. G., and Martin, T. A.: Inter-rotational Effects of Fertilization and Weed Control on Juvenile Loblolly Pine Productivity and Nutrient Dynamics, Soil Sci Soc Am J, 78, S152-S167, 10.2136/sssaj2013.08.0345nafsc, 2014.

Togashi, H. F., Atkin, O. K., Bloomfield, K. J., Bradford, M., Cao, K. F., Dong, N., Evans, B. J., Fan, Z. X., Harrison, S. P., Hua, Z., Liddell, M. J., Lloyd, J., Ni, J., Wang, H., Weerasinghe, L. K., and Prentice, I. C.: Functional trait variation related to gap dynamics in tropical moist forests: A vegetation modelling perspective, Perspect Plant Ecol Evol Syst, 35, 52-64, 2018.

Thum, T., MacBean, N., Peylin, P., Bacour, C., Santaren, D., Longdoz, B., Loustau, D., and Ciais, P.: The potential benefit of using forest biomass data in addition to carbon and water flux measurements to constrain ecosystem model parameters: Case studies at two temperate forest sites, Agr Forest Meteorol, 234-235, 48-65, 10.1016/j.agrformet.2016.12.004, 2017.

Vangenuchten, M. T.: A closed-form equation for predicting the hydraulic conductivity of unsaturated soils, Soil Sci Soc Am J, 44, 892-898, 1980.

Van Wijk, M. T., Dekker, S. C., Bouten, W., Bosveld, F. C., Kohsiek, W., Kramer, K., and Mohren, G. M. J.: Modeling daily gas exchange of a Douglas-fir forest: comparison of three stomatal conductance models with and without a soil water stress function, Tree Physiol, 20, 115-122, 2000.

Walker, A. P., Beckerman, A. P., Gu, L., Kattge, J., Cernusak, L. A., Domingues, T. F., Scales, J. C., Wohlfahrt, G., Wullschleger, S. D., and Woodward, F. I.: The relationship of leaf photosynthetic traits – Vcmax and Jmax – to leaf nitrogen, leaf phosphorus, and specific leaf area: a meta-analysis and modeling study, Ecology and Evolution, 4, 3218-3235, 2014.

Wallach, D., and Goffinet, B.: Mean squared error of prediction as a criterion for evaluating and comparing system models, Ecol Model, 44, 299-306, 10.1016/0304-3800(89)90035-5, 1989.

Wang, Y. X., Zhu, X. D., Bai, S. B., Zhu, T. T., Qiu, W. T., You, Y. J., Wu, M. J., Berninger, F., Sun, Z. B., Zhang, H., and Zhang, X. H.: Effects of forest regeneration practices on the flux of soil CO2 after clear-cutting in subtropical China, J Environ Manage, 212, 332-339, 10.1016/j.jenvman.2018.02.038, 2018.

Wösten, J. H. M., Lilly, A., Nemes, A., and Le Bas, C.: Development and use of a database of hydraulic properties of European soils, Geoderma, 90, 169-185, 1999.

Wutzler, T., Wirth, C., and Schumacher, J.: Generic biomass functions for Common beech (Fagus sylvatica) in Central Europe: predictions and components of uncertainty, Can J Forest Res, 38, 1661-1675, 10.1139/x07-194, 2008.

Yousefpour, R., Augustynczik, A. L. D., Reyer, C. P. O., Lasch-Born, P., Suckow, F., and Hanewinkel, M.: Realizing Mitigation Efficiency of European Commercial Forests by Climate Smart Forestry, Sci Rep, 8, 10.1038/s41598-017-18778-w, 2018.

Zhang, X. Z., Guan, D. X., Li, W. B., Sun, D., Jin, C. J., Yuan, F. H., Wang, A. Z., and Wu, J. B.: The effects of forest thinning on soil carbon stocks and dynamics: A meta-analysis, Forest Ecol Manag, 429, 36-43, 10.1016/j.foreco.2018.06.027, 2018.

SUPPLEMENTARY MATERIAL. Energy, water and carbon exchanges in managed forest ecosystems: description and evaluation of the INRAE GO+ model, version 3.0.

Virginie Moreaux[1,11], Simon Martel[1,10], Alexandre Bosc[1], Delphine Picart[1], David Achat[1], Christophe Moisy[1], Raphael Aussenac[1], Christophe Chipeaux[1], Jean-Marc Bonnefond[1], Soisick Figuères[1], Pierre Trichet[1], Rémi Vezy[2], Vincent Badeau[3], Bernard Longdoz[3], André Granier[3], Olivier Roupsard[4], Manuel Nicolas[5], Kim Pilegaard[6], Giorgio Matteucci[7], Claudy Jolivet[8], Andrew T. Black[9], Olivier Picard[10], and Denis Loustau[1]

[1]Bordeaux-Sciences-Agro, INRAE, UMR ISPA, Villenave d'Ornon, F-33140, France
[2]AMAP, Univ Montpellier, CIRAD, CNRS, INRAE, IRD, Montpellier, France
[3]INRAE, UMR SILVA 1434, Champenoux, F-54280, France
[4]Eco&Sols, Univ. Montpellier, CIRAD, INRAE, IRD, Montpellier SupAgro, Montpellier, France
[5]ONF, Département RDI, Fontainebleau, F-77300, France
[6]Technical University of Denmark, Department of Environmental Engineering, 2800 Kgs. Lyngby, Denmark
[7]CNR,ISAFOM, I-80056 Ercolano (NA) Italy
[8]INRAE, US1106 InfoSol, Orléans, F-45075, France
[9]Faculty of Land and Food Systems, Vancouver, BC - V6T 1Z4, Canada
[10]CNPF-IDF, Paris, F-75000 France
[11]Université de Grenoble-ALpes,CNRS, UMR IGE 5001, Grenoble, F-38058, France

Correspondence: Denis Loustau (denis.loustau@inrae.fr)

1 introduction

This supplementary material is including details of the equations and algorithms cited in the main article. It is organised in different sections corresponding to specific processes included in the GO+ model. Some additional illustrations of the sensitivity analysis, uncertainty analysis and model evaluation are also provided in the last section number 9. The tables and figures are presented at the end of the document for readability. The main table, Table S1, shows the complete list of the model parameters. Each parameter refers to one or several entities that are denoted in the third column, namely:

- entire vegetation layers, either the trees, T, or understorey, U;
- individual tree, t;
- soil, S;
- "air" or "water" for the parameters related to the air or water physical constants or thermodynamic properties.

The Table S1 is organised in subsections corresponding to the physical constants, radiative transfer, latent and sensible heat transfer, physiological parameters, canopy structure, phenology, soil hydraulics and soil carbon. Further details on variables and parameters as well as the GO+V3 version code are available at https://github.com/DenisLOUSTAU/GOplus_model_INRAE.

2 Radiative transfer

2.1 Canopy foliage

We have assumed that, providing adequate values of the parameters are used, the de Pury and Farquhar (1997, further abbreviated as dPF) model for the 400–700 nm domain may be extended to the entire shortwave domain (300–1200 nm). The calculations are identical for both canopy layers and all values are expressed on a ground area basis. As the first step, the sunlit leaf area index of the layer c is given by :

$$LAI_{sun,c} = 1 - LAI_{shade,c} = \frac{1-\exp(-k_{b,c}\times LAI_c)}{k_{b,c}} \tag{S1}$$

where LAI_c is the leaf area index and $k_{b,c}$ the canopy extinction coefficient for direct beam radiation that is:

$$k_{b,c} = \frac{k_{bh,c}}{sin\beta} \tag{S2}$$

$k_{bh,c}$ being the extinction coefficient for a beam normal to the canopy (dPF, Eq.18). The canopy reflection coefficients for direct radiation and a uniform leaf distribution are given by :

$$\begin{gathered}\rho_{b,c}(\beta) = 1-\exp[\frac{-2\times\rho_{h,c}\times k_{b,c}}{(1+k_{b,c})}]\\ \rho_{h,c} = \frac{1-(1-\sigma_l)^{1/2}}{1+(1-\sigma_l)^{1/2}}\end{gathered} \tag{S3}$$

where $\rho_{h,c}$ is the reflection coefficient from the horizontal surface and σ_l is the leaf scattering coefficient that is $\rho_l+\tau_l$ (dPF eq. A19 to A20). For sake of simplicity, the diffuse radiation reflection coefficient for the canopy is fixed at a constant value $\rho_{d,c} = 0.036$ rather than calculated as the $\rho_{b,c}$ integral over $\pi/2$. For accounting for the scattering of radiation, extinction coefficients including scattered radiations are introduced (dPF Eq. A4):

$$\begin{gathered}k'_{b,c} = k_{b,c}(1-\sigma_l)^{0.5}\\ k'_{d,c} = k_{d,c}(1-\sigma_l)^{0.5}\end{gathered} \tag{S4}$$

The irradiance absorbed by the sunlit fraction of each canopy layer is given as the sum of direct, diffuse and scattered-beam components:

$$
\begin{aligned}
SW_a(sun) = {} & \\
& SW_{dir} \times (1-\sigma_c) \times [1-\exp(-k_{b,c} \times LAI_c)] \\
& + (SW_{dif}\downarrow + SW_{dif}\uparrow) \times (1-\rho_{d,c}) \times [1-\exp(-(k'_{d,c}+k_{b,c}) \times LAI_c)] \times \frac{k'_{d,c}}{(k'_{d,c}+k_{b,c})} \\
& + SW_{dir} \times (1-\rho_{b,c}) \times [1-\exp(-(k'_{b,c}+k_{b,c}) \times LAI_c) \times \frac{k'_{b,c}}{(k'_{b,c}+k_{b,c})}] \\
& - (1-\sigma_c) \times \frac{[1-\exp(-2 \times k_{b,c} \times LAI_c)]}{2}
\end{aligned}
\tag{S5}
$$

where α, ρ_{cd} and ρ_{cb} are the leaf absorbance and diffuse and direct beam canopy reflectance respectively (Eq. 20-b, to 20-d dPF). The total amount of SW radiation absorbed is :

$$SW_a = (1-\rho_b) \times SW_b \times [1-\exp(-k'_b \times LAI)] + (1-\rho_d) \times SW_d \times [1-\exp(-k'_d \times LAI)] \tag{S6}$$

The amount of shortwave radiation that is absorbed by the shaded canopy fraction is then :

$$SW_a(shade) = SW_a - SW_a(sun) \tag{S7}$$

The longwave radiation absorbed by a canopy layer is given by:

$$LW_{a,c} = (LW\downarrow_{I,c} + LW\uparrow_{I,c}) - (LW\downarrow_{S,c} + LW\uparrow_{S,c}) \tag{S8}$$

where the subscripts I and S stand for intercepted and scattered radiation. These are calculated following Berbigier and Bonnefond (1995) assuming a fixed partitioning of the scattering of intercepted radiation between reflection (0.75) and transmission (0.25) :

$$
\begin{aligned}
& LW\downarrow_{I,c} = LW\downarrow_{c-1} \times (1-\exp[(k_{LW1}+k_{LW2} \times LAI_c) \times LAI_c] \\
& LW\uparrow_{I,c} = LW\uparrow_{c+1} \times (1-\exp[(k_{LW1}+k_{LW2} \times LAI_c) \times LAI_c] \\
& LW\uparrow_{S,c} = (1-\epsilon) \times (LW\downarrow_{I,c} \times 0.75 + LW\uparrow_{I,c} \times 0.25) \\
& LW\downarrow_{S,c} = (1-\epsilon) \times (LW\downarrow_{I,c} \times 0.25 + LW\uparrow_{I,c} \times 0.75)
\end{aligned}
\tag{S9}
$$

The subscript c refers to the layer number increasing from the top to the bottom of the canopy.

2.2 Canopy Woody parts

The wood area index (WAI) intercepting radiation and rainfall accounts for the interception by the tree trunks and branches. WAI is function of the stem standing stock, SD, mean trunk diameter (D_{130}, cm) and height (H_c) and a tree stand shape factor,f, that is the ratio of stand tree stem volume over the product $BA \times H_c$ (m^3), and branches biomass (kg dry matter m^{-2}) :

$$WAI = \frac{f \times SD \times H_c \times D_{130} \times \cos(75)}{100 \times area} + \frac{4 \times W_{T,branches} \times \cos(45)}{d_{wood} \times 1000 \times \Pi \times D_{130}/100/5} \tag{S10}$$

The first part of the left member refers to the stem and the second part to the branches, where the mean angle between beam radiation –or rainfall– is here 75 and 45 degrees for trunks and branches respectively and the mean branch diameter is $1/5$ of the stem diameter. These values are species specific. The interception of throughfall by the understorey woody parts is neglected.

3 Rainfall interception model

The wet and dry fractions of each canopy and soil layer are calculated dynamically using Gash's (1979) canopy water balance model resolved at an hourly time step, $S_{W,c,h}$. The rainfall amounts intercepted by the canopy, $Rain_{I,c}$, and the throughfall and stemflow dripping from the canopy layer, $Rain_{TS,c}$ are calculated :

$$Rain_{I,c} = Rain \times [1 - \exp(k_{R,f} \cdot LAI + k_{R,w} \cdot WAI))] \tag{S11}$$

$$Rain_{TS,c} = [S_{w,c,h-1} + Rain_{I,c} - E_{wet,c}] - S_{Wmax,c} \tag{S12}$$

$$S_{W,c,h} = S_{w,c,h-1} + Rain_{I,c} - E_{wet,c} - Rain_{TS,c} \tag{S13}$$

$$f_{dry,c,h} = 1 - \frac{S_{W,c,h}}{S_{Wmax,c}} \tag{S14}$$

where k_R are rainfall extinction coefficients for the canopy and $S_{Wmax,c}$ the canopy storage capacity that is $(LAI_c \times S_{Wmax,f} + WAI_c \times S_{Wmax,w})$ with S_{Wmax} the storage capacity per unit area of LAI or WAI area.

4 Water transfer model

- The mean tree water capacitance, C_T (kg $\mathrm{H_2O}$ m^{-2} leaf area MPa^{-1}, Eq. 21) is taken from Loustau et al. (2000).

  $$C_T = \frac{0.07 \times W_T}{13} \tag{S15}$$

  where W_T is the tree biomass (kg d.m. m^{-2}soil area).

- The calculation of soil water potential in the soil rooted zone comes from Van Genuchten (1980):

  $$\psi_{soil} = \frac{-1}{\alpha_{VG}} \times [(\frac{\theta_{rootlayer} - \theta_{WP}}{\theta_{FC} - \theta_{WP}})^{\frac{-1}{m_{VG}}} - 1]^{1-m_{VG}} \times 10^{-3} \tag{S16}$$

  where 10^{-3} converts unit from kPa to MPa.

5 Photosynthesis

The photosynthetic carbon uptake by each canopy layer is formalised in GO+ following de Pury and Farquhar (1998) and Farquhar et al. (1980) as :

$$Anet_c = (1 - \frac{\Gamma^*}{c_c}) \times min(W_{c,c}, W_{c,j}) - R_d \tag{S17}$$

The net carbon assimilation is calculated separately for shaded and sunlit fractions of the foliage but apart from the amount of light absorbed per unit leaf area, the calculations are identical and are not duplicated here. The two terms $W_{c,c}$ and $W_{c,j}$ are the Ribulose biPhosphate carboxylation rate limited by the RubisCO activity and the rate of regeneration of Ribulose -biPhosphate limited by electron transport respectively.

$$W_{c,c} = \frac{c_c \times V_{cmax,c}}{c_c + K_c \times (1 + O_2/K_o)} \qquad W_{c,j} = \frac{J_{c,c}}{4 + 8 \times \Gamma^*/c_c} \tag{S18}$$

The electron transport rate, J_c (μmol e- m^{-2} s^{-1}), with $Q_{c,a}$ being the amount of light absorbed by unit leaf area (μmol photons m^{-2} s^{-1}) and α the quantum efficiency of electron transport (mol e- mol photons $^{-1}$), is:

$$J_c = \frac{\alpha \times Q_{c,a} + J_{max,c} - \sqrt{(\alpha \times Q_{c,a} + J_{max,c})^2 - 4 \times \theta \times \alpha \times Q_{c,a} \times J_{max,c}}}{2 \times \theta} \tag{S19}$$

The conversion of the amount of SW radiation absorbed by a vegetation layer and exposure class — sunlit or shaded —, $SW_{a,c,s}$, into moles of photons in the band 400-700 nm absorbed by a unit area of leaf, $Q_{a,c,s}$, is:

$$Q_{a,c,s} = \frac{SW_{a,c,s}}{LAI_{c,s}} \times 4.6 \times 10^{-6} \tag{S20}$$

For tree species, the internal leaf conductance to the CO2 transport, $g_{m,c}$ (mol m $^{-2}$ s^{-1}) is taken from Ellsworth et al. (2015):

$$g_{m,c} = r_{m,c}^{-1} = -0.04 \times 10^{-6} + 1.34 \times g_{s,c,t} \tag{S21}$$

For understorey species, no internal resistance is included. In Eq. S18 to S21, parameters are the mean value for the entire layer and may differ from values obtained using e.g. gas exchange measurements calculations at leaf level. Following Bernacchi et al. (2001) and Medlyn et al. (2002) and with $k_{\mathrm{T,\,c}}$ a temperature factor used for describing the temperature dependency of metabolic parameters, the following temperature response functions are used:

$$k_{\mathrm{T},c} = \frac{T_{\mathrm{K,c}} - T_{\mathrm{K,ref}}}{R \times T_{\mathrm{K},c} \times T_{\mathrm{K,ref}}} \tag{S22}$$

$$V_{cmax,c} = V_{cmax25,c} \times \exp(Ea(Vc) \times k_{\mathrm{T},c}) \tag{S23}$$

$$J_{max,c} = J_{opt,c} \times \frac{H_d \times \exp(H_a \times k_{\mathrm{Topt},c})}{H_d - H_a \times (1 - \exp(H_d \times k_{\mathrm{Topt},c}))} \tag{S24}$$

$$K_{c,c} = K_{c25,c} \times \exp(Ea(Kc) \times k_{\mathrm{T},c}) \tag{S25}$$

$$K_{o,c} = K_{o25,c} \times \exp(Ea(Ko) \times k_{\mathrm{T},c}) \tag{S26}$$

$$K_{m,c} = K_{c,c} \times (1 + O_2/K_{o,c}) \tag{S27}$$

$$\Gamma^*_c = \Gamma^*_{25} \times \exp(Ea(\Gamma^*) \times k_{\mathrm{T},c}) \tag{S28}$$

where $T_{\mathrm{K},c}$ is the mean temperature of foliage layer (in K), and other parameters are detailed in the Table S1.

6 Calculation of the total amount of nitrogen in the tree living biomass

The living fraction of the stem biomass in a tree, $W^{*}_{stem,t}$, is estimated for each individual tree t as follows:

$$W^{*}_{\text{stem},t} = W_{\text{stem},t} \times (1 - W^{+}_{\text{stem, t}}) \tag{S29}$$

where the heartwood biomass,$W^{+}_{stem,t}$, is:

$$W^{+}_{\text{stem},t} = d_{wood} \times [(\pi \times (\frac{D_{130,t}}{4})^2 - SA_t)] \times \frac{h_t}{3} \tag{S30}$$

and the living wood — or sapwood — cross sectional area, SA_t, is derived from McDowell et al. (2002),assuming the ratio between the canopy leaf area and the cross sectional sapwood area at 1.3m height, $A_l{:}A_s$, is related to the tree height.

$$SA_t = \frac{A_{l,t}}{A_l{:}A_s}$$

and

$$A_l{:}A_s = k_{H,1} + k_{H,2} \times h_t^{k_H,3} \tag{S31}$$

The amount of nitrogen in the living stem biomass, N^{*}_{stem}, is :

$$N^{*}_{stem} = kN_{stem} \times W^{*}_{stem} \tag{S32}$$

where kN_{stem} is the nitrogen content of living stem part and W^{*}_{stem} the living stem biomass (kg d.m. m^{-2}). Whereas the live fraction of the foliage and fine roots is assumed constant to 0.8 for coniferous and 1.0 for broadleaf species, the live fraction of the other tree parts (the branches and root parts denoted by x), W^{*}_{x}, is assumed to be linearly depending on the tree age:

$$\begin{aligned} W^{*}_{x} &= k_{MX,x} - (k_{MX,x} - k_{MN,x}) \times \frac{Age}{100} \qquad \text{if } Age < 100, \\ W^{*}_{x} &= k_{MN,x} \qquad \text{if } Age \geq 100. \end{aligned} \tag{S33}$$

The Table S1 lists the kN_x and $k_{MN,MX,x}$ default values used of the maritime Pine species.

7 Carbon allocation and growth

This section details the allocation equations used for different tree species in the GO+ model. The parameter values for tree biomass, D_{130} and height computations are summarised in Table S2. This section details the equations used for three species.The following equations continue the main text Eq. (31). The stem diameter,tree height and biomass values are in cm, m and kg dry matter tree^{-1} respectively.

7.1 Maritime pine (*Pinus pinaster* Ait.)

The allocation algorithm was derived from allometric equations (Shaiek et al. 2011, Achat et al. 2018). For clarity, we keep the same parameter name (k_1 to k_4) throughout the equations, their default values being listed in Table S2.

Step 3.1. Calculation of stem diameter, D_{130} and height, h, from the tree aboveground biomass, $W_{a,i}$.

$$D_{130_i} = k_1 \times W_{a,i,}^{k_2} \times Age^{k_3}, \tag{S34}$$

$$h_{i,} = k_1 \times W_{a,i,}^{k_2} \times Age^{k_3} \tag{S35}$$

Step 3.2. Calculation of the biomass of each tree parts (subscript i is not repeated for clarity).

$$W_{leaf,cohort=1} = k_1 \times W_a^{k_2} \times Age^{k_3} \tag{S36}$$

$$W_{stem} = k_1 \times W_a^{k_2} \times Age^{k_3} \tag{S37}$$

$$W_{leaftotal} = k_1 \times W_a^{k_2} \times Age^{k_3} \tag{S38}$$

$$W_{branches} = W_a - W_s - W_l \tag{S39}$$

$$W_{tr} = W_r \times min(k_1, k_2 \times D_{130}^{-k_3}), \tag{S40}$$

$$W_{cr} = W_r \times max(k_1, k_2 \times log(D_{130}) - k_3), \tag{S41}$$

$$W_{sr} = W_r \times min(k_1, k_2 \times D_{130}^{-k_3}), \tag{S42}$$

$$W_{fr} = W_r - W_{tr} - W_{cr} - W_{sr} \tag{S43}$$

where W_{tr}, W_{cr}, W_{sr} and W_{fr} are biomass variables of taproot, coarse roots (> 20 mm), small roots (2-20 mm) and fine roots (< 2 mm), respectively.

7.2 Douglas fir (*Pseudotsuga menziesii*)

Allometric equations of aboveground compartments were derived from Gholz et al. (1979). The relationship between height and aboveground biomass was computed using the GIS coop database (Seynave et al., 2018).

$$D_{130} = k_1 \times W_a^{k_2} \tag{S44}$$

$$h = k_1 \times W_a^{k_2} \tag{S45}$$

$$W_{stem} = k_1 \times W_a^{k_2} \tag{S46}$$

$$W_{leaf,cohort=1} = k_1 \times W_a^{k_2} \times Age^{k_3} \tag{S47}$$

$$W_{leaftotal} = k_1 \times W_a^{k_2} \tag{S48}$$

$$W_{branches} = W_a - W_{stem} - W_{leaftotal} \tag{S49}$$

The biomass of different root classes are simulated as follows (Achat et al. 2018):

$$W_{cr} = W_r \times max(k_1, k_2 \times log(D_{130}) - k_3), \tag{S50}$$

$$W_{fr} = W_r \times min(k_1, k_2 \times D_{130}^{-k_3}), \tag{S51}$$

$$W_{tr} = (W_r - W_{cr} - W_{fr}) \times \frac{(-k_1 \times D_{130} + k_2)}{(-k_1 \times D_{130} + k_2) + (-k_3 \times D_{130} + k_4)}, \tag{S52}$$

$$W_{sr} = (W_r - W_{cr} - W_{fr}) \times \frac{(-k_3 \times D_{130} + k_4)}{(-k_1 \times D_{130} + k_2) + (-k_3 \times D_{130} + k_4)}, \tag{S53}$$

where W_{tr}, W_{cr}, W_{sr} and W_{fr} are biomasses of stump plus taproot, coarse roots (> 40 mm), small roots (2–40 mm) and fine roots (< 2 mm), respectively.

7.3 European beech (*Fagus sylvatica*)

Equations for the stem, branches and foliage biomass are taken from Wutzler et al. (2008) and include covariates (altitude (m), tree age (yr) or site index(m)). Biomass of root parts are simulated following Achat et al. (2018).

$$D_{130} = k_1 \times W_a^{k_2} \times h^{k_3} \tag{S54}$$

$$W_l = k_1 \times D_{130}^{k_2} \times h^{k_3} \tag{S55}$$

$$W_{stem} = k_1 \times D_{130}^{k_2} \times h^{k_3} \tag{S56}$$

$$W_{branches} = k_1 \times D_{130}^{k_2} \times h^{k_3} \tag{S57}$$

$$W_{cr} = W_r \times \begin{cases} k_1 & \text{for } D_{130} < 4 \text{ cm} \\ k_2 - k_3 \times e^{-k_4 \times D_{130}} & \text{otherwise} \end{cases} \tag{S58}$$

$$W_{fr} = W_r \times min(k_1, k_2 \times D_{130}^{-k_3}) \tag{S59}$$

$$W_{tr} = (W_r - W_{cr} - W_{fr}) \times \frac{(k_1 \times D_{130} + k_2)}{(k_1 \times D_{130} + k_2) + (-k_3 \times D_{130} + k_4)} \tag{S60}$$

$$W_{sr} = (W_r - W_{cr} - W_{fr}) \times \frac{(-k_3 \times D_{130} + k_4)}{(k_1 \times D_{130} + k_2) + (-k_3 \times D_{130} + k_4)} \tag{S61}$$

The algorithm for the calculation of individual tree height (Le Mogedec and Dhôte, 2012) reads:

$$\begin{aligned} m &= 1.218, \qquad K = 55 \\ Cm &= \exp(1+m) \times (1 - \log 10(1+m)) \\ H0 &= K \times \exp[-((\log 10(K/1.3))^{-m} + \frac{(0.4 \times m \times Cm)}{K} \times (Age - 5))^{-1/m}] \\ alpha &= H0 - 1.3 + \pi \times 0.412 \times D_{130,i} \\ h_i &= 1.3 + \frac{alpha - \sqrt{alpha^2 - 4 \times \pi \times 0.412 \times 0.98764 \times (h0 - 1.3) \times D_{130,i}}}{2 \times 0.98764} \end{aligned} \tag{S62}$$

where W_{tr} , W_{cr} , W_{sr} and W_{fr} are the biomass of stump, coarse roots (> 40 mm), small roots (2-40 mm) and fine roots (< 2 mm), respectively.

8 Vegetation phenology and growth

8.1 Tree species

Table S3 details the references used for simulating the lifecycle of the foliage for three European tree species and Table S4 lists the equations and parameters used for modelling the senescence of living organs of the individual trees. They include a temperature dependent budburst date and a fixed foliage lifecycle for the coniferous needles. The onset of senescence of beech leaves depends on the amount of incident shortwave radiation accumulated from budburst until DOY 258.

8.2 Understorey

The phenology of the understorey vegetation is shown in Table S5. It includes a simple thermal time model for leaf unfolding and a mechanistic model of foliage growth, as described in the main text, that is sensitive to temperature and soil moisture. The maximal foliage life duration is fixed and is shortened by high water deficit of the soil or low air temperature.

9 Sensitivity and uncertainty analysis

9.1 Sensitivity assessment

Figures S1 to S3 show the values of the sensitivity value index (Eq. 38 of the main text) of 14 output variables related to the main energy, water and CO_2 fluxes to 28 model parameters and for the years 1994 (wet), 2005 (wet) and the full rotation cycle 1970–2010 in a coniferous stand at Le Bray. The following figures S4 and S5 illustrate the long-term sensitivity of "fluxes" and "stocks" variables to meteorological forcing variables over a forest rotation (1970-2010).

9.2 Uncertainty assessment

The normalized uncertainty values of key model variables calculated for the Le Bray site are shown Figs. S6–S8. The variables are split by canopy layers whereas the overall ecosystem values are given in Figs. 10–11 of the main text. The uncertainty is calculated from the uncertainty of the 14 most influential parameters of the model (Table 3 of the main text) using the MonteCarlo method with 2500 runs for the year 1994 at the Le Bray site.

9.3 Model evaluation

Table S7 presents the variance fraction accounted for by model predictions at different time spans of the latent heat, net radiation Rn, latent heat flux, λE and net ecosystem exchange, NEE. It continues the table 7 of the main article.

References

Achat, D. L., Martel, S., Picart, D., Moisy, C., Augusto, L., Bakker, M. R., and Loustau, D.: Modelling the nutrient cost of biomass harvesting under different silvicultural and climate scenarios in production forests, For Ecol Manag, 429, 642-653, 2018.

Berbigier, P., and Bonnefond, J. M.: Measurement and Modeling of Radiation Transmission within a Stand of Maritime Pine (Pinus-Pinaster Ait), Ann For Sci, 52, 23-42, 1995.

Berbigier, P., Bonnefond, J. M., and Mellmann, P.: CO2 and water vapour fluxes for 2 years above Euroflux forest site, Agric For Meteorol, 108, 183-197, 2001.

Bernacchi, C. J., Singsaas, E. L., Pimentel,C., Portis Jr A. R., and Long S. P.: Improved temperature response functions for models of Rubisco-limited photosynthesis, Plant Cell Environ 24(2): 253-259, 2001.

Bosc, A., Grandcourt, A. D., and Loustau, D.: Variability of stem and branch maintenance respiration in a Pinus pinaster tree, Tree Physiol, 23, 227-236, 2003.

Chen, J. M. and Black, T. A.: Defining leaf area index for non-flat leaves, Plant Cell Environ, 15, 421-429, 1992.

Coleman K., and Jenkinson:, D.D.: RothC - 26.3 - A model for the turnover of carbon in soil. , in: Evaluation of soil organic matter models using existing, long-term datasets., edited by: Powlson D.S., Smith P., and J.U., S., NATO ASI Series I, Springer Verlag, Heidelberg, Germany, 237-246, 1996.

DePury, D. G. G. and Farquhar, G. D.: Simple scaling of photosynthesis from leaves to canopies without the errors of big-leaf models, Plant Cell Environ, 20, 537-557, 1997.

Desprez-Loustau, M. L., and Dupuis, F.: Variation in the phenology of shoot elongation between geographic provenances of maritime pine (Pinus pinaster)-implications for the synchrony with the phenology of the twisting rust fungus, Melampsora pinitorqua, Ann Sci Forest, 51, 553-568, 1994.

Ellsworth, D. S., Crous, K. Y., Lambers, H., and Cooke, J.: Phosphorus recycling in photorespiration maintains high photosynthetic capacity in woody species, Plant Cell Environ, 38, 1142-1156, 10.1111/pce.12468, 2015.

Farquhar, G. D., von Caemmerer, S., and Berry, J.: A biochemical model of photosynthetic CO2 assimilation in leaves of C3 species, Planta, 149, 78-90, 1980.

Gash, J. H. C.: Analytical model of rainfall interception by forests, Q J Roy Meteor Soc, 105, 43-55, 10.1002/qj.49710544304, 1979.

Gholz, H. L. : Limits on aboveground net primary pro- duction, leaf area, and biomass in vegetational zones of the Pacific Northwest. Dissertation. Oregon State University, Corvallis, Oregon, USA, 1979.

Granier, A., and Loustau, D.: Measuring and modelling the transpiration of a maritime pine canopy from sap-flow data, Agr Forest Meteorol, 71, 61-81, 1994.

Granier, A., Bréda, N., Longdoz, B., Gross, P., and Ngao, J.: Ten years of fluxes and stand growth in a young beech forest at Hesse, North-eastern France, Ann For Sci, 65, 704-704, 2008.

Harrington, C. A., Gould, P. J., and St Clair, J. B.: Modeling the effects of winter environment on dormancy release of Douglas-fir, Forest Ecol Manag, 259, 798-808, 10.1016/j.foreco.2009.06.018, 2010.

Kramer, K.: Selecting a Model to Predict the Onset of Growth of Fagus-Sylvatica, Journal of Applied Ecology, 31, 172-181, 1994.

Le Moguedec, G., and Dhote, J. F.: Fagacees: a tree-centered growth and yield model for sessile oak (Quercus petraea L.) and common beech (Fagus sylvatica L.), Ann Sci For, 69, 257-269, 10.1007/s13595-011-0157-0, 2012.

Loustau, D., Domec, J. C., and Bosc, A.: Interpreting the variations in xylem sap flux density within the trunk of maritime pine (Pinus pinaster Ait.): application of a model for calculating water flows at tree and stand levels, Ann Sci For, 55, 29-46, 1998.

McDowell, N., Barnard, H., Bond, B. J., Hinckley, T., Hubbard, R. M., Ishii, H., Kostner, B., Magnani, F., Marshall, J. D., Meinzer, F. C., Phillips, N., Ryan, M. G., and Whitehead, D.: The relationship between tree height and leaf area:sapwood area ratio, Oecologia, 132, 12-20, 2002.

Medlyn, B. E., Barton, C. V. M., Broadmeadow, M. S. J., Ceulemans, R., De Angelis, P., Forstreuter, M., Freeman, M., Jackson, S. B., Kellomäki, S., Laitat, E., Rey, A., Roberntz, P., Sigurdsson, B. D., Strassemeyer, J., Wang, K., Curtis, P. S., and Jarvis, P. G.: Stomatal conductance of forest species after long-term exposure to elevated CO2 concentration: a synthesis, New Phytol, 149, 247-264, 10.1046/j.1469-8137.2001.00028.x, 2001.

Medlyn, B. E., Dreyer, E., Ellsworth, D., Forstreuter, M., Harley, P. C., Kirschbaum, M. U. F., Le Roux, X., Montpied, P., Strassemeyer, J., Walcroft, A., Wang, K., and Loustau, D.: Temperature response of parameters of a biochemically based model of photosynthesis. II. A review of experimental data, Plant Cell Environ, 25, 1167-1179, 2002.

Mohren, G. M. J., and Bartelink, H. H.: Modeling the effects of needle mortality-rate and needle area distribution on dry-matter production of Douglas-fir, Neth J Agr Sci, 38, 53-66, 1990.

Moreaux, V.: Observation et modélisation des échanges d'énergie et de masse de jeunes peuplements forestiers du Sud-Ouest de la France., Ph. D.thesis., Ecole Doctorale 304 "Sciences et Environnements", Thématique "Physique de l'Environnement", Université de Bordeaux-1, Bordeaux, 262 pages pp., 2012.

Nakai, T., Sumida, A., Daikoku, K. i., Matsumoto, K., van der Molen, M. K., Kodama, Y., Kononov, A. V., Maximov, T. C., Dolman, A. J., Yabuki, H., Hara, T., and Ohta, T.: Parameterisation of aerodynamic roughness over boreal, cool- and warm-temperate forests, Agr Forest Meteorol, 148, 1916-1925, https://doi.org/10.1016/j.agrformet.2008.03.009, 2008.

Penningdevries, F. W., Brunsting, A. H., and Vanlaar, H. H.: Products, requirements and efficiency of biosynthesis - Quantitative approach, J Theor Biol, 45, 339-377, 1974.

Pilegaard, K., Ibrom, A., Courtney, M. S., Hummelshøj, P., and Jensen, N. O.: Increasing net CO2 uptake by a Danish beech forest during the period from 1996 to 2009, Agric For Meteorol, 151, 934-946, 2011.

Porté, A., and Loustau, D.: Variability of the photosynthetic characteristics of mature needles within the crown of a 25-year-old Pinus pinaster, Tree Physiol, 18, 223-232, 1998.

Ryan, M. G.: Effects of climate change on plant respiration, Ecol Appl, 1, 157-167, 1991.

Scartazza, A., Moscatello, S., Matteucci, G., Battistelli, A., and Brugnoli, E.: Seasonal and inter-annual dynamics of growth, non-structural carbohydrates and C stable isotopes in a Mediterranean beech forest, Tree Physiol, 33, 730-742, 2013.

Seynave, I., Bailly, A., Balandier, P., Bontemps, J.-D., Cailly, P., Cordonnier, T., Deleuze, C., Dhôte, J.-F., Ginisty, C., Lebourgeois, F., Merzeau, D., Paillassa, E., Perret, S., Richter, C., and Meredieu, C.: GIS Coop: networks of silvicultural trials for supporting forest management under changing environment, Ann For Sci, 75, 48, 10.1007/s13595-018-0692-z, 2018.

Shaiek, O., Loustau, D., Trichet, P., Meredieu, C., Bachtobji, B., Garchi, S., and El Aouni, M. H.: Generalized biomass equations for the main aboveground biomass components of maritime pine across contrasting environments, Ann Sci For, 68, 443-452, 2011.

Vangenuchten, M. T.: A closed-form equation for predicting the hydraulic conductivity of unsaturated soils, Soil Sci Soc Am J, 44, 892-898, 1980.

Villar, R., Held, A. A., and Merino, J.: Dark leaf respiration in light and darkness of an evergreen and a deciduous Plant Species, Plant Physiol., 107, 421, 1995.

Wutzler, T., Wirth, C., and Schumacher, J.: Generic biomass functions for Common beech (Fagus sylvatica) in Central Europe: predictions and components of uncertainty, Can J For Res, 38, 1661-1675, 10.1139/x07-194, 2008.

Table S1: List of the model parameters. Default values are for Pine species unless specified. Additional values of other tree species are downloadable with the GO+ software package.

Symbol	Definition and entity concerned		Unit	Default value	Ref
Physical constants					
γ	Psychrometric constant	air	Pa K^{-1}	66.1 at 293 K	
λ	Latent heat of vaporisation	water	MJ Kg^{-1}	2.45 at 293 K	
ρ_a	dry air density	air	kg m^{-3}	1.20 at 293 K	
σ	Stefan-Boltzmann constant	all	W m^{-2}K^{-4}	5.6703 E-8	
c_p	Specific heat capacity	air	J kg^{-1} K^{-1}	1010	
D_{CO2}	CO_2 diffusivity	air	m^2 s^{-1}	1.47 E-7	
D_{H2O}	H_2O diffusivity	air	m^2 s^{-1}	2.42 E-7	
g	Acceleration due to gravity	air	m^2 s^{-1}	9.8067	
k	Von Karman constant	air	-	0.41	
R	Gas constant	air	J K^{-1} mol^{-1}	8.3144	
s	Slope of temperature - saturation water vapour pressure relationship	air	Pa K^{-1}	145 at 293 K	
Radiation transfer					
α	Leaf absorptance of SW	T,U		1 - σ_l	
ϵ	Long wave emissivity	T,U,S		0.98	
τ_l	Leaf transmittance (SW)	T,U		0.014	
ρ_l	Leaf reflectance (SW)	T,U		0.09	
σ_l	Leaf scattering coefficient (SW)	T,U		0.104	
$\rho_{b,c}$	Canopy reflection coefficient in direct SW	T,U			
$\rho_{d,c}$	Canopy reflection coefficient in diffuse SW	T,U		0.036	
$\rho_{h,c}$	Canopy reflection coefficient for a beam normal to the surface	T,U		0.0274	
a	Soil albedo	S		0.25	
$k_{bh,c}$	Canopy extinction coefficient for beam normal to the surface	T,U		0.33	2
$k_{b,c}$	Canopy extinction coefficient for SW beam radiation	T,U		$= k_{bh,c} \times \sin\beta^{-1}$	

Table S1: (continued) List of the model parameters.

Symbol	Definition and entity concerned		Unit	Default value	Ref
$k'_{b,c}$	Canopy extinction coefficient for direct SW including scattering	T,U		$= k_{b,c} \times (1 - \sigma_l)^{0.5}$	
$k_{d,c}$	Canopy extinction coefficient for diffuse SW radiation	T,U		0.467	2
$k'_{d,c}$	Canopy extinction coefficient for diffuse SW including scattering	T,U		$= k_{d,c} \times (1 - \sigma_l)^{0.5}$	
$k_{b,w}$	Woody parts extinction coefficient for direct SW radiation	T,U		1.0	
$k_{d,w}$	Woody parts extinction coefficient for diffuse SW radiation	T,U		1.0	
k_{LW1-2}	Extinction coefficient of LW radiation	T,U		-0.548, 0.0177	2
Latent and sensible Heat transfer					
$g_{smax,c}$	Maximal stomatal conductance	T,U	m s^{-1}	0.004	
$k_{SW,c}$	parameter for g_s response to incident SW radiation	T,U	W m^{-2}, -	50	
$k_{c,1-2}$	parameters for displacement height d_c	T,U		0.000724/ 0.273	3
$k_{CO2,c}$	parameters for g_s response to the air CO_2 concentration	T,U	-	0.9	4
$k_{e,c,1-2}$	parameters for g_s response to the air water vapor saturation deficit	T,U	Pa^{-1}, -	750 / 1.0	
$k_{\psi,c,1-2}$	parameters for g_s response to the leaf water potential	T,U	MPa^{-1}, -	-1.45 / 15	
τ	Time constant for stomatal response	T,U	mn	12	
Physiological parameters - Photosynthesis					
α_c	Quantum efficiency of electron transport	T,U	mol e mol $phot.^{-1}$	0.138/ 0.187	8
Γ^*_c	Photosynthetic compensation point for CO_2 at 25^oC	T,U	μmolCO_2 mol air^{-1}	42.75	4
$Ea(\Gamma^*)$	Activation energy for Γ^*	T,U,	J mol^{-1}	37 830	9
$Ea(K_c)$	Activation energy for K_c	T,U,	J mol^{-1}	79 430	10
$Ea(K_o)$	Activation energy for K_o	T,U,	J mol^{-1}	36 380	10

Table S1: (continued) List of the model parameters.

Symbol	Definition and entity concerned		Unit	Default value	Ref
$Ea(V_c)$	Activation energy for V_{cmax}	T,U,	J mol^{-1}	62 220	10
$H_{a,c}$	Activation energy for J_{max}	T,U	J mol^{-1}	34 830	10
$H_{d,c}$	Deactivation energy for J_{max}	T,U	J mol^{-1}	2.0E5	10
$J_{max25,c}$	Maximal electron transport rate at T=25^{o}C	T,U	μmol e$^-$m^{-2} s^{-1}	77.37	10
$V_{cmax25,c}$	Maximal carboxylation rate	T,U	μmolCO$_2$ m^{-2} s^{-1}	45.0	10
$K_{c25,c}$	RubisCO Michaelis constant for CO$_2$	T,U,	μmolCO$_2$ mol air^{-1}	404.9	10
$K_{o25,c}$	RubisCO Michaelis constant for O$_2$	T,U,	mmolCO$_2$ mol air^{-1}	278.4	10
K_m	RubisCO Michaelis constant	T,U,	μmolCO$_2$ mol air^{-1}		
$Topt(J_{max})$	Optimal temperature for J_{max}	T,U	K	310.02	10
Physiological parameters - Respiration					
Q_{10}	Respiration multiplier for a 10^{o}C increase	T,U		1.7 -2.0 according to organs	11
$R_{d,T15,c}$	Foliage respiration at T=25^{o}C	T,U	μmolCO$_2$ m^{-2} s^{-1}	0.80	10
$Ea(R_d)$	Activation energy for R_d	T,U,	J mol^{-1}	46 390	10
$R_{N,T15}$	Woody parts respiration at T=15^{o}C	T,U	gC gN^{-1} hr^{-1}	0.0064	12
-	Min. and max. fractions of tissues alive in a given organ	T		0.01 -1.0 (organs)	
R_g	Respiration associated with growth	T,U	gC gC^{-1}	0.28	13
-	Photoinhibition of leaf mitochondrial respiration	T,U,		0.51 /0.65	20
kN_{leaf}	Nitrogen content of foliage	T	gN kg^{-1}d.m	10	15
kN_{stem}	Nitrogen content of stem	T	gN kg^{-1}d.m	0.05	15
kN_{branch}	Nitrogen content of branches	T	gN kg^{-1}d.m	2.5	15
kN_{tr}	Nitrogen content of tap root	T	gN kg^{-1}d.m	1.2	15
kN_{cr}	Nitrogen content of coarse roots	T	gN kg^{-1}d.m	1.4	15
kN_{sr}	Nitrogen content of small roots	T	gN kg^{-1}d.m	2.9	15
kN_{fr}	Nitrogen content of fine roots	T	gN kg^{-1}d.m	8.2	15
$k_{MN,MX,br}$	parameters of the live fraction of branches	T,t	-, year^{-1}	0.10, 0.50	
$k_{MN,MX,tr}$	same for taproot	T,t	-, year^{-1}	0.05, 0.10	
$k_{MN,MX,cr}$	same for coarse roots	T,t	-, year^{-1}	0.05, 0.20	
$k_{MN,MX,sr}$	same for small roots	T,t	-, year^{-1}	0.10, 0.25	

Table S1: (continued) List of the model parameters.

Symbol	Definition and entity concerned		Unit	Default value	Ref
Physiological parameters - Plant water relations					
C_T	Global capacitance of the root-to-leaf water pathway	T	kg H_2O m^{-2} leaf area Mpa^{-1}	$0.05 \times \frac{W}{15}$	9
$k_{H,1-3}$	Leaf area to sapwood area ratio	t	m^2 cm^{-2}	0.20/ -0.07 /0.8	14
$k_{x,0-2}$	Root-to-Leaf hydraulic resistance parameters	T,U	MPa m^2LAI s kg H_2O $^{-1}$ m^{-1}	5000/7500/0.7	
Canopy structure 1. Generic					
SLA	Specific leaf area (area to mass ratio)	T,U	m^2 area kg^{-1} d.m.	6.5	
-	Biomass carbon content	T,U	gC kg d.m.$^{-1}$	480	
λ_i	Coefficient of distribution of GPP_T among tree parts	t	-	-	
d_{wood}	Wood basic density	t	10^3 kg d.m. m^{-3}	0.45	
$k_{\lambda,1-3}$	Root-shoot partitioning coefficient Λ	T	-	0.2/1.0/3.0	
$k_{N,c}$	Nitrogen content of living parts of biomass	T, U	mg N g d.m.$^{-1}$	0.5	15
$k_{R,f}$	Extinction coefficient of precipitations by foliage	T,U	-	0.3	
$k_{R,w}$	Extinction coefficient of precipitations by stem and branches	T, U	-	0.5	
$S_{wmax,c}$	Canopy water storage capacity	T,U	kg H_2O $m^{-2}LAI$ or WAI	0.2	
ξ	Leaf or needle area to LAI ratio	T,t	-	0.5	1
DPM/RPM	Decomposable over Resistant plant material ratios (organs)	T,U	-	0.15-5.0	6
	Age of plant material input into the soil	T,U	yr	1-30	6
Canopy structure 2. Understorey					
$\lambda_f, \lambda_p, \lambda_r,$	Allocation of NPP_U to understorey biomass parts	U	-	0.45/0.10/0.45	
$W_{max,f,p,r}$	Peak value of the biomass of understorey parts	U	kg d.m. m^{-2}	0.25	

Table S1: (continued) List of the model parameters.

Symbol	Definition and entity concerned		Unit	Default value	Ref
h_{max}	Maximal height of understorey canopy	U	m	0.8	
Phenology- 1.Tree species					
BB_T	Heat sum for Pine needles bud burst	T	^{o}C day	1400	18
-	Life duration of leaf cohort	T	days	1002	17
-	fractions of needle cohort lifecycle - (fixed)	T		0.42/0.55/0.80	17
-	parameter Tmin of the equation of chilling rate	T		-17.02	19
-	parameter Tmax of the equation of chilling rate	T		92.15	19
-	parameter Topt of the equation of chilling rate	T		-1.34	19
-	base temperature of the sequential phenology model	T	^{o}C	0.0	19
-	chilling rate threshold (fitted)	T	^{o}C day	102.83	19
-	forcing rate threshold (fitted)	T	^{o}C day	7.05	19
-	k parameters of the forcing rate equation	T		1.0/-0.12/-20.54	19
-k_{1-2}	parameters 1-2 of the broadleaf leaf life duration	T	days, m^2 W^{-1}	0.0023/110	
-	parameter a/b/c of secondary growth model (-)	T		105.5/2.084/62.8	
$k_{S1,S2,S3}$	Parameters of branch turn-over rate	t	yr^{-1}, -,-	0.3678/1.097/-1.256	
$k_{S1,S2,S3}$	Parameters of root turn-over rate	t	yr^{-1}, -,-	0.8/0.5/0.0	
Phenology- 2.Understorey					
BB_U	Heat sum for understorey foliage bud burst	T	^{o}C day	600	
GD	Maximal duration of understorey growth	U	day	130	
$k_{S1,S2}$	Parameters setting up understorey leaf senescence	T	day m^{-2} W^{-1}	7.5E-3, -63.4	
k_p	Sigmoid function parameter	U	-	calculated	

Table S1: (continued) List of the model parameters.

Symbol	Definition and entity concerned		Unit	Default value	Ref
k_s	Flattening coefficient of the derivative of the sigmoid growth function	U	-	0.01	
$SMD_{G,U}$	Soil moisture deficit limiting growth	U	-	0.85	
$T_{G,U}$	Temperature threshold of growth	U	^{o}C	5.0	
T_{MU}	Temperature threshold for mortality	U	^{o}C	0, -8, 0	
DOY_{MU}	day of the year triggering mortality	U	-	288	
SMD_{MU}	Soil moisture deficit threshold of mortality	U	-	0.95	
M_{rate}	Rate of mortality (Date, air T, soil moisture)	U	day^{-1}	0.05, 0.025, 0.01	
Soil hydraulics					
$c/si/s$	soil clay/silt/sand contents	S	pct		
-	Basic density	S	t m^{-3}		
α_{VG}	Van Genuchten α	S	cm^{-1}	0.0003	5
m_{VG}	Van Genuchten m	S	cm^{-1}	0.75	5
θ_{FC}	Water content at Field capacity	S	kg H_2O m^{-3}	150	16
θ_{SAT}	Water content at saturation	S	kg H_2O m^{-3}	275	16
θ_{WP}	Water content at wilting point	S	kg H_2O m^{-3}	65	16
$Tref_S$	Reference temperature of the soil	S	^{o}C	13.5	
D_{max}	Maximal drainage rate	S	kg H_2O m^{-2} d^{-1}	2.5	
z_{min}	Depth at which groundwater discharge = 0	S	m	2.5	
k_w	Power of the discharge curve equation	S		2.0	
h	Thermal conductivity	S	J m^{-2} s^{-1}	1.7	
z_{root}	Rooting depth	S	m	0.8	
Soil carbon					
k_{Ta}	parameters of the force-restore model of the soil temperature for respiration	S	-	0.005	
k_{Tref}	parameters of the force-restore model of the soil temperature for respiration	S	-	0.005	
k_{HUM}	decomposition rate of the HUM fraction	S	yr^{-1}	0.02	6
k_{BIO}	decomposition rate of the BIO fraction	S	yr^{-1}	0.66	6

Table S1: (continued) List of the model parameters.

Symbol	Definition and entity concerned		Unit	Default value	Ref
k_{DPM}	decomposition rate of the DPM fraction	S	yr^{-1}	10	6
k_{RPM}	decomposition rate of the RPM fraction	S	yr^{-1}	0.16	6
k_{plow}	amplification factor of decomposition rate by plowing	S	-	3.0	7
τ_{plow}	half time duration of the plowing effect	S	day	182	7

(1) Chen et al. (1991), (2) Berbigier and Bonnefond (1995), (3) Nakai et al. (2008), (4) Medlyn et al. (2001)

(5) Van Genuchten (1980), (6) Coleman and Jenkinson (1996), (7) Moreaux (2012), (8) Porte and Loustau (1998)

(9) Loustau et al. (1998), (10) Medlyn et al. (2002), (11) Bosc et al.(2003), (12) Ryan (1991), (13) Penning de Vries et al. (1974)

(14) McDowell et al. (2002), (15) Achat et al. (2018), (16) Roman-Dobarco et al. (2019)

(17) Granier and Loustau. (1994), (18) Desprez-Loustau and Dupuis (1994), (19) Kramer (1994), (20) Villar et al. (1995)

Table S2. Allometric coefficient values used for *Pinus pinaster, Pseudotsuga menziesii* and *Fagus sylvatica*.

Tree species	Tree part	k_1	k_2	k_3	k_4	Eq.	Reference
$Pinus$	D_{130}	3.221	0.0403	0.0	-	S34	Shaiek et al. (2011)
$pinaster$	h	1.60	0.381	0.12	-	S35	Shaiek et al. (2011)
	W_{stem}	0.344	1.063	0.131	-	S37	Shaiek et al. (2011)
		1.010	0.796	-0.694	-	S36	Shaiek et al. (2011)
	$W_{leafcohort=1}$						
	$W_{leaftotal}$	1.563	0.835	-0.67	-	S38	Shaiek et al. (2011)
	W_{tr}	0.285	0.499	0.21	-	S40	Achat et al. (2017)
	W_{cr}	0	0.206	0.2218	-	S41	Achat et al. (2017)
	W_{sr}	0.159	0.262	0.259	-	S42	Achat et al. (2017)
	D_{130}	2.574	0.403	0	-	S44	Gholz et al. (1979)
$Pseudotsuga$							
$mensiezii$	h	2.10	0.41	0	-	S45	GIS Coop data set
	W_{stem}	0.686	1.037	0	-	S46	Gholz et al. (1979)
		0.401	0.796	-0.602	-	S47	
	$W_{leafcohort=1}$						
	$W_{leaftotal}$	0.290	0.686	0	-	S48	Gholz et al. (1979)
	W_{tr}	0.002	0.400	0.003	0.315	S52	Achat et al. (2017)
	W_{cr}	0	0.212	0.335	-	S50	Achat et al. (2017)
	W_{sr}	0.002	0.400	0.003		S53	Achat et al. (2017)
	W_{fr}	0.606	0.512	0.603	-	S51	Achat et al. (2017)
$Fagus$	D_{130}	$k_1 = 0.0551 + 30 \times 2.39 \cdot 10^{-4} - 4.68 \cdot 10^{-6} \times Altitude$				S54	(site index=30)
$sylvatica$			$k_2 = 2.11$				Wutzler et al. (2008)
				$k_3 = 0.589 + 4.06 \cdot 10^{-4} \times Age$			
	h		cf. Eq. S62		Le Moguedec and Dhote (2012)		
	W_l	0.038	2.43	-0.913	-	S55	Wutzler et al. (2008)
	W_{stem}	$k_1 = 0.00347 + 30 \times 6.72 \cdot 10^{-4} + 8.11 \cdot 10^{-6} \times Altitude$					Wutzler et al. (2008)
			1.84	1.04		S56	(site index=30)
	W_{branch}	0.122	3.09		-	S57	Wutzler et al. (2008)
		$k_3 = -0.151 - 0.0309 \times 30 - 9.87 \cdot 10^{-4} \times Altitude + 3.06 \cdot 10^{-5} \times 30 \times Altitude$					
	W_{tr}	0.0023	0.082	0.001	0.234	S60	Achat et al. (2017)
	W_{cr}	0	0.542	0.757	0.115	S58	Achat et al. (2017)
	W_{sr}	0.002	0.082	0.001	0.234	S61	Achat et al. (2017)
	W_{fr}	0.489	4.670	1.106	-	S59	Achat et al. (2017)

Table S3. Models of phenology and life cyle of leaf cohorts implemented in the GO+ v3.0

Model type (species)	Budburst	Lifecycle	End of senescence
Thermal time (Maritime Pine)	$\sum_{DOY=1}^{n} T_{a,mean}(DOY) = 1400^{o}C$ Desprez-Loustau and Dupuy (1994)	Beadle et al. (1982) Granier and Loustau (1994)	$age = 1002$ days
Parallel (Douglas Fir)	Harrington et al. (2010)	Mohren and Bartelink (1990)	$age = 2555$ days
Alternate (European Beech)	Kramer (1994)		$BB + [k_1 \cdot \sum_{BB}^{258} SW\downarrow] - k_2$

$SW\downarrow$ is the daily mean incident shortwave radiation, k_1 and k_2 are parameters listed in Table S1.

Table S4. Equations and parameters used for modelling the senescence of living organs of the individual trees.

Tree part	Senescence model	Reference
Branch	$S_{br}(\text{kg dmyear}^{-1}) = k_{\text{S},1} \times W_{br}^{k_{\text{S},2}} \times Age^{k_{\text{S},3}}$	unpublished
Roots	$S_{r}(\text{kg dmyear}^{-1}) = k_{\text{S},1} \times \frac{W_r}{1+W_r^{1-k_{\text{S},2}}} \times Age^{k_{\text{S},3}}$	unpublished

Table S5. Models of phenology and life cycle of the understorey vegetation parts implemented in the GO+ v3.0

Phase	Model		Reference
Budburst	$\sum_{DOY=1}^{n} T_{a,mean} = 600^{o}C$		unpublished
Growth	Soil moisture and Temperature threshold : SMD_{GU}, T_{GU} $dW_{l,p,r} = min($Max. Growth rate, C available$)$		Moreaux (2012)
Senescence	Temperature: $T_{MU,l,p,r}$	$\Rightarrow M_{rate} = 0.05, 0.001, 0.05 day^{-1}$	Moreaux (2012)
	Soil moisture :$SMD_{MU,l,p,r}$	$\Rightarrow M_{rate} = 0.025, 0.003, 0.025 day^{-1}$	
	Date: $DOY_{MU,l,p,r}$	$\Rightarrow M_{rate} = 0.05, 0.001, 0.05 day^{-1}$	

Table S6. Characteristics of the sites selected for long term series of tree (ΔD_{130}) and stand growth (ΔBA)

Site name (code)	Lat / Lon (°)	Annual temperature (°C) / rainfall(mm yr^{-1})	Main species	Tree age (yr)	Period	Reference
St Pardoux	45.44 / 1.45	11.5/1020	Douglas fir	28-42	1997-2011	1
Ecouves	48.50 / 0.10	11.0/750	Douglas fir	21-62	1969-2010	1
Quartier	45.80 / 3.60	11.5/720	Douglas fir	12-21	2004-2013	1
La Houve	49.35 / 5.99	10.7/760	Douglas fir	11-22	2000-2011	1
Soroe (DK-Sor)	55.49 / 11.6	8.2 / 660	European beech	88-97	2000-2009	2
Collelongo (IT-Col)	41.85 / 13.59	6.3 / 1180	European beech	130-140	2002-2012	3
Hesse	48.67 / 7.07	9.2 / 820	European beech	33-44	1999-2010	4
Solling	51.47 /9.37	6.5/1090	European beech	148	1996-2014	European database
Le Bray (FR-LBr)	44.72 / -0.77	13.5/ 930	Maritime pine	26-37	1987-2008	5
Vielle	44.03 / -0.18	9.2 / 820	Maritime pine	33-46	1991-2014	1
Pompogne	44.25 / 0.04	9.2 / 820	Maritime pine	33-43	1993-2009	1

(1) https://www6.inra.fr/giscoop, Seynave et al. (2018); (2)European database, Pilegaard et al. (2011);(3) European database, Scartazza et al. (2013); (4)European database, Granier et al. (2008); (5) European database, Berbigier et al. (2001)

Table S7. Variance fraction (R^2) of latent heat,λE, net radiation, R_n, and net ecosystem exchange, NEE, accounted for by the model predictions at different time spans in five sites. The number of data values used is given in the bottom section.

Time span: (day)	1/24	1	5	10	30	90	180	365
Rn								
BC Campbell 49		0.97	0.97	0.98	0.98	0.98	0.40	0.00
BC Campbell 88		0.95	0.97	0.97	0.97	0.97	0.95	0.33
Collelongo	0.71	0.56	0.75	0.76	0.66	0.73	0.00	0.00
Hesse		0.75	0.90	0.92	0.95	0.96	0.44	0.42
Soroe	0.71	0.63	0.86	0.90	0.92	0.85	0.07	0.35
Le Bray		0.68	0.87	0.91	0.84	0.96	0.39	0.05
λE								
BC Campbell 49		0.76	0.86	0.89	0.93	.94	0.00	0.10
BC Cambpell 88		0.68	0.75	0.77	0.81	0.84	0.20	0.77
Collelongo	0.30	0.22	0.27	0.24	0.23	0.19	0.31	0.44
Hesse		0.70	0.72	0.85	0.87	0.88	0.10	0.28
Soroe	0.28	0.44	0.63	0.69	0.78	0.87	0.09	0.10
Le Bray		0.18	0.24	0.29	0.31	0.57	0.51	0.30
NEE								
BC Campbell 49		0.67	0.70	0.70	0.72	0.85	0.81	0.14
BC Campbell 88		0.25	0.19	0.16	0.15	0.34	0.38	0.76
Collelongo	0.29	0.23	0.30	0.29	0.31	0.28	0.01	0.03
Hesse		0.57	.070	0.75	0.80	0.80	0.05	0.18
Soroe	0.32	0.34	0.44	0.47	0.50	0.47	0.08	0.14
Le Bray		0.15	0.19	0.20	0.27	0.50	0.30	0.57
Number of values								
BC Campbell 49		4002	797	394	130	42	20	9
BC Campbell 88		2110	415	208	69	22	10	4
Collelongo	53601	2654	653	358	145	56	29	14
Hesse		4414	878	433	146	50	23	12
Soroe	105178	4381	886	430	145	46	22	10
Le Bray		3559	704	349	120	40	20	9

Figure S1. Values of the sensitivity index I_k of 14 model variables for the year 1994 (wet year). Variables are grouped into three processes, energy balance, water balance and carbon balance. Within each group, the heading are the variable symbol, nominal value (annual sum) and unit. The numbers in boxes are the highest I_k value per variable whereas bold numbers show I_k values that are greater than half the maximum value, $0.5 \times I_{kmax}$, e.g. 2.2 MJ $\mathrm{m}^{-2} yr^{-1}$ for I_{Rn} (1994). The numbers in normal font show values between $0.1 \times I_{kmax}$ and $0.5 \times I_{kmax}$, that are within $[0.22, 2.2]$ $MJm^{-2}yr^{-1}$ for I_{Rn} (1994). Empty cells denotes $I_k$values less than $0.1 \times I_{kmax}$.

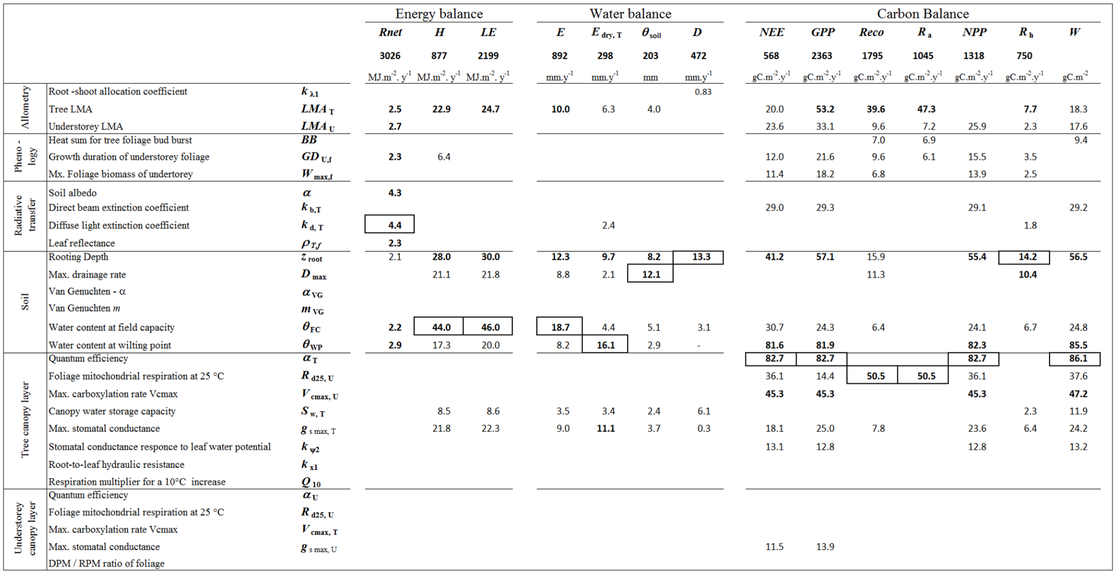

			Energy balance			Water balance				Carbon Balance						
			Rnet	***H***	***LE***	***E***	$E_{dry,T}$	θ_{soil}	***D***	***NEE***	***GPP***	***Reco***	R_a	***NPP***	R_h	***W***
			3026	**877**	**2199**	**892**	**298**	**203**	**472**	**568**	**2363**	**1795**	**1045**	**1318**	**750**	
			$MJ.m^{-2}.y^{-1}$	$MJ.m^{-2}.y^{-1}$	$MJ.m^{-2}.y^{-1}$	$mm.y^{-1}$	$mm.y^{-1}$	mm	$mm.y^{-1}$	$gC.m^{-2}.y^{-1}$	$gC.m^{-2}.y^{-1}$	$gC.m^{-2}.y^{-1}$	$gC.m^{-2}.y^{-1}$	$gC.m^{-2}.y^{-1}$	$gC.m^{-2}.y^{-1}$	$gC.m^{-2}$
Allometry	Root -shoot allocation coefficient	$k_{\lambda 1}$							0.83							
	Tree LMA	LMA_T	**2.5**	**22.9**	**24.7**	**10.0**	6.3	4.0		20.0	**53.2**	**39.6**	**47.3**		**7.7**	18.3
	Understorey LMA	LMA_U	**2.7**							23.6	33.1	9.6	7.2	25.9	2.3	17.6
Pheno - logy	Heat sum for tree foliage bud burst	BB										7.0	6.9			9.4
	Growth duration of understorey foliage	$GD_{U,f}$	**2.3**	6.4						12.0	21.6	9.6	6.1	15.5	3.5	
	Mx. Foliage biomass of undertorey	$W_{max,f}$								11.4	18.2	6.8		13.9	2.5	
Radiative transfer	Soil albedo	α	**4.3**													
	Direct beam extinction coefficient	$k_{b,T}$								29.0	29.3			29.1		29.2
	Diffuse light extinction coefficient	$k_{d,T}$	$\boxed{\mathbf{4.4}}$				2.4								1.8	
	Leaf reflectance	$\rho_{T,f}$	**2.3**													
Soil	Rooting Depth	z_{root}	2.1	**28.0**	**30.0**	**12.3**	**9.7**	**8.2**	$\boxed{\mathbf{13.3}}$	**41.2**	**57.1**	15.9		**55.4**	$\boxed{\mathbf{14.2}}$	**56.5**
	Max. drainage rate	D_{max}		21.1	21.8	8.8	2.1	$\boxed{\mathbf{12.1}}$				11.3			**10.4**	
	Van Genuchten - α	α_{VG}														
	Van Genuchten *m*	m_{VG}														
	Water content at field capacity	θ_{FC}	**2.2**	$\boxed{\mathbf{44.0}}$	$\boxed{\mathbf{46.0}}$	$\boxed{\mathbf{18.7}}$	4.4	5.1	3.1	30.7	24.3	6.4		24.1	6.7	24.8
	Water content at wilting point	θ_{WP}	**2.9**	17.3	20.0	8.2	$\boxed{\mathbf{16.1}}$	2.9	-	**81.6**	**81.9**			**82.3**		**85.5**
Tree canopy layer	Quantum efficiency	α_T								$\boxed{\mathbf{82.7}}$	$\boxed{\mathbf{82.7}}$			$\boxed{\mathbf{82.7}}$		$\boxed{\mathbf{86.1}}$
	Foliage mitochondrial respiration at 25 °C	$R_{d25,U}$								36.1	14.4	$\boxed{\mathbf{50.5}}$	$\boxed{\mathbf{50.5}}$	36.1		37.6
	Max. carboxylation rate Vcmax	$V_{cmax,U}$								**45.3**	**45.3**			**45.3**		**47.2**
	Canopy water storage capacity	$S_{w,T}$		8.5	8.6	3.5	3.4	2.4	6.1						2.3	11.9
	Max. stomatal conductance	$g_{s\,max,T}$		21.8	22.3	9.0	**11.1**	3.7	0.3	18.1	25.0	7.8		23.6	6.4	24.2
	Stomatal conductance responce to leaf water potential	$k_{\psi 2}$								13.1	12.8			12.8		13.2
	Root-to-leaf hydraulic resistance	k_{x1}														
	Respiration multiplier for a 10°C increase	Q_{10}														
Understorey canopy layer	Quantum efficiency	α_U														
	Foliage mitochondrial respiration at 25 °C	$R_{d25,U}$														
	Max. carboxylation rate Vcmax	$V_{cmax,T}$														
	Max. stomatal conductance	$g_{s\,max,U}$								11.5	13.9					
	DPM / RPM ratio of foliage															

Figure S2. Values of the sensitivity index I_k of 14 model variables for the year 2005 (dry year).

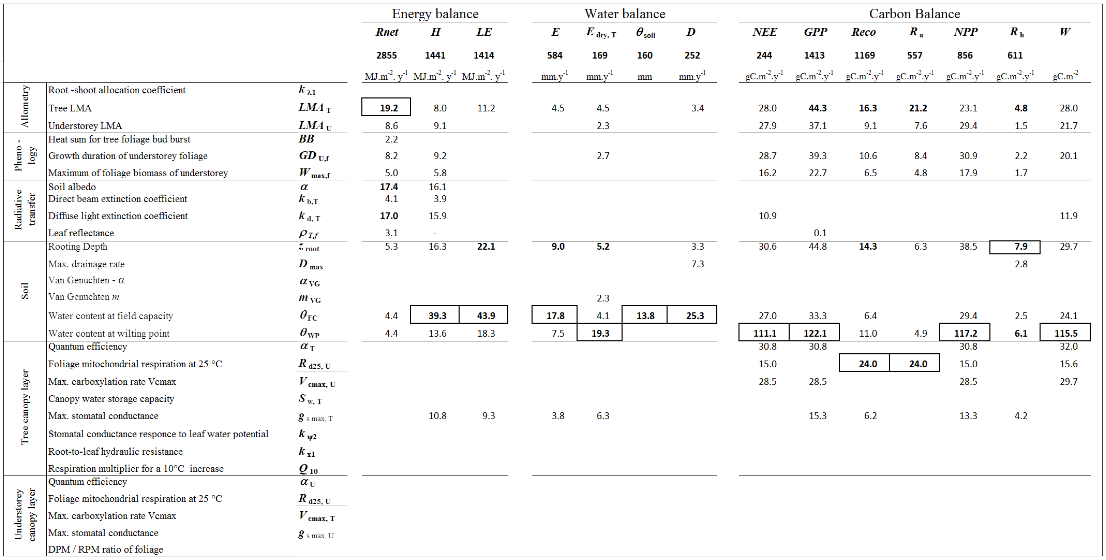

			Energy balance			Water balance				Carbon Balance						
			Rnet	***H***	***LE***	***E***	$E_{dry,T}$	θ_{soil}	***D***	***NEE***	***GPP***	***Reco***	R_a	***NPP***	R_h	***W***
			2855	**1441**	**1414**	**584**	**169**	**160**	**252**	**244**	**1413**	**1169**	**557**	**856**	**611**	
			$MJ.m^{-2}.y^{-1}$	$MJ.m^{-2}.y^{-1}$	$MJ.m^{-2}.y^{-1}$	$mm.y^{-1}$	$mm.y^{-1}$	mm	$mm.y^{-1}$	$gC.m^{-2}.y^{-1}$	$gC.m^{-2}.y^{-1}$	$gC.m^{-2}.y^{-1}$	$gC.m^{-2}.y^{-1}$	$gC.m^{-2}.y^{-1}$	$gC.m^{-2}.y^{-1}$	$gC.m^{-2}$
Allometry	Root -shoot allocation coefficient	$k_{\lambda 1}$														
	Tree LMA	LMA_T	$\boxed{\mathbf{19.2}}$	8.0	11.2	4.5	4.5		3.4	28.0	**44.3**	**16.3**	**21.2**	23.1	**4.8**	28.0
	Understorey LMA	LMA_U	8.6	9.1			2.3			27.9	37.1	9.1	7.6	29.4	1.5	21.7
Pheno - logy	Heat sum for tree foliage bud burst	BB	2.2													
	Growth duration of understorey foliage	$GD_{U,f}$	8.2	9.2			2.7			28.7	39.3	10.6	8.4	30.9	2.2	20.1
	Maximum of foliage biomass of understorey	$W_{max,f}$	5.0	5.8						16.2	22.7	6.5	4.8	17.9	1.7	
Radiative transfer	Soil albedo	α	**17.4**	16.1												
	Direct beam extinction coefficient	$k_{b,T}$	4.1	3.9												
	Diffuse light extinction coefficient	$k_{d,T}$	**17.0**	15.9						10.9						11.9
	Leaf reflectance	$\rho_{T,f}$	3.1	-							0.1					
Soil	Rooting Depth	z_{root}	5.3	16.3	**22.1**	**9.0**	**5.2**		3.3	30.6	44.8	**14.3**	6.3	38.5	$\boxed{\mathbf{7.9}}$	29.7
	Max. drainage rate	D_{max}							7.3						2.8	
	Van Genuchten - α	α_{VG}														
	Van Genuchten *m*	m_{VG}					2.3									
	Water content at field capacity	θ_{FC}	4.4	$\boxed{\mathbf{39.3}}$	$\boxed{\mathbf{43.9}}$	$\boxed{\mathbf{17.8}}$	4.1	$\boxed{\mathbf{13.8}}$	$\boxed{\mathbf{25.3}}$	27.0	33.3	6.4		29.4	2.5	24.1
	Water content at wilting point	θ_{WP}	4.4	13.6	18.3	7.5	$\boxed{\mathbf{19.3}}$			$\boxed{\mathbf{111.1}}$	$\boxed{\mathbf{122.1}}$	11.0	4.9	$\boxed{\mathbf{117.2}}$	**6.1**	$\boxed{\mathbf{115.5}}$
Tree canopy layer	Quantum efficiency	α_T								30.8	30.8			30.8		32.0
	Foliage mitochondrial respiration at 25 °C	$R_{d25,U}$								15.0		$\boxed{\mathbf{24.0}}$	$\boxed{\mathbf{24.0}}$	15.0		15.6
	Max. carboxylation rate Vcmax	$V_{cmax,U}$								28.5	28.5			28.5		29.7
	Canopy water storage capacity	$S_{w,T}$														
	Max. stomatal conductance	$g_{s\,max,T}$		10.8	9.3	3.8	6.3				15.3	6.2		13.3	4.2	
	Stomatal conductance responce to leaf water potential	$k_{\psi 2}$														
	Root-to-leaf hydraulic resistance	k_{x1}														
	Respiration multiplier for a 10°C increase	Q_{10}														
Understorey canopy layer	Quantum efficiency	α_U														
	Foliage mitochondrial respiration at 25 °C	$R_{d25,U}$														
	Max. carboxylation rate Vcmax	$V_{cmax,T}$														
	Max. stomatal conductance	$g_{s\,max,U}$														
	DPM / RPM ratio of foliage															

Figure S3. Values of the sensitivity index I_k of 14 model variables over a complete forest rotation from 1970 (plantation) to 2010 (clearcut).

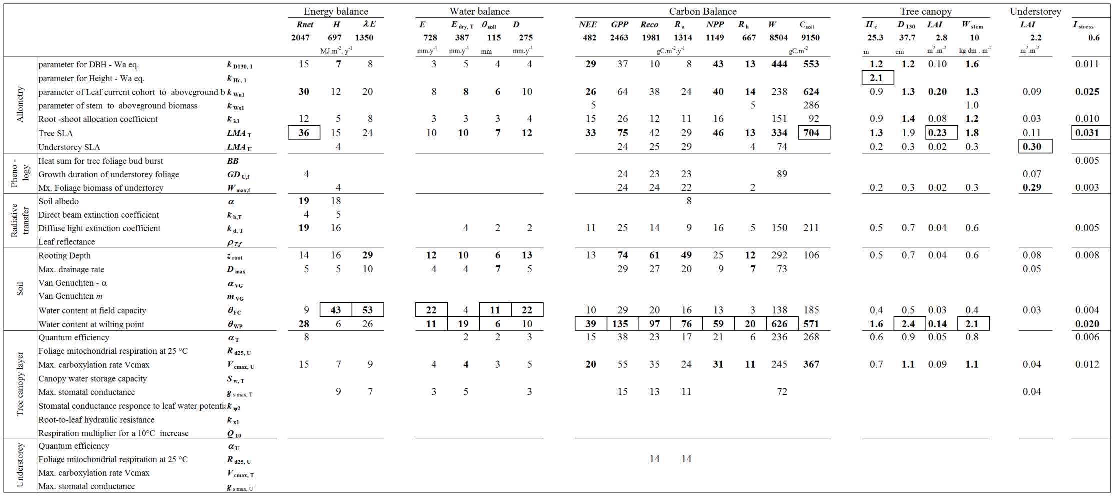

			Energy balance			Water balance				Carbon Balance								Tree canopy				Understorey	
			$Rnet$	H	λE	E	$E_{\mathrm{dry,T}}$	θ_{soil}	D	NEE	GPP	$Reco$	R_{a}	NPP	R_{h}	W	C_{soil}	H_{c}	D_{130}	LAI	W_{stem}	LAI	I_{stress}
			2047	**697**	**1350**	**728**	**387**	**115**	**275**	**482**	**2463**	**1981**	**1314**	**1149**	**667**	**8504**	**9150**	**25.3**	**37.7**	**2.8**	**10**	**2.2**	**0.6**
			$\mathrm{MJ.m^{-2}.\,y^{-1}}$			$\mathrm{mm.y^{-1}}$	$\mathrm{mm.y^{-1}}$	mm	$\mathrm{mm.y^{-1}}$	$\mathrm{gC.m^{-2}.y^{-1}}$						$\mathrm{gC.m^{-2}}$		m	cm	$\mathrm{m^2.m^{-2}}$	$\mathrm{kg\ dm\ .\ m^{-2}}$	$\mathrm{m^2.m^{-2}}$	
Allometry	parameter for DBH - Wa eq.	$k_{\mathrm{D130,1}}$	15	**7**	8	3	5	4	4	**29**	37	10	8	**43**	**13**	**444**	**553**	**1.2**	**1.2**	0.10	**1.6**		0.011
	parameter for Height - Wa eq.	$k_{\mathrm{Hc,1}}$																$\boxed{\mathbf{2.1}}$					
	parameter of Leaf current cohort to aboveground b	k_{Wn1}	**30**	12	20	8	**8**	**6**	10	**26**	64	38	24	**40**	**14**	238	**624**	0.9	**1.3**	**0.20**	**1.3**	0.09	**0.025**
	parameter of stem to aboveground biomass	k_{Ws1}								5					5		286				1.0		
	Root -shoot allocation coefficient	$k_{\lambda 1}$	12	5	8	3	3	3	4	15	26	12	11	16		151	92	0.9	**1.4**	0.08	**1.2**	0.03	0.010
	Tree SLA	LMA_{T}	$\boxed{\mathbf{36}}$	15	24	10	**10**	**7**	**12**	**33**	**75**	42	29	**46**	**13**	**334**	$\boxed{\mathbf{704}}$	**1.3**	1.9	$\boxed{\mathbf{0.23}}$	**1.8**	0.11	$\boxed{\mathbf{0.031}}$
	Understorey SLA	LMA_{U}		4							24	25	29		4	74		0.2	0.3	0.02	0.3	$\boxed{\mathbf{0.30}}$	
Pheno -logy	Heat sum for tree foliage bud burst	BB																					0.005
	Growth duration of understorey foliage	$GD_{\mathrm{U,f}}$	4								24	23	23			89						0.07	
	Mx. Foliage biomass of undertorey	$W_{\mathrm{max,f}}$		4							24	24	22		2			0.2	0.3	0.02	0.3	**0.29**	0.003
Radiative transfer	Soil albedo	α	**19**	18									8										
	Direct beam extinction coefficient	$k_{\mathrm{b,T}}$	4	5																			
	Diffuse light extinction coefficient	$k_{\mathrm{d,T}}$	**19**	16			4	2	2	11	25	14	9	16	5	150	211	0.5	0.7	0.04	0.6		0.005
	Leaf reflectance	$\rho_{T,f}$																					
Soil	Rooting Depth	z_{root}	14	16	**29**	**12**	**10**	**6**	**13**	13	**74**	**61**	**49**	25	**12**	292	106	0.5	0.7	0.04	0.6	0.08	0.008
	Max. drainage rate	D_{max}	5	5	10	4	4	**7**	5		29	27	20	9	**7**	73						0.05	
	Van Genuchten - α	α_{VG}																					
	Van Genuchten *m*	m_{VG}																					
	Water content at field capacity	θ_{FC}	9	$\boxed{\mathbf{43}}$	$\boxed{\mathbf{53}}$	$\boxed{\mathbf{22}}$	4	$\boxed{\mathbf{11}}$	$\boxed{\mathbf{22}}$	10	29	20	16	13	3	138	185	0.4	0.5	0.03	0.4	0.03	0.004
	Water content at wilting point	θ_{WP}	**28**	6	26	**11**	$\boxed{\mathbf{19}}$	**6**	10	$\boxed{\mathbf{39}}$	$\boxed{\mathbf{135}}$	$\boxed{\mathbf{97}}$	$\boxed{\mathbf{76}}$	$\boxed{\mathbf{59}}$	$\boxed{\mathbf{20}}$	$\boxed{\mathbf{626}}$	**571**	**1.6**	$\boxed{\mathbf{2.4}}$	**0.14**	$\boxed{\mathbf{2.1}}$		**0.020**
Tree canopy layer	Quantum efficiency	α_{T}	8				2	2	3	15	38	23	17	21	6	236	268	0.6	0.9	0.05	0.8		0.006
	Foliage mitochondrial respiration at 25 °C	$R_{\mathrm{d25,U}}$																					
	Max. carboxylation rate Vcmax	$V_{\mathrm{cmax,U}}$	15	7	9	4	**4**	3	5	**20**	55	35	24	**31**	**11**	245	**367**	0.7	**1.1**	0.09	**1.1**	0.04	0.012
	Canopy water storage capacity	$S_{\mathrm{w,T}}$																					
	Max. stomatal conductance	$g_{\mathrm{s\,max,T}}$		9	7	3	5		3		15	13	11			72						0.04	
	Stomatal conductance responce to leaf water potenti	$k_{\psi 2}$																					
	Root-to-leaf hydraulic resistance	k_{x1}																					
	Respiration multiplier for a 10°C increase	Q_{10}																					
Understorey	Quantum efficiency	α_{U}																					
	Foliage mitochondrial respiration at 25 °C	$R_{\mathrm{d25,U}}$										14	14										
	Max. carboxylation rate Vcmax	$V_{\mathrm{cmax,T}}$																					
	Max. stomatal conductance	$g_{\mathrm{s\,max,U}}$																					

Figure S4. Values of the relative sensitivity index I_k of "fluxes" variables to meteorological variables over a complete forest rotation from 1970 (planting) to 2010 (clear-cut). Each box shows the relative sensitivity value of nine output variables to one of the six forcing input variables.

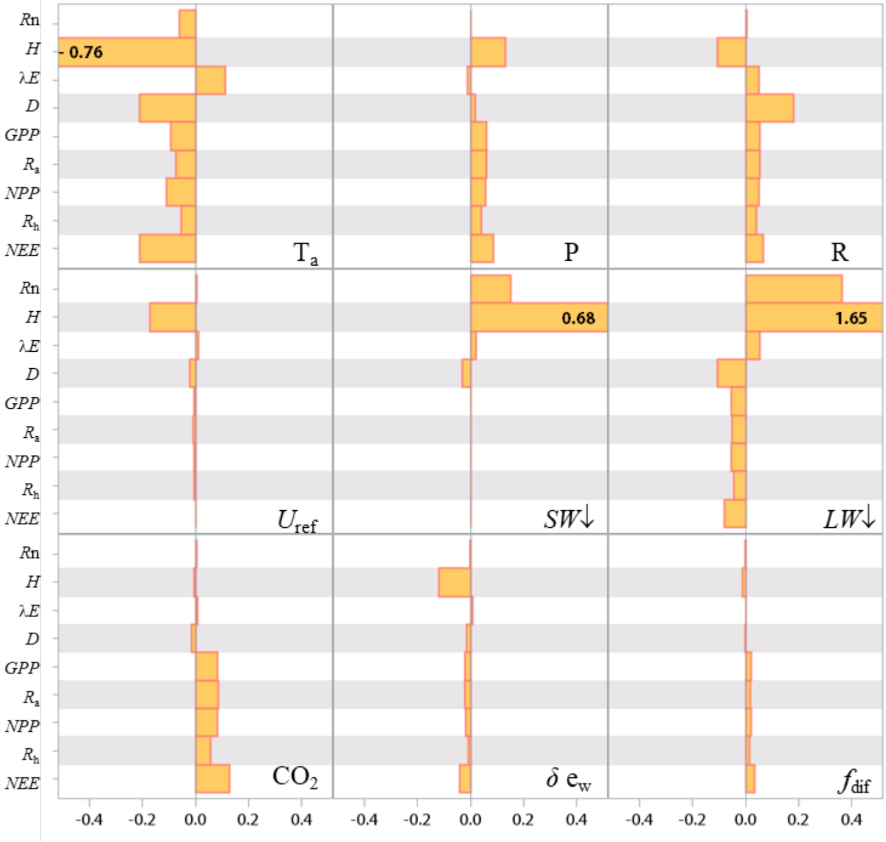

Figure S5. Relative sensitivity of soil water, stress index, tree stand variables and soil carbon stock to meteorological variables over a complete forest rotation from 1970 (planting) to 2010 (clear-cut).

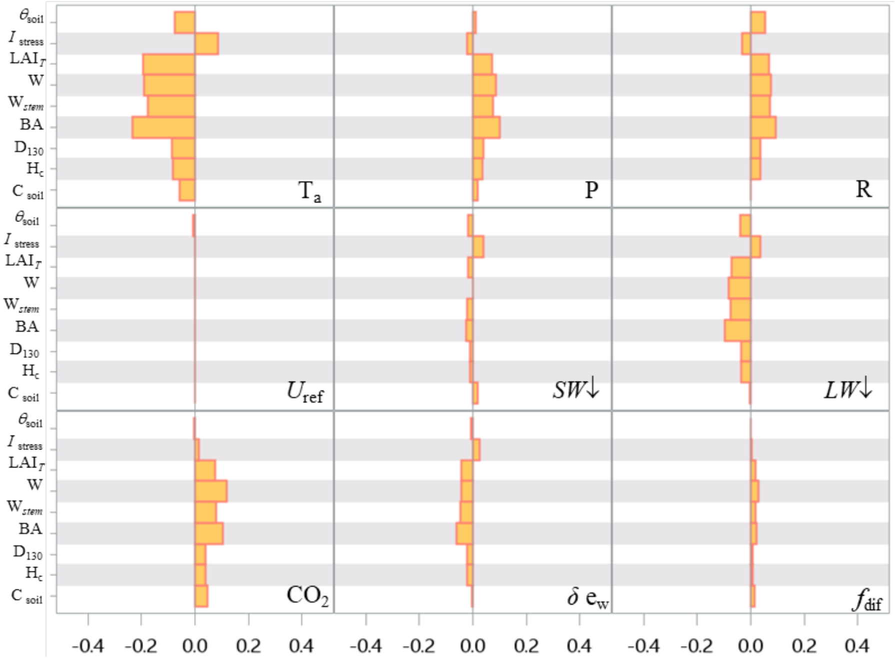

Figure S6. Normalized uncertainty of the annual mean values of the energy balance components calculated for the year 1994 at Le Bray. Red curve is the normal distribution fitted and inset numbers are the standard deviation.

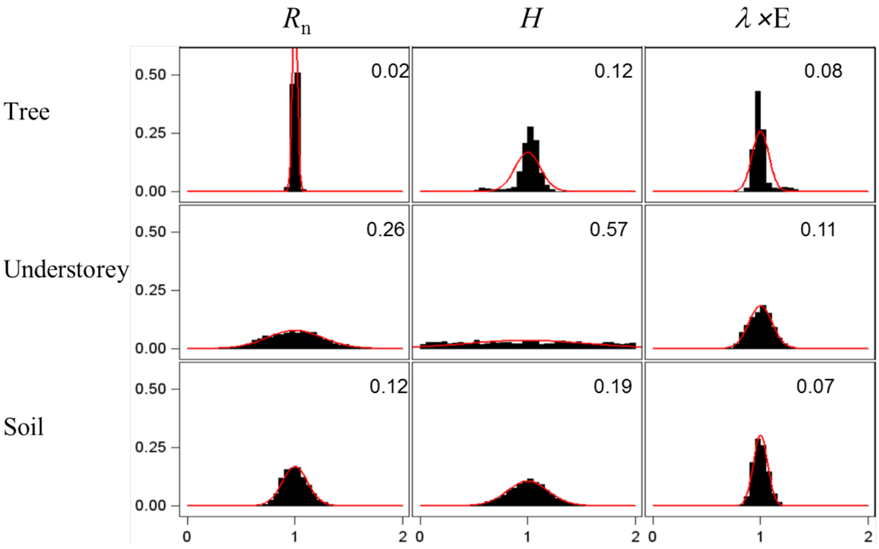

Figure S7. Normalized uncertainty of the annual mean values of the carbon balance components calculated for the year 1994 at Le Bray. The red curve is the normal distribution fitted and inset numbers are the standard deviation.

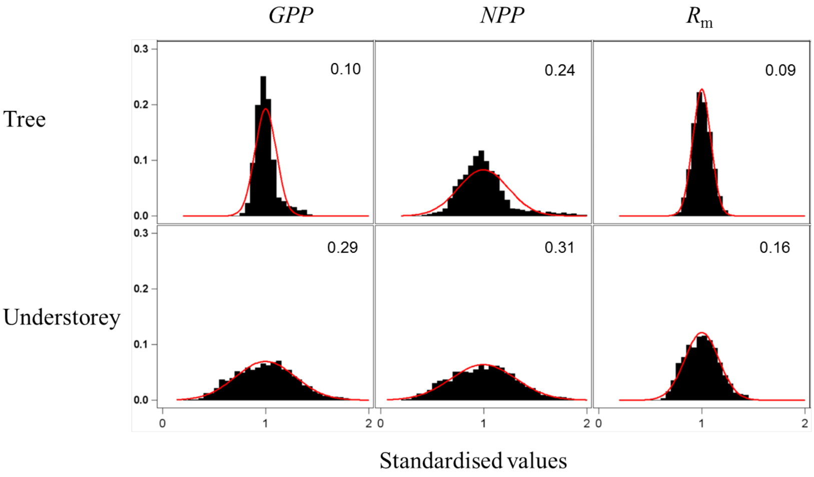

Figure S8. Normalized uncertainty of the annual mean values of the biomass components calculated for the year 1994 at Le Bray. The red curve is the normal distribution fitted and inset numbers are the standard deviation.